

ICSSST 2019

The Everly Hotel, Putrajaya
11th – 13th November

ABSTRACTS BOOK



7th International Conference on
Solid State Science & Technology 2019

SPECIAL THANKS TO OUR SPONSORS



HI - TECH INSTRUMENTS
Your Ultimate Strategic Partner

Biotek Abadi
Sdn. Bhd.
(964217-K)

Solutions Beyond Expectation

Imaging topmost surface electron with confidence



HITACHI UHR FESEM

- Beam deceleration for ultra-low landing voltages
- Signal detection flexibilities for topmost surface, molecular step, grain and composition contrast
- Reduction of charge and edge effect with Super ExB refinements

Ultimate Raman Spectroscopy sensitivity & class leading resolutions



HORIBA Raman Microscope

- True 3D CONFOCAL Raman solution
- Tip Enhanced Raman Spectroscopy (TERS), Stimulated and Polarized TERS and Tip Enhanced Photoluminescence (TEPL)
- Nano spectroscopy with spatial resolution down to few nanometers

Scanning Probe Microscopy measurement is not difficult !
Operating is simple



HITACHI SPM

- One instrument – Two technologies (Self-detection & Laser Optic)
- One-Click automatic measurement (ease of system operation)
- Nano Scale Quality Control make available

Your Ultimate Strategic Partner



HI-TECH INSTRUMENTS SDN. BHD. (Head Office) (388534-U)
19, Jalan BP4/8, Bandar Bukit Puchong, 47120 Puchong, Selangor, Malaysia.
HI-TECH INSTRUMENTS PTE. LTD. (Singapore Office) (200103160-C)
HI-TECH INSTRUMENTS INC. (Philippines Office) (A200110681)
HI-TECH IMAGING CO., LTD. (Thailand Office) (0105549128429)

Tel: +603 - 8061 2228
Tel: +65 - 6899 9218
Tel: +632 - 873 3009
Tel: +662 024 1400

Fax: +603 - 8061 6668
Fax: +65 - 6899 0989
Fax: +632 - 873 3010
Fax: +662 024 1401

General Email: sales@htimail.com.my, service@htimail.com.my

<http://www.htiweb.com>

7th ICSSST 2019

On behalf of the members of committee, I am honored and delighted to welcome the keynote speakers, presenters and participants to the 7th International Conference on Solid State Science and Technology (ICSSST 2019), which is co-organized by The Malaysian Solid State and Technology Society (MASS). It is an inaugural event, which aims to provide a premier platform for students, academicians, researchers, scientist and practitioners to share insights and relevant information in regards to the innovations, trends and challenges encountered in world of research. Especially on the sustainable achievement in the domain of Solid State Science and Technology.

The theme of ICSSST19 this year, *'Enhancing Science and Technology of Advanced Materials for the Fourth Industrial Revolution'*, will need academicians, researchers, scientists and practitioners to be more prepared in idea and knowledge comprised of various Science and Technology scope. We are delighted to have with us in ICSSST19, four distinguished keynote speakers namely, Prof. Dr. Muralidhar Miryala (Shibaura Institute of Technology), Prof. Dr. Imad Hamadneh (University of Jordan), Prof. Dr. Paul A. Bingham (Sheffield Hallam University, UK) and Prof. Emeritus Dato' Dr. Wan Md Zin Wan Yunus (National Defence University of Malaysia). We are proud to announce the submission of **167** manuscripts received from various research and academic institutions from all over the world for this conference that will be presented in oral and poster sessions.

Finally, further thanks are due to all members of the organising committee for struggling together, dedicating their valuable time and energy towards making this conference successful and memorable. I would like to express my appreciation to our great keynote speakers for their commitment to be here with us and also to all sponsors who made this conference possible. Last but not least, my sincere thanks to all presenters and participants for their generous support and outstanding contributions. I wish all an enjoyable and successful conference.

Thank you.

Major Prof. Ts. Dr. Muhd Zu Azhan Yahya
Chairman of ICSSST 2019

Cluster: Biomedical/ Nanotechnology/ Nanomaterials

Paper ID	Paper Title	Name	Sub-theme	Page
ICSSST2019-001	Synthesis, Characterization, Antimicrobial Activity and in vitro Bioactivity of Chitosan Hydroxyapatite Composite Doped with Strontium	Ismaila Abdullahi	Biomaterials	13
ICSSST2019-073	Effect of Mechanical Agitation on Cr-Al ₂ O ₃ Nanocomposite Coatings Fabricated from Trivalent Chromium Electrodeposition	Eydar Tey	Electrochemical and Solid State	36
ICSSST2019-057	Influence of Surfactant on the Synthesis of NiO Nanoparticles by a Sol-gel Method	Noor Hidayah Aniza Zakaria	Material and Energy	43
ICSSST2019-085	Effect of Particles Size on Cu (II) Ion Removal from Aqueous Solutions using Fe ₃ O ₄ Nanoparticles Adsorbents Synthesized from Mill Scale Waste	Syazana Sulaiman	Material and Energy	44
ICSSST2019-020	Synthesis and Controlled Release Properties of Nanohybrid Zinc-Aluminium Layered Double Hydroxide -Captopril	Dr. Zaemah Jubri	Nanoscience and Nanotechnology	53
ICSSST2019-028	Study on the Impact of pH Adjustment to Remove Metallic Ions using Membranes	Dr. Norherdawati Kasim	Nanoscience and Nanotechnology	54
ICSSST2019-045	Nanocellulose-based Filters as Novel Barrier Systems for Chemical Warfare Agents	Dr. Mohd Nor Faiz Norrrahim	Nanoscience and Nanotechnology	56
ICSSST2019-046	Synthesis of Calcium/Aluminium-Ciprofloxacin-Layered Double Hydroxide for A New Antibacterial Drug Formulation	Monica Limau Anak Jadam	Nanoscience and Nanotechnology	56
ICSSST2019-089	Multi-walled Carbon Nanotubes Functionalized with Amide for Acetone Detection in VENUE Temperature	Assoc. Prof. Dr. Noor Azilah Mohd Kasim	Nanoscience and Nanotechnology	57
ICSSST2019-123	Supramolecular Interactions in Aromatic Structural Units for Non-Optical and Optical Detection	Dr. Juan Matmin	Nanoscience and Nanotechnology	58
ICSSST2019-024	Mechanical Properties and Thermal Behavior of Poly(lactic acid) Composites Reinforced with TiO ₂ Nanofiller	Nur Ain Syafiqah Sudin	Polymers and Composites	72
ICSSST2019-135	Thermomechanical, Crystallization and Melting Behavior of Plasticized Poly (lactic acid) Nanocomposites	Nur Ain Syafiqah Sudin	Polymers and Composites	77
ICSSST2019-015	Solution process growth of Co, Bi and Mn Doped Zinc Oxide Nanowires by Hydrothermal Method	Syed Jamal Ahmed Kazmi	Thin Films and Nanostructures	83
ICSSST2019-064	Synthesis and Characterization of Polyaniline Thin Film: The Effect of pH and Concentration	Nur Atikah Shaari	Thin Films and Nanostructures	84
ICSSST2019-070	Influence of Applied Potential on Electrodeposited ZnSe/ZnO Nanostructured Films for Photoelectrochemical Cell	Laimy Mohd Fudzi	Thin Films and Nanostructures	84
ICSSST2019-138	The Optical Properties of Thin Films Tin Oxide with Triple Doping (Aluminum, Indium, and Fluorine) for Electronic Device	Assoc. Prof. Dr. Aris Doyan	Thin Films and Nanostructures	86

List of Oral Presenter

Cluster: Electrics/ Electronics/ Magnetics

Paper ID	Paper Title	Name	Sub-theme	Page
ICSSST2019-042	Preliminary Electrical Studies on Enzyme- Based BioSensor	Ainil Hawa Jasni	Biomaterials	13
ICSSST2019-182	CO ₂ Gas Sensor Based on Polyaniline/ Cu-ZnS Hollow Microsphere Composite	Dr. Zubair Ahmad	Carbon and related materials	18
ICSSST2019-172	Towards Dye Extraction using a Magnetic Aerogel	Assoc. Prof. Dr. Ing Kong	Ceramics and Glasses	30
ICSSST2019-051	The Response of Ion Selective Electrode Based on Aryl Methyl Carbonylamino Thiazole Derivatives as Ionophore	Noor Wahidah Zainol Jamil	Electrochemical and Solid State	35
ICSSST2019-077	The Electrochemical Performance of Superconcentrated Na ⁺ Salt in Ionic Liquid- Based Gel Electrolytes for Application in Sodium Rechargeable Batteries	Noorhaslin Che Su	Electrochemical and Solid State	37
ICSSST2019-037	Electrochemical Studies of Polymer Gel Electrolytes based on Agarose:LiBOB and P(VP-co-VAc):LiBOB	Muhammad Syahir Sak Ari	Material and Energy	42
ICSSST2019-147	Structural and Conductivity Properties of Na ₂ ZnSiO ₄ -Py ₁₄ TFSI Hybrid Solid Electrolyte for Sodium-ion Batteries	Nur Sofina Mohamad Johari	Material and Energy	49
ICSSST2019-160	Improved Performance of Inverted Type Organic Solar Cell Using Copper Iodide-doped P3HT:PCBM as Active Layer	Assoc. Prof. Dr. Chi Chin Yap	Material and Energy	49
ICSSST2019-170	Effect of Vanadium Doping on Thermoelectric Properties of CaMnO ₃ using First Principle Calculations	Assoc. Prof. Dr. Abdullah Chik	Material and Energy	50
ICSSST2019-035	High Dielectric Permittivity of La _{0.88} Bi _{0.12} Mn _{0.80} Ni _{0.20} O ₃ Composite	Aaliyawani Ezzerin Sinin	Optical and Dielectric Materials	59
ICSSST2019-063	Dielectric and ac Conductivity Studies of SrXLiTeO ₆ (X=La, Nd) Double Perovskites	Muhammad Zharfan Mohd Halizan	Optical and Dielectric Materials	59
ICSSST2019-183	Study of Dielectric Properties of Polycrystalline Ex situ Magnesium Diboride	Assoc. Prof. Dr. Soo Kien Chen	Optical and Dielectric Materials	61
ICSSST2019-030	Conductivity Mapping of SWCNT Dispersed in Conducting Polymer	Nurul Syahirah Nasuha binti Sa'aya	Organic Materials and Application	63
ICSSST2019-065	Microwave Absorption Properties of Monovalent Doped La _{0.85} Ag _{0.15} MnO ₃ La _{0.85} Ag _{0.15} MnO ₃ Manganite Prepared by Solid State Method	Nur Ain Athirah Che Apandi	Other Solid State Research	68
ICSSST2019-067	Electroresistance Effect Due to Mo Substitution at Mn-site in La _{0.85} Ag _{0.15} Mn _{1-x} Mo _x O ₃ (x = 0.00 and 0.05) Monovalent doped Manganites	Dr. Norazila Binti Ibrahim	Other Solid State Research	68
ICSSST2019-078	Effect of Fe Partial Substitution at Mn-site on Electroresistance Behaviour in La _{0.7} Ba _{0.3} Mn _{1-x} Fe _x O ₃ (x = 0 and 0.02) Manganites	Muhammad Suffian Sazali	Other Solid State Research	69
ICSSST2019-120	Effect of Fe Doping on the Structural, Electrical and Magnetic Properties of La _{0.7} Ca _{0.3} Mn _{1-x} Fe _x O ₃ (x = 0, 0.01, 0.03 and 0.05) Perovskite Manganite Materials	Dr. Nor Azah Nik Jaafar	Other Solid State Research	70

List of Oral Presenter

Paper ID	Paper Title	Name	Sub-theme	Page
ICSSST2019-054	Physical and Electrical Studies of High Molecular Weight Poly(Methyl Methacrylate) Based Solid Polymer Electrolytes	Assoc. Prof. Ab Malik Marwan Ali	Polymers and Composites	74
ICSSST2019-162	Localized Deep and Shallow Traps of α -Peaks from Thermally Stimulated Current (TSC) Measurement on Thermoplastic Polymers	Assoc. Prof. Dr. Norhana Abdul Halim	Polymers and Composites	78
ICSSST2019-113	Structural and Electronic Properties of Ag-doped in Ba-site of $YBa_{2-x}Cu_3O_7$ using Density Functional Theory via First Principle Study	Siti Fatimah Saipuddin	Superconductors	80
ICSSST2019-142	AC Susceptibility and Superconducting Properties of Low Density $Bi_{1.6}Pb_{0.4}Sr_2(Ca_{2-x}Yb_x)_2Cu_3O_y$ Superconductor	Prof. Dr. Azhan bin Hashim @ Ismail	Superconductors	81
ICSSST2019-143	Rare-Earths, Alkali and Transition Metals Effects on the Tl-1212 Type Phase Superconductors	Prof. Dato' Dr. Roslan Abd Shukur	Superconductors	81
ICSSST2019-148	Ferrimagnetic Cr_2S_3 Effect on (Bi,Pb)-Sr-Ca-Cu-O Superconductor	Masnita Mat Jusoh	Superconductors	82
ICSSST2019-169	Impact of Zinc Ferrite Nanoparticles on Transport and Superconducting Properties of $(Tl_{0.85}Cr_{0.15})Sr_2CaCu_2O_{7.5}$ Bulk Superconductors	Nurul Auni Khalid	Superconductors	82
ICSSST2019-049	Impact of Ba/Fe Molar Ratio on the Structural and Magnetic Properties of $BaFe_{12}O_{19}$ Film Synthesized by a Sol-gel Method	Assoc. Prof. Dr. Noor Baa'Yah Ibrahim	Thin Films and Nanostructures	83

Cluster: Glass/ Ceramics/ Other Materials

Paper ID	Paper Title	Name	Sub-theme	Page
ICSSST2019-164	Physical, Structural and Mechanical Properties of Glass Ionomer Cement Derived from Fluoroaluminosilicate Glass with Different Ageing Time	Mohammad Zulhasif Ahmad Khiri	Biomaterials	14
ICSSST2019-006	Effect of Samarium Oxide on Structural and Optical Properties of Zinc Silicate Glass Ceramics from Waste Material	Assoc. Prof. Dr. Auwalu Inusa Abubakar	Ceramics and glasses	18
ICSSST2019-011	Preparation of Alumina-Based Ceramics Foam with Corn Starch as Pore Former	Assoc. Prof. Dr. Hamimah Abd.Rahman	Ceramics and glasses	19
ICSSST2019-013	FTIR and Optical Properties of Samarium Doped Zinc Borotellurite Glasses	Siti Nasuha Mohd Rafien	Ceramics and glasses	19
ICSSST2019-014	Optical Properties of Silica Borotellurite Glass Doped with Samarium (iii) Oxide	Nurul Asyikin Ahmad Sukri	Ceramics and glasses	20
ICSSST2019-016	Structural and Electrical Properties of $La_{0.7}Ca_{0.3}MnO_3 / \alpha-Fe_2O_3$ Composites	Lik Nguong Lau	Ceramics and glasses	20
ICSSST2019-017	Effect of TiO_2 Concentration on the Structural and Electrical Properties of $Nd_{0.67}Sr_{0.33}MnO_3$ Composites	Assoc. Prof. Dr. Kean Pah Lim	Ceramics and glasses	21
ICSSST2019-019	Effect of Holmium Oxide on Optical Performance of Borotellurite Glass	Dr. Muhammad Noorazlan Abd Azis	Ceramics and glasses	21

List of Oral Presenter

Paper ID	Paper Title	Name	Sub-theme	Page
ICSSST2019-022	Structural and Electrical Properties of Nd-Sr-Mn-O/CuO by Solid-state Reaction Method	Amirah Natasha Ishak	Ceramics and glasses	22
ICSSST2019-031	The Forming and Non-Forming Phases of LaZrTa ₃ O ₁₁ Analogues	Dr. Fadhlna Che Ros	Ceramics and glasses	22
ICSSST2019-032	Fabrication of Silica (SiO ₂) as-derived from Rice Husk Ash Foam via Polymeric Replication Method	Assoc. Prof. Dr. Hariati Taib	Ceramics and glasses	23
ICSSST2019-039	Comparative Spectroscopic Studies on Luminescence Performance of Er ³⁺ Doped Tellurite Glass Embedded with Nanoparticles at 0.55 μm Emission	Prof. Dr. Md Rahim Sahar	Ceramics and glasses	23
ICSSST2019-043	Chemical and Mineralogical Characterization of Electric Arc Furnace (EAF) Steel Slag Waste: The Potential Green Resource for Geopolymer Ceramic Production	Dr. Pao Ter Teo	Ceramics and glasses	24
ICSSST2019-060	Elastic Properties of (80-x)B ₂ O ₃ -xTeO ₂ -10Li ₂ O-10Al ₂ O ₃ Mixed Network Former Glass System	Nurul Ain Mohd Samsudin	Ceramics and glasses	25
ICSSST2019-102	Photoluminescence and Spectroscopic Properties of Erbium Doped Bio-Silica Borotellurite Glasses Containing Silver Oxide	Abdulkarim Muhammad Hamza	Ceramics and glasses	26
ICSSST2019-118	Effect of SLS Glass Doping on ZnO Varistor Ceramics: Dry Milling Process	Nur Quratul Aini Ismail	Ceramics and glasses	27
ICSSST2019-130	Nonlinearity Characteristics of ZnO Varistors Tailored by Perovskite-BaTiO ₃ and Cobalt Dopants	Muhamad Syaizwadi Shaifudin	Ceramics and glasses	27
ICSSST2019-133	Effect of Heat Treatment to The Properties of Zinc Silicate Based Glass-Ceramics	Dr. Mohd Hafiz Mohd Zaid	Ceramics and glasses	28
ICSSST2019-173	A Brief Review on the Fundamentals of Multiferroic Materials and their Possible Applications	Prof. Dr. Abdul Halim Shaari	Ceramics and Glasses	31
ICSSST2019-174	UV-Vis Spectroscopy of Samarium Doped Wollastonite - CaSiO ₃ :Sm ³⁺	Prof. Dr. Sidek Ab Aziz	Ceramics and Glasses	32
ICSSST2019-010	Human Detection for Thermal and Visible Images	Dr. Mazlinda Ibrahim	Defence and security	34
ICSSST2019-023	Effects of Convective Boundary Conditions and Heat Transfer on MHD Stagnation Point Nanofluid Flow Past a Shrinking Sheet	Nor Ain Azeany Mohd Nasir	Defence and security	34
ICSSST2019-112	Phase Formation and Morphology of NiO-BCZY Anode Functional Layer for Proton Conducting Fuel Cell	Lidayatty Abdul Malik	Electrochemical and Solid State	38
ICSSST2019-003	Key Properties and Benefits of Clay in Environmental Protection	Muntari Mudi Yaradua	Material and Energy	41
ICSSST2019-029	Effect of Gamma Radiation on Micromechanical Behaviour in Microelectronic Packaging	Noor Fadhilah Rahmat	Material and Energy	41
ICSSST2019-050	Enhanced Mg Ion Transport in Cellulose Acetate based Gel Polymer Electrolytes: Effect of Plasticizer	Dr. Siti Zafirah Zainal Abidin	Material and Energy	42
ICSSST2019-091	Screen Printing Methods for The Fabrication of Solid Oxide Fuel Cells (SOFCs): A Short Review	Assoc. Prof. Dr. Hamimah Abd.Rahman	Material and Energy	44

List of Oral Presenter

Paper ID	Paper Title	Name	Sub-theme	Page
ICSSST2019-098	Relationship Between Spectroscopic and Thermal Analysis of Poly(ethylene oxide) (PEO) - 50% Epoxidized Natural Rubber (ENR50) Complexed with Sodium Trifluoromethanesulfonate Based Polymer Electrolyte	Dr. Siti Aminah Mohd Noor	Material and Energy	45
ICSSST2019-117	Acoustic Performance of Natural Fibres of Oil Palm Frond (OPF) and Empty Fruit Bunch (EFB)	Mageswaran A/L Ravi Chandran	Material and Energy	47
ICSSST2019-121	Band Structure and Thermoelectric Properties of $Ni_{(x)}Zn_{(1-x)}Fe_2O_4$	Dr. Lim Joon Hoong	Material and Energy	47
ICSSST2019-139	The Effect of Cooling Rate at the Cooling Bed Step on the Volume Fraction of the Constituent Phases of the Tempcore Steel Rebar	Ahmed Elsherbiny	Metal and Alloys	52
ICSSST2019-012	Corrosion and Microbial Inhibition Characteristic of Local Herb (Petai Belalang) on Stainless Steel (316L) in Seawater	Wan Mohamad Ikhmal Wan Mohamad Kamaruzzaman	Organic Materials and Application	62
ICSSST2019-034	Feasibility of Irradiated Corn-Based Bioplastics as Packaging Material	Dr. Siti Amira Othman	Organic Materials and Application	64
ICSSST2019-134	Green Approach in Anti-Corrosion Coating by using <i>Andrographis paniculata</i> Leaves Extract as Additives of Stainless Steel 316L in Seawater	Maria Fazira Binti Mohd Fekeri	Organic Materials and Application	66
ICSSST2019-090	Green Approach of Rice (MR 219) Treatment using a 2-D Clinostat: Factorial Design Analysis	Prof. Dr. Ong Keat Khim	Other Solid State Research	69
ICSSST2019-150	Solid State Synthesis and Characterization of Cu(II) and Ni(II) Polynuclear Metal Complexes With Ligand Derived from 3-Methoxy-4-Hydroxy Benzaldehyde and L-Leucine	Zainab Sulaiman	Other Solid State Research	71
ICSSST2019-178	Computational Designing of Energy Materials for Futuristic Technological Applications	Dr. Rashid Ahmed	Other Solid State Research	71
ICSSST2019-179	GPU Based Computing For Application In Material Physics	Maqsood Ahmed	Other Solid State Research	72
ICSSST2019-038	Fatigue Crack Growth of Natural Rubber/Butadiene Rubber Blend Containing Waste Tyre Rubber Powders	Dayang Habibah Abang Ismawi Hassim	Polymers and Composites	73
ICSSST2019-053	Enhancement of Heat Ageing Properties of Epoxidised Natural Rubber Blend for Automotive Application	Dr. Mazlina Mustafa Kamal	Polymers and Composites	73
ICSSST2019-071	Thermomechanical Study and Thermal Behavior of Plasticized Poly(lactic Acid) Composites	Mohammed Zorah	Polymers and Composites	75
ICSSST2019-127	Influence of Hydroxymethylated Lignin on Mechanical Properties and Payne Effect of NR/BR Compounds	Nor Anizah Binti Mohamad Aini	Polymers and Composites	76
ICSSST2019-159	Nonlinearity Characteristics of Zn-Bi-Ti-O Varistor Ceramics Doped with Sb_2O_3 Prepared by Co-Precipitation Method	Assoc. Prof. Dr. Mohd Sabri Mohd Ghazali	Semiconductors and Devices	79
ICSSST2019-058	Effect of Cr_2O_3 on the Tc and Phase Formation of $Tl_{2-x}Cr_xBa_2CaCu_2O_{8.5}$ Superconductor	Syahrul Humaidi	Superconductors	80
ICSSST2019-156	Influence of Target to Substrate Distance on Structural, Microstructure and Optical Properties of Sputtered Gd-doped ZnO Thin Films	Dr. Siti Nooraya Mohd Tawil	Thin Films and Nanostructures	87

List of Oral Presenter

Cluster: Nanomaterials/ Nanotech/ Other Materials

Paper ID	Paper Title	Name	Sub-theme	Page
ICSSST2019-171	Graphene Exfoliation and Its Stability in Microcrystalline Cellulose Solution	Amirul Hadi Bin Azmi	Carbon and Related Materials	17
ICSSST2019-075	BiFeO ₃ assisted with Different Weight Ratio of Polymer Chitosan: Structural, Optical and Photocatalytic Properties	Muhammad Safwan Bin Sazali Muhammad Safwan	Ceramics and glasses	25
ICSSST2019-104	The Effects of Tungsten Carbide WC-Co Thermal Spray Coating on Mechanical Properties of Carbon Steel	Mohamad Ariff Bin Moh Halmi	Ceramics and glasses	26
ICSSST2019-145	Gold Nanoparticles Activated Enhanced Photoluminescence of Samarium Ions Inside Tellurite Amorphous Host	Dr. Yakubu Aliyu Tanko	Ceramics and glasses	28
ICSSST2019-128	Generalized Function Projective Synchronization of 4D Chaotic Laser System for a Secure Communication	Dr. Nur Aisyah Abdul Fataf	Laser and Optoelectronics	40
ICSSST2019-083	Controlled Growth of Root-Free Ni ₃ Si ₂ Nanowires for High Performance Supercapactor Electrode	Dr. Goh Boon Tong	Material and Energy	43
ICSSST2019-146	Development of a Computer-based Data Acquisition and Performance Analysis of Fuzzy-PID Hybrid γ Temperature Control for Torrefaction	Jailani Jamaludin	Material and Energy	48
ICSSST2019-176	Fabrication of Porous ZnO:Al Nanostructures Using Microwave Assisted Hydrothermal Method	Assoc. Prof. Dr. Mohammad Hafizuddin Jumali	Material and Energy	51
ICSSST2019-036	Effect of Different Drying Method on the Morphology of Nanocellulose	Nurjahirah Janudin	Nanoscience and Nanotechnology	55
ICSSST2019-094	Synthesis and Controlled Release Properties of Nanohybrid Zinc-Aluminium Layered Double Hydroxide – Captopril	Anissa Azlan	Nanoscience and Nanotechnology	57
ICSSST2019-076	Sol Precursor Concentration Effect on Synthesis and Characterization of ZnO Nanoparticles Film	Tan Huey Jing	Thin Films and Nanostructures	85
ICSSST2019-115	Synthesis of Silver Nanoparticles by Plasma-Assisted Hot-Filament Evaporation for Luminance Enhancement of Organic Light Emitting Diode	Abtisam Hasan Hamood Al-Masoodi	Thin Films and Nanostructures	85

List of Oral Presenter

Cluster: Optical/ Photonics/ Other Materials

Paper ID	Paper Title	Name	Sub-theme	Page
ICSSST2019-175	Role of Sm ³⁺ ions on the Optical Properties of Borotellurite Glass Under 480 nm Excitation Wavelength	Dr. Azman Kasim	Ceramics and Glasses	32
ICSSST2019-080	The Effect of Blast Exposure Distance on Hardness and Reduced Modulus Properties of Lead Free Solder	Dr. Wan Yusmawati Wan Yusoff	Metal and Alloys	52
ICSSST2019-033	Enhanced Optical Efficiency of Graphene Oxide-coated Tellurite Glasses Doped with Erbium for Advanced Fiber Optics	Azlina Yahya	Nanoscience and Nanotechnology	55
ICSSST2019-177	High-Sensitivity Single/Double Layer Coating Side Polished Optical Fiber Refractive Index Sensor Based on Surface Plasmon Resonance	Assoc. Prof. Dr. Rozalina Zakaria	Optical and Dielectric Materials	60
ICSSST2019-187	Structural and Optical Properties of Europium Doped and Dysprosium Co-Doped with Yttrium Aluminium Garnet Nanocrystalline Powders Prepared by Combustion Synthesis	Ts. Dr. Abd Rahman Tamuri	Optical and Dielectric Materials	61
ICSSST2019-004	Computational Insights of Some Ruthenium Complexes with Azobenzene Derivatives for Non-Linear Optic Application	Dr. Fazira Ilyana Abdul Razak	Other Solid State Research	67
ICSSST2019-061	Optimum Lasing Cavity for Erbium Doped Zinc Tellurite Glass Doped with Ag Nanoparticles	Nur Aina Mardia Adnan	Other Solid State Research	67
ICSSST2019-108	Investigation of Chemical and Optical Properties of Polystyrene/Silver Nanocomposites	Jibrin Alhaji Yabagi	Polymers and Composites	75

Cluster: Synthesis/ Carbon-based Materials

Paper ID	Paper Title	Name	Sub-theme	Page
ICSSST2019-044	Evaluation of Superoleophilic-Hydrophobic Kapok Fiber as Effective Oil Sorbents	Normaisarah Yunos	Carbon and related materials	13
ICSSST2019-052	Oil Sorbents Derived from Carbonization of Disposable Baby Diapers	Jee Khan Lim	Carbon and related materials	15
ICSSST2019-069	Synthesis of Graphene Oxide from Waste Tyre using Sodium Nitrate and Phosphoric Acid as Precursor in Hummer's Method	Ain Zanaya Zanuri	Carbon and related materials	15
ICSSST2019-093	The Optimization of a-CN _x Thin Films and its Humidity Sensing Properties at Different Substrate Temperature by Radio Frequency-plasma Enhanced Chemical Vapor Deposition	Dr. Rozidawati Awang	Carbon and related materials	16
ICSSST2019-131	Ni Catalytic Effects on the Growth of PECVD and HF-PECVD Transfer-free Graphene	Dr. Richard Ritikos	Carbon and related materials	16
ICSSST2019-140	Effect of Prekotac as Filter Aids on Pressure Drop and Particle Penetration in Pilot Plant Fabric Filtration System	Dr. Nor Ruwaida Jamian	Carbon and related materials	17
ICSSST2019-163	Synthesis and Enhancement of Luminescence Properties of Co ²⁺ : Zn ₂ SiO ₄ Willemite Based Glass Ceramic Derived for Potent Optoelectronic Applications	Siti Aisyah Abdul Wahab	Ceramics and glasses	29

List of Oral Presenter

Paper ID	Paper Title	Name	Sub-theme	Page
ICSSST2019-161	The Impact of Zr Substitution on the Crystal Structure of Yb doped BaCeO ₃ Solid Solution Prepared by a Sol-gel Method	Assoc. Prof. Dr. Nafisah Osman	Crystallography	33
ICSSST2019-109	Modification of Gold Electrodes using Reduced Graphene Oxide for Cortisol Electrochemical Biosensor	Dr. Ahmad Farid Mohd Azmi	Electrochemical and Solid State	38
ICSSST2019-116	Ionic Conductivity in Carboxymethyl cellulose (CMC) Biopolymer membrane incorporated with Ammonium Thiocyanate, NH ₄ SCN	Dr. Rosnah Binti Zakaria	Electrochemical and Solid State	39
ICSSST2019-158	Effect of pH and Immersion Time on the Corrosion Protection of SDBS-ZnSO ₄ Pre-Treated Mild Steel in Sodium Chloride Solution	Ismaliza Ismail	Electrochemical and Solid State	40
ICSSST2019-110	The Effect of Sintering Temperature on Structural and Microwave Properties of Barium Hexaferrite Derived from Mill Scale	Nurshahiera Rosdi	Material and Energy	46
ICSSST2019-125	Photocatalyst Degradation of Methylene Blue by Using TiO ₂ -Graphene Composite	Mohd Fairul Sharin Abdul Razak	Material and Energy	48
ICSSST2019-009	Synthesis, Characterization and Catalytic Activity of Pd Nanoparticles Supported on Anatase (Pd/TiO ₂)	Dr. Norli Abdullah	Nanoscience and Nanotechnology	53
ICSSST2019-027	Biosynthesis of Silver Particles Using <i>Citrus Microcarpa</i> Peel's Extract	Wee Jie Gong	Organic Materials and Application	63
ICSSST2019-040	Synthesis of Antidote Conjugation with Oximes for Chemical Warfare Agents	Mas Amira Idayu Abdul Razak	Organic Materials and Application	64
ICSSST2019-048	Synthesis of Carbide Lime Derived Solid Superbase Catalyst for Biodiesel Production	Lim Hong Hua	Organic Materials and Application	65
ICSSST2019-099	Discovering Picrocrocic from the Extraction of <i>Crocus</i> Species	Assoc. Prof. Ibtisam Abdul Wahab	Organic Materials and Application	65
ICSSST2019-137	Synthesis and Characterization Barium M-Hexaferrites (BaFe _{12-2x} Co _x Mn _x Ni _x O ₁₉) as a Microwave Absorbent Material	Assoc. Prof. Dr. Susilawati	Other Solid State Research	70
ICSSST2019-062	A Study on Milling Time and Composition of Mechanical Milled Graphite Powder Effect as Filler in MDPE Composite to Physical and Tensile Properties	Dr. Engku Abd Ghapur Che Engku Ali	Polymers and Composites	74

Paper ID	Paper Title	Name	Sub-theme	Page
ICSSST2019-018	From Kaolin to Kalsilite: The Effect of KOH Concentrations and Reaction Temperature	Eddy Mohd Farid Mohd Yusslee	Advanced Material Synthesis and Crystal Growth Technology	88
ICSSST2019-066	Elastic Properties of Sodium Potassium Borotellurite Glass System	Dr. Rosdiyana Hasham@Hisam	Ceramics and Glasses	88
ICSSST2019-082	γ -Ray Shielding Parameter of Barium-Boro-Tellurite Glass	Dr. Azuraida Amat	Ceramics and glasses	89
ICSSST2019-103	Experimental and Theoretical Approach on The Elastic Properties of $50\text{B}_2\text{O}_3-(50-x)\text{Na}_2\text{O}-x\text{Fe}_2\text{O}_3$ Glasses	Syafawati Nadiah Mohamed	Ceramics and Glasses	89
ICSSST2019-111	Structural and Ionic Conductivity of $\text{Mg}_{0.5}\text{Ti}_2(\text{PO}_4)_3$ NASICON-Structured Ceramic Electrolytes	Dr. Nur Amalina Mustaffa	Ceramics and Glasses	90
ICSSST2019-136	Effect of Li Substitution on the Structure and Electrical Properties of Potassium Sodium Niobate Piezoceramics	Dr. Zalita Zainuddin	Ceramics and Glasses	90
ICSSST2019-153	Structural and Elastic Properties of Binary Bismuth Borate Glass Systems	Nuraidayani Effendy	Ceramics and Glasses	91
ICSSST2019-165	Effect of Tungsten Oxide on Elastic Properties of Zinc Borotellurite Glass System	Prof. Dr. Halimah Mohamed Kamari	Ceramics and Glasses	91
ICSSST2019-144	Influence of Ruthenium Doping on the Structural and Magnetic Properties of $\text{Pr}_{0.67}\text{Ba}_{0.33}\text{Mn}_{1-x}\text{Ru}_x\text{O}_3$	Zakiah Mohamed	Crystallography	92
ICSSST2019-059	Preliminary Study: Entrance Surface Dose Verification using Nanodot Optically Stimulated Luminescence (OSL) For Chest X-Ray Examinations in 4 Health Clinic in Perak	Moh Tarmizi Saidin	Devices and Materials for Biology and Medicine	92
ICSSST2019-092	An Antifouling Electrode as a Sensing Platform for the Development of an Electrochemical Immunosensor for the Determination of Glycosylated Hemoglobin (HbA1c)	Dr. Safura Taufik	Devices and Materials for Biology and Medicine	93
ICSSST2019-026	Carboxymethyl Chitosan Based Biopolymer Electrolyte with Imidazolium Ionic Liquid	Dr. Intan Juliana Shamsudin	Electrochemical and Solid State	94
ICSSST2019-132	Synthesis and characterization of $\text{Li}_2\text{FeP}_2\text{O}_7$ composite by sol-gel method	Maziidah Hamidi	Electrochemical and Solid State	94
ICSSST2019-041	The Effect of Etching Conditions on CdS/CdTe Solar Cells Efficiency	Dr. Nor Azlian	Material and Energy	95
ICSSST2019-055	Texturization of SiNW Process for P-Type Silicon Wafer	Mohd Norizam Md Daud	Material and Energy	95
ICSSST2019-081	Ferroelectric and Pyroelectric Effect of Annealed Copolymer P(VDF-TrFE)	Nurazlin binti Ahmad	Material and Energy	96
ICSSST2019-167	Effect of film thickness on electrochemical properties of $\text{LiCo}_{0.6}\text{Co}_{0.4}\text{O}_2$ cathode material for solid oxide fuel cell application	Wan Nor Anasuhah Wan Yusoff	Material and Energy	96

List of Poster Presenter

Paper ID	Paper Title	Name	Sub-theme	Page
ICSSST2019-168	An Overview of Working Principle and Criteria for Composite Cathode in Solid Oxide Fuel Cell	Azreen Junaida Abd Aziz	Material and Energy	97
ICSSST2019-101	Influence of Zr Additive on the Reduction Behaviour of MoO ₃ in Carbon Monoxide Atmosphere	Dr. Alinda Samsuri	Metal and Alloys	98
ICSSST2019-141	The Role of Sr on Microstructure and Mechanical Properties of Al A356 Reinforced Al ₂ O ₃ Composite	Anne Zulfia	Metal and Alloys	99
ICSSST2019-180	Effect of Titanium and Aluminium Addition on Microstructure and Corrosion Behaviour of AISI 430 Ferritic Stainless Steel Welds	Nabil Bensaid	Metal and Alloys	99
ICSSST2019-181	Effect of Filler Metal Types on Microstructure and Mechanical Behavior of HSLA-X70/304L SS Dissimilar Welds	Mohamed Farid Benlamnour	Metal and Alloys	100
ICSSST2019-184	Mechanical Properties of Highly Deformed Sn-3.0Ag-0.5Cu Solder Wire	Dr. Norliza Ismail	Metal and Alloy	100
ICSSST2019-185	Synthesis and Characterization of Copper Selenide and Tin Selenide Powders by Mechanical Alloying Method	Loh Yen Nee	Metal and Alloy	101
ICSSST2019-087	Synthesis Optimization and Characterization of Chitosan-coated Magnetite Nanoparticles Extracted from Mill Scales Waste	Nur Asyikin Ahmad Nazri	Nanoscience and Nanotechnology	102
ICSSST2019-096	Effect of TEOS on the Synthesis of Silica-coated Iron Oxide Nanoparticles	Nurul Izza Taib	Nanoscience and Nanotechnology	103
ICSSST2019-106	Determination of Hygroscopic Growth and Water Activities of Continentals and Desert Aerosols	Muhammad Dahiru Audu	Nanoscience and Nanotechnology	103
ICSSST2019-149	Facile Synthesis and Characterizations of Silver Nanoparticle-Reduced Graphene Oxide Hybrid	Dr. Nurul Izrini Ikhsan	Nanoscience and Nanotechnology	104
ICSSST2019-154	DFT and Spectroscopic Study of a Zin-porphyrin Beta-substitution with Indene-dioxo Group for Potential Dye-sensitized Solar Cell (DSSCs) use	Dr. Alvie Lo Sin Voi Lo	Nanoscience and Nanotechnology	104
ICSSST2019-186	Comparative Study on Micronized and Nanosized <i>Carica Papaya</i> Seed Modified Pullulan as Biocoagulant in Wastewater Treatment	Deong Jing Lie	Nanoscience and Nanotechnology	105
ICSSST2019-025	Pt Coated Carbon Nanotubes for Optical Limiting Applications	Dr. Noor Aisyah Ahmad Shah	Optical and Dielectric Materials	106
ICSSST2019-008	Vibrational Spectroscopy Analysis of Oligomer Blend Film	Dr. Siti Zulaikha Nghah Demon	Organic Materials and Application	106
ICSSST2019-126	Corrosion Inhibition of Mild Steel by Electrodeposited Poly(M-Aminophenol) Coating	Sabrina M Yahaya	Organic Materials and Application	107
ICSSST2019-002	Fatigue Lifetime Prediction of Bamboo Laminated Composites	Prof. Dr. Aidy Ali	Polymers and Composites	107
ICSSST2019-088	Conversion of Bacterial Cellulose to Cellulose Nitrate with High Nitrogen Content as Propellant Ingredient	Dr. Siti Hasnawati Jamal	Polymers and Composites	108

List of Poster Presenter

Paper ID	Paper Title	Name	Sub-theme	Page
ICSSST2019-119	Effects of Ammonium Bromide on Methylcellulose Biopolymer Electrolytes in Optical and Electrical Studies	Dr. Nik Aziz Nik Ali	Polymers and Composites	108
ICSSST2019-157	Study of π - π Interaction and Covalent Bond of Hybridized Polypyrrole with Reduced Graphene Oxide Composites	Nur Atikah Md Jani	Polymers and Composites	109
ICSSST2019-152	Semiconductor Devices Lifetime Prediction Methodology for Hot Carrier Injection Tests	Yew Huang Lau	Semiconductors and Devices	110
ICSSST2019-047	Synthesis and Characterization of Low Density Bi-2223 Cuprates Superconductor Doped Eu_2O_3 Nanoparticles	Nurbaisyatul Ermiza Suhaimi	Superconductors	111
ICSSST2019-166	Enhanced Transport Critical Current Density of TI-1212 Bulk Superconductor Added with Nickel-Zinc Ferrite Nanoparticles	Assoc. Prof. Dr. Wei Kong	Superconductors	112
ICSSST2019-188	Assessment of Magnetic Property between Fe and Ni doped ZnO Nanoparticles Synthesized by Microwave Assisted Synthetic Method	Prof. Dr. Abdul Halim Shaari	Semiconductors and Devices	113

v

Biomaterials

ICSSST2019-001

Synthesis, Characterization, Antimicrobial Activity and in vitro Bioactivity of Chitosan Hydroxyapatite Composite Doped with Strontium

Ismaila Abdullahi

Chemistry Department, University of Abuja PMB 117, Abuja, FCT, Nigeria

Abstract. The objective of this work is to report the synthesis, characterization and in vitro response of a novel strontium doped chitosan-hydroxyapatite composite. For this reason hydroxyapatite (HA), strontium doped HA, chitosan-hydroxyapatite composite and the novel strontium doped chitosan-hydroxyapatite composite were synthesised via in situ co-precipitation method. The effects of strontium and chitosan incorporation on the structural properties of the samples were studied by X-ray diffraction (XRD), Fourier transformed infrared spectroscopy (FTIR), thermogravimetric analysis (TGA), differential thermal analysis (DTA), and energy dispersive X-ray spectroscopy (EDX). Bioactivity studies of the samples in simulated body fluid (SBF) and antimicrobial activity against E. coli were carried out. The incorporation of strontium and chitosan into the lattice of the HA influenced the crystallinity, crystallite size and lattice parameters of the HA. The chemical composition of the novel strontium doped chitosan-HA composite is found to have resemblance to that of bone mineral. The novel strontium doped chitosan-HA showed improved bioactivity in SBF over other samples. Field emission scanning electron microscopy (FESEM) images of the novel composite material also showed a good apatite forming ability. The novel composite material show substantial antimicrobial effect against the E. coli bacteria.

ICSSST2019-042

Preliminary Electrical Studies on Enzyme- Based BioSensor

Ainil Hawa Jasni

Centre of Chemical Defence, National Defence University of Malaysia, Kem Sungai Besi, 57000 Kuala Lumpur, Malaysia

Abstract. The integration of biomolecules such as enzymes with semiconductors to form sensing devices has been recently the subject of intense scientific research especially in volatile organic chemicals (VOCs), chemical warfare agent (CWA) and pesticides detection. The need of new sensors exhibiting a high selectivity and a total reliability in connection with smart systems and actuators for real time detection of lethal gaseous has driven wonderful development for pre-detection and post-detection technology. Problem statements: Currently, analytical techniques such as gas and liquid chromatography are being used due to its sensitivity and reliable. However it unable carried out infield, expensive and time consuming. Thus, the development of rapid, cost-effective, selective and able to used infield is critical. Enzymes based biosensor have potential application in biosensor due to it high substrate specificity and catalytic activity which provide rapid and effective hydrolysis process Objective: The preliminary development of a rapid, and highly selective biosensor using enzyme immobilized on functionalized carbon nanotubes (CNT) for the detection of leaving group from hydrolysis process. The electrochemical behavior and the optimization will be investigated using cyclic voltammetry measurement. Methodology: Amylase and Trypsin enzymes reaction with their specific substrates of glucose and milk protein characterization, functionalization with CNT and the immobilization of the nanocomposite on the screen-printed electrode (SPE) as well as sample characterization using field emission scanning electron microscopy (FESEM), Fourier Transform infrared spectroscopy (FTIR), full name (GC-MS) and full name (CHNOS) are reported. Conclusion: An excellent sensing performance of enzyme biosensor is achieved due to the synergistic effect of the individual components in the system. These features will offer an excellent biosensing platform for rapid, sensitive, selective detection and also to further develop the sensing mechanism behind the charge exchange between the environment, the active site vacancies and the nanoparticles.

ICSSST2019-164

Physical, Structural and Mechanical Properties of Glass Ionomer Cement Derived from Fluoroaluminosilicate Glass with Different Ageing Time

Mohammad Zulhasif Ahmad Khiri, Khamirul Amin Matori^a, Mohd Hafiz Mohd Zaid^b, Che Azuranim Che Abdullah^c, Norhazlin Zainuddin^d, Wan Nurshamimi Wan Jusoh^e, Rohaniah Abdul Jalil^f, Nadia Asyikin Abdul Rahman^g, Siti Aisyah Abdul Wahab^h

^akhamirul@upm.edu.my, ^bmhmzaid@gmail.com, ^cazuranim@upm.edu.my, ^dnorhazlin@upm.edu.my, ^emimieywanjusoh@gmail.com, ^fniajalil20@gmail.com, ^gnadiarahman84@gmail.com, ^haisyahwahab94@gmail.com

Material Synthesis and Characterization Laboratory, Institute of Advanced Technology, Universiti Putra Malaysia, 43400 UPM Serdang, Selangor, Malaysia.

Abstract. Glass Ionomer Cement (GIC) is produced from acid-base reaction between calcium fluoro-alumino-silicate (CFAS) glass powder and polyacrylic acid (PAA) with the presence of water. In this research, CFAS glass was derived from waste materials such as soda-lime-silica (SLS) glass and clamshell (CS) which are sources of silica and calcium oxide respectively. CFAS glass has been synthesized by using the conventional melt-quenching method. The different physical behaviour of CFAS glass was closely related to the CaF₂ content in the glass system. CFAS glass is commonly used in dental restoration due to fluoride ion leaching act as an antibacterial agent to fight oral caries. To study the influence of ageing time on physical, structural and mechanical properties of GIC, deionized water was used as a soaking medium. The ageing time of GIC was evaluated from 7 to 28 days. From the XRD result, some GIC was indicating amorphous structure was detected during ageing until 28 days. However, GIC shows the mechanical properties increase by ageing time through the compressive test. FTIR analysis shows this phenomenon occurs due to the deformation of Si-OH bonding and formation of Si-O-Si simultaneously in the presence of water. Thus, the observed results in this study promise the GIC derived from waste materials have a high potential in dental application due to excellence structural and mechanical properties against ageing.

Carbon and Related Materials

ICSSST2019-044

Evaluation of Superoleophilic-Hydrophobic Kapok Fiber as Effective Oil Sorbents

Normaisarah Yunos

Department of Physics, School of Fundamental Science, Universiti Malaysia Terengganu

maisarahyunos96@gmail.com

Abstract. Offshore oil spills can cause instant and lasting damage to aquatic life and wildlife around the shores, chemical toxicity to water security, ecological changes, food supply threats and consequently affecting tourism industry. Superhydrophobic and superoleophilic materials have been proven to be effective oil spill clean-up candidate. This work demonstrated the production of hydrophobic and superoleophilic low cost Kapok Aerogel (KA) carbonised from *Kapok*. The KAs show significant hydrophobic-superoleophilic features with water and oil contact angles of $> 90^\circ$ and $< 5^\circ$, respectively. The entangled assembly and nano-pores appeared on each fibers is the key reason the KAs exhibit hydrophobic and superoleophilic with max oil sorption capacity of 60 g oil/sorbent's weight (g). Moreover, the KAs retained approximately 100% of oil for one hours, suggesting the KAs are effective oil sorbents which are feasible to deploy on hectic waterway.

ICSSST2019-052

Oil Sorbents Derived from Carbonization of Disposable Baby DiapersJee Khan Lim^{1,a}, Oon Jew Lee^{1,b*} and Zainal Abidin Talib^{2,c}¹School of Fundamental Science, Universiti Malaysia Terengganu, 21030 Kuala Nerus, Terengganu, Malaysia²Department of Physics, Faculty of Science, Universiti Putra Malaysia, Serdang, 43400 Seri Kembangan, Selangor.^ajeekhanlim95@outlook.com, ^{b*}oonjew@umt.edu.my, ^czainalat@upm.edu.my

Abstract. With the massive need for fossil fuel energy in today's world, offshore and shorelines waters have been polluted by frequent oil spill due to the exploration, extraction and transportation of oil. Catastrophic effect of oil spill incident on the scale of Exxon Valdez and Deepwater Horizon has haunted the globes. This work presents an enticing method to expedite oil spills recovery which involves oil absorbents derived from the disposable baby diapers. The disposable baby diapers were carbonized to form water repelling oil absorbent with water and oil contact angles of 131° and 0°, respectively. These oil absorbents exhibited maximum oil sorption of 10.62 g_{gasoline oil}/g_{absorbent} as compared to non-biodegradable polypropylene with oil sorption capacity of 7 g_{gasoline oil}/g_{absorbent}. The polypropylene is the most commonly used oil absorbent for offshore oil spill cleaning due to the ease in mass production. They are capable of absorbing oil selectively from water and simultaneously the absorbed oil can be retrieved by compressing it. This work gives the disposable baby diapers a new life with the Waste to Wealth concept.

v

ICSSST2019-069

Synthesis of Graphene Oxide from Waste Tyre using Sodium Nitrate and Phosphoric Acid as Precursor in Hummer's MethodAin Zanaya Zanuri^{1,a}, Noor Najmi Bonnia^{1,b*} and Noor Asnida Asli^{2,c}¹School of Physics and Materials Science, Faculty of Applied Sciences, Universiti Teknologi MARA, 40450 Shah Alam, Selangor, Malaysia²NANO-SciTech Centre, Institute of Science, Universiti Teknologi MARA, 40450 Shah Alam, Selangor, Malaysia^aainzanaya@rocketmail.com, ^{b*}noornajmi@salam.uitm.edu.my, ^casnida1462@salam.uitm.edu.my

Abstract. Graphene oxide have been widely used in many industries and attract much interest among researchers due to its desirable properties. Top down and bottom up method can be used to synthesis graphene oxide. Recently, Hummer's method has become popular due to its simple top down synthesis but there is an issue due to the releasing of nitrate gaseous which harmful to environment. Thus, phosphoric acid has been used to replace sodium nitrate. Large waste of carbon tyre in landfills has led researcher to find various ways to overcome this problem. This research was carried out using waste carbon tyre as a carbon source to synthesis graphene oxide. Waste tyre is one of carbon rich material and can be easily found in the world with low cost. The obtained samples were investigated and analyzed using FESEM, EDX, XRD and RAMAN Spectroscopy. FESEM analysis shows a rough surface micrograph of graphene oxide with the elemental composition of carbon and oxygen were confirmed by EDX which are 83.91 % and 16.09 % respectively which indicate good composition of graphene oxide. XRD analysis shows broad peak of 2 theta which indicate that the sample is an amorphous. Raman analysis was confirmed that graphene oxide was successfully synthesized by showing peaks of D band and G band at 1354 cm⁻¹ and 1574 cm⁻¹ respectively. Lastly, the improved Hummer's method using phosphoric acid and using waste carbon tyre as carbon source was successfully synthesized yet have the same quality as graphene oxide that synthesis using convectional Hummer's method.

ICSSST2019-093

The Optimization of a-CN_x Thin Films and its Humidity Sensing Properties at Different Substrate Temperature by Radio Frequency-plasma Enhanced Chemical Vapor DepositionSiti Aisyah Abd Aziz^a and Rozidawati Awang^{b*}

Pusat Pengajian Fizik Gunaan, Fakulti Sains dan Teknologi, Universiti Kebangsaan Malaysia 43600 UKM Bangi, Selangor Darul Ehsan, Malaysia

^asitiaisyahabdaziz@gmail.com, ^{b*}rozida@ukm.edu.my

Abstract. An amorphous carbon nitride (a-CN_x) thin film has been widely investigated for its use in humidity sensor applications. In this work, a-CN_x thin films were deposited on quartz substrates by varying substrate temperature using radio-frequency plasma enhanced chemical vapour deposition (RF-PECVD). These films were prepared using a mixture of acetylene (C₂H₂) at 20 sccm and nitrogen (N₂) gases at 50 sccm. The bonding properties and film disorder were investigated using FTIR and Raman spectroscopy. The FTIR analysis exhibited that a-CN_x thin films resulted the formation of double (C=N) and triple (C≡N) bonds. The highest intensity ratio of the D and G peaks, (I_D/I_G) ratio and the decrease in sp² cluster size for films deposited at 100°C show highest disorder phase in the film graphite and the sp² hybridization size. This result show nitrogen induces carbon to form sp² graphitic clusters. The a-CN_x thin films morphology were characterized by field emission scanning electron microscopy (FESEM). FESEM image indicates that the a-CN_x thin film surface exhibit cauliflower-like structure morphology with a grain size of ~ 10 nm. The a-CN_x thin films show good sensor properties such as good repeatability and fast response to humidity changes. The a-CN_x thin films with optimum substrate temperature were deposited at 100°C. The sample at this optimum condition clearly indicates the presence of high C-C/C=C/C-H, C=N, C≡N, N-sp³C (N-C) and N-sp²C (N=C) bonds from the XPS spectrum. In conclusion, the high content of C-N, C=C, C=N, C≡N, C-H and N-H bonds in a-CN_x film deposited using acetylene gas are then major factors affecting the electrical properties of the a-CN_x thin film and also increases the sensitivity of the a-CN_x thin film to humidity. Particularly, at an optimum substrate temperature of 100°C, the sensor exhibits high sensitivity, fast response (23 s) and short recovery time (19 s) as compared to the a-CN_x sample in the previous study with an increase of 40%. The hydrophobic nature of the a-CN_x thin film makes it highly appropriate to be used in the humidity sensors. The results of the study can then be a reference to other researchers to explore the electrical properties of a-CN_x thin-film for application as an electronic device as well as a sensor application that can be used by the community in the future.

ICSSST2019-131

Ni Catalytic Effects on the Growth of PECVD and HF-PECVD Transfer-free GrapheneMaisara Othman^{1,a}, Richard Ritikos^{2,b*} and Saadah Abdul Rahman^{2,c}¹New Energy Science & Engineering, Xiamen University, 43900, Sepang, Selangor, Malaysia²Low Dimensional Materials Research Centre, Department of Physics, University of Malaya, 50603, Kuala Lumpur, Malaysia^amysaraothman@gmail.com, ^{b*}richardr@um.edu.my, ^csaadah.abdulrahman@gmail.com

Abstract. Transfer-free graphene were synthesized via PECVD and HF-PECVD using Ni catalyst at relatively low temperature. The Ni layer was used as a catalyst to assist the formation of graphene at the Ni-substrate interface. Prior to the deposition of graphene, a thin Ni film was deposited onto the SiO₂ substrate using the sputtering technique. The increase in temperature from the radiant heat of the filament using HF-PECVD changed the Ni grains from nano-sized to micro-sized and reduced the formation of Ni grains boundaries. Instead of additional process of Ni annealing, the direct thermal heat effect promoted the formation of a less defective graphene with a more ordered structure, which could be achieved by larger Ni grain size and grains boundaries. This resulted in the formation of better quality of graphene as compared to graphene grown from PECVD system alone due to better catalytic effects during graphene deposition. The resulting transfer-free graphene films were investigated for their structural, chemical bonding and morphology.

ICSSST2019-140

Effect of Prekotac as Filter Aids on Pressure Drop and Particle Penetration in Pilot Plant Fabric Filtration SystemA.Nurnadia^{1,3,a*}, M.Rashid^{1,b}, S.Hajar^{1,c}, M.R. Ammar² and J. NorRuwaida¹¹Malaysia-Japan International Institute of Technology, 54100 UTM Kuala Lumpur, Malaysia²AMR Environmental Sdn Bhd, Johor Bahru, Malaysia ammar_amrgroup@yahoo.com.my³Pusat Pentropikalan, Universiti Pertahanan Nasional Malaysia, 57000, Kem Sungai Besi, Malaysia^{a*}nurnadia@upnm.edu.my, ^brashidyusof.kl@utm.my, ^chajarahim@hotmail.com

Abstract. Filter aids is used in air filtration system to fulfil the needs to extend the life span of filter media in fabric filtration system. In this study, the effect of a filter aids performance known as PrekotAC on pressure drop and particle penetration in a filtration system with varying filtration velocities of 1 to 3 m/min was evaluated. The PrekotAC is a admixture of PrekotTM and activated carbon mixed in different weight compositions. Result showed that the pressure drop across the fabric media decreases with the addition of PrekotTM in the PrekotAC admixture due to its wide range of non-uniform particle size distribution that gives higher porosity of filter cake during filtration process. The finding also showed that the total particle penetration through the fabric media was proportionally related to addition of PrekotTM in the PrekotAC admixture under a constant material loading. The study suggests that the addition of PrekotTM in the formulation of filter aids significantly affect both pressure drop and particle penetration of the fabric filter media.

ICSSST2019-171

Graphene Exfoliation and Its Stability in Microcrystalline Cellulose SolutionAmirul Hadi Bin Azmi^a, Shaharin Fadzli Bin Abd Rahman^b

Universiti Teknologi Malaysia, Malaysia

^aahadi67@graduate.utm.my, ^bshaharinfadzli@utm.my

Abstract. Graphene has drawn a lot of attention as a promising material for a conductive ink due to its high electrical conductivity and abundant source. Selection of solvent for ink formulation is crucial to obtain the desired result. For instance, graphene may be efficiently exfoliated and stabilized in certain solvent. Cyrene and NMP are two examples of high performance solvent which can produce high conduction and sufficient stability. In this work, cellulose solution is investigated as alternative solvent for conductive ink formulation. Although the viability of the cellulose solution was already presented in other works, further thorough a systematic study is highly required. Cellulose solution was prepared using microcrystalline cellulose and sodium hydroxide aqueous solution. Graphite was expanded under 800W microwave for 40s. The expanded graphite with a concentration of 4 mg/ml was added into the cellulose solution. The ratio of graphene to cellulose was 20:1. The mixture was exfoliated inside ultrasonic bath for 8 to 20 hours. The exfoliation can be observed within 30 minutes as the solution turned to black. The stability of the prepared ink was recorded for 24 hours under room temperature. To measure the conductivity of the ink, graphene thin film was formed by drop-casting 20 microliters on four different types of paper substrates. Sheet resistance was measured using 4 point probe configuration. Based on the obtained result, cellulose solution seems to be suitable for graphene exfoliation process. However, the ink stability needs to be improved for practical applications of conductive ink.

ICSSST2019-182

CO₂ Gas Sensor Based on Polyaniline/ Cu-ZnS Hollow Microsphere CompositeZubair Ahmad¹, Jolly Bhadra¹, Shoaib Mallick², Hemalatha Parangusan¹ and Noora Al-Thani¹¹Centre for Advanced Materials (CAM), Qatar University, P.O. Box 2713 Doha, Qatar.²Department of Electrical Engineering, College of Engineering, Qatar University, P.O. Box 2713 Doha, Qatar.

Abstract. In this work, we have investigated the Polyaniline/Cu-ZnS composites for the fabrication of CO₂ gas sensor applications. PANI coated Cu-ZnS hollow microsphere structures have been synthesized by the hydrothermal method and in-situ polymerization process. The spin coating technique has been used to deposit the composite film on the ITO glass electrode. The structural, thermal stability and surface morphology of the PANI/Cu-ZnS composites were investigated by X-ray diffraction analysis (XRD), Thermal gravimetric analysis (TGA), Field emission electron microscopy (FESEM) and Atomic force microscopy (AFM). The XRD patterns indicate that PANI and Cu-ZnS have been successfully synthesized by in situ-polymerization method. It has been observed that PANI/Cu-ZnS composite has higher thermal stability as compared to the pure PANI. The morphology of the film indicates that uniform porous and rough structure developed at the surface of the composite film. PANI/Cu-ZnS composite based gas sensors exhibit high thermal stability, repeatable and stable response as compared to the pure PANI. The response and recovery times of the PANI/ 1wt% Cu-ZnS have been found to be 35s and 55s, respectively.

v

Ceramics and Glasses

ICSSST2019-006

Effect of Samarium Oxide on Structural and Optical Properties of Zinc Silicate Glass Ceramics from Waste Material

Auwalu Inusa Abubakar

Department of Physics, Faculty of Science, Kano University of Science and Technology, Wudil, P.M.B.3244
Kano-Nigeria

Abstract. This work indicates the synthesis of samarium doped zinc silicate (willemite) glass ceramics with different weight concentrations. Solid-state reaction technique was used to make up the samples, with waste rice husks as silicate source. The measurement of X-ray diffraction revealed sharp and broad diffraction peaks. Besides, the Field emission scanning electron microscope exhibited the poly grains morphology of the crystalline samples. Consequently, samarium strips were growing in size as the weight percent of dopant was increased. While Fourier transforms infrared spectra, showed slight variation peaks with diverse dopant concentrations. Then the energy band gaps of samarium doped willemite glass ceramics were reduced with the increment of samarium dopant concentrations. The photoluminescence measurement exhibited the red emission which agreed to the $4G5/2 \rightarrow 6H11/6$ (646.71 nm) under the blue excitation.

ICSSST2019-011

Preparation of Alumina-Based Ceramics Foam with Corn Starch as Pore Former

Hamimah binti Abd.Rahman and Wan Muhammad Syahmi bin Wan Azhan

Faculty of Mechanical & Manufacturing Engineering, Universiti Tun Hussein Onn Malaysia

Abstract. Ceramic foams have mechanical strength and thermal stabilities higher than the commonly employed polymeric foams. In this study, ceramic foams is produced using starch consolidation casting method. This research focuses on the preparation of alumina-based ceramic foam by using corn starch as a pore-forming agent. Other materials such as silica and polyethylene glycol (PEG) are used as an additive and a dispersing agent respectively. The mixture of the suspension compositions used are 64-58 wt% of alumina, 55 wt% of deionized water, 1 wt% of polyethylene glycol and 1 wt% of silica to increase the strength of the ceramic foam. Corn starch is added in the amount of 4, 6, 8 and 10 wt%. Then, the sample is preheated at 70 °C in 90 minutes for gelation and coagulation process. After that, the samples were dried at 110 °C. The process was followed by sintering at 1250 °C for 2 hours. The obtained flexural strength is between 0.594 MPa to 1.996 MPa. For the compressive strength test, the value attained was between 0.026 N/mm² to 0.244 N/mm². Meanwhile, the average of total porosity ranges from 54.05% to 70.70%. In conclusion, the preparation of alumina-based ceramic foam using corn as a pore former was successfully demonstrated through a starch consolidation casting method. From this study, the suitable amount of corn starch in alumina foam is 4 wt% as the obtained values of porosity, flexural and compressive strength is appropriate for ceramic foams.

v

ICSSST2019-013

FTIR and Optical Properties of Samarium Doped Zinc Borotellurite Glasses

Siti Nasuha Binti Mohd Rafien, Dr Azman B. Kassim, Prof. Dr Azhan B. Hashim, Dr Wan Aizuddin B. Wan Razali And Miss Norihan Yahya

Univeristi Teknologi Malaysia

Abstract. Zinc borotellurite glasses doped with Sm³⁺ ions of the system (70-x)TeO₂-20B₂O₃-10ZnO-xSm₂O₃ where x varies from 0.0 to 2.5 mol % were prepared by a melt-quenching technique. The studies on structural and optical characterization of Sm³⁺ ions have been carried out through Fourier transform infrared spectroscopy (FTIR), absorption spectra, optical band gap, E_{opt} and Urbach energy, ΔE. From the FTIR analysis, the presence of BO₃, BO₄, TeO₃, TeO₄ and B – O - structural units in the prepared glasses were identified. Three strong absorption peaks in the ultraviolet and visible regions were observed and resolved from absorption spectra due to transition between the ground state and various excited state of Sm³⁺ ions. The value of optical band gap, E_{opt} lies between 2.605 eV to 2.982 eV for the direct transition and 2.768 eV to 3.198 eV for the indirect transition respectively. Meanwhile, the Urbach energy, ΔE was observed in the range of 0.112 eV to 0.694 eV respectively. Some other results will be analysed and discussed in details.

ICSSST2019-014

Optical Properties of Silica Borotellurite Glass Doped with Samarium (iii) OxideNurul Asyikin Binti Ahmad Sukri, Halimah Mohamed Kamari^a, Amirah Abdul Latif^b

Department of Physics, Faculty of Science, Universiti Putra Malaysia, 43400 UPM Serdang, Selangor, Malaysia

^ahalimahmk@upm.edu.my, ^bamirahlatif@upm.edu.my

Abstract. Rice husk is a by-product from a rice milling industry that usually being disposed through open burning. This process would release carbon dioxide into the atmosphere and give a negative impact to the environment. Therefore, a waste to wealth technology has been introduced to fully utilize the waste rice husk by extracting the valuable element which is silica. The waste rice husk that is rich in silica content was used as a substitute for silica and was included in the glass composition. A series of silica borotellurite glass doped with samarium (III) oxide were successfully synthesized by using melt-quenching method. The chemical composition of the prepared glasses is as follow; $\{[(\text{TeO}_2) 0.7 (\text{B}_2\text{O}_3) 0.3]0.8 [\text{SiO}_2] 0.2\}1-x \{\text{Sm}_2\text{O}_3\} x$, where $x=0.01, 0.02, 0.03, 0.04$ and 0.05 molar fraction. In this research, the influence of Sm_2O_3 on the structural, physical and optical properties of glasses has been studied using different characterization tools. The amorphous nature of the glass samples was proven by XRD pattern. The vibration mode of silica, borate and tellurite group were detected by FTIR spectra. Meanwhile, the density of the glass samples increased with the addition of more Sm_2O_3 into the glass system. The optical properties have been investigated by using UV-Vis spectroscopy in the range of 300-2000 nm at room temperature. The values for optical band gap, refractive index and Urbach energy were obtained from the absorption spectra. The direct and indirect optical band gap have values in the range of 1.848 to 1.930 eV and 1.951 to 1.995 eV respectively. The refractive index and Urbach energy values show an increment from 0.01 to 0.02 molar fraction, however the values show a decreasing pattern with increasing concentration of Sm_2O_3 .

ICSSST2019-016

Structural and Electrical Properties of $\text{La}_{0.7}\text{Ca}_{0.3}\text{MnO}_3 / \alpha\text{-Fe}_2\text{O}_3$ CompositesLau Lik Nguong, K.P. Lim^a, A.N. Ishak^b, M.M. Awang Kechik^c, S.K. Chen^d, N.B. Ibrahim^e, S.A. Halim^f, Eijin Lim^g

Superconductor and Thin Film Laboratory, Department of Physics, Faculty of Science, Universiti Putra Malaysia, 43400 UPM Serdang, Selangor Darul Ehsan, Malaysia.

^alimkp@upm.edu.my, ^bamirahnatasha.ir@gmail.com, ^cmmak@upm.edu.my, ^dchensk@upm.edu.my, ^ebaayah@ukm.edu.my, ^fahalim@upm.edu.my, ^gforget03282@gmail.com

Abstract. Colossal magnetoresistive (CMR) materials have huge potential in modern application and it has been widely used in magnetic sensing industry. From the previous studies, an incorporation of secondary insulating phase into mixed-valence manganites could improve its extrinsic effect especially low-field magnetoresistance (LFMR). In this work, the structural and electrical properties of $\text{La}_{0.7}\text{Ca}_{0.3}\text{MnO}_3$ (LCMO) were investigated by adding the $\alpha\text{-Fe}_2\text{O}_3$ nanoparticle with ratio of 0, 0.05, 0.10, 0.15 and 0.20 as the artificial grain boundaries. The LCMO compound has been synthesized using sol-gel route. The samples were sintered at 800 °C to obtain the LCMO phase by referring to the thermogravimetric analysis (TGA). The structural properties were investigated by an X-ray diffractometer (XRD) while electrical properties were measured by a four point probe (4PP) system. XRD patterns show the coexistence of two phases (LCMO & $\alpha\text{-Fe}_2\text{O}_3$). LCMO is having orthorhombic structure with space group Pnma while $\alpha\text{-Fe}_2\text{O}_3$ is in hexagonal form with space group R-3c. As the content of $\alpha\text{-Fe}_2\text{O}_3$ increases, the resistivity of the samples increase drastically. However, the addition of iron oxide has no significant effect on the metal-insulator transition temperature (T_{MI}). From the XRD and 4PP analysis, it can be deduced that the $\alpha\text{-Fe}_2\text{O}_3$ nanoparticle does not react with LCMO compound and successfully formed the $\text{La}_{0.7}\text{Ca}_{0.3}\text{MnO}_3 / \alpha\text{-Fe}_2\text{O}_3$ composites.

ICSSST2019-017

Effect of TiO₂ Concentration on the Structural and Electrical Properties of Nd_{0.67}Sr_{0.33}MnO₃ CompositesLim Kean Pah, L.N. Lau^a, A.N. Ishak^b, M.M. Awang Kechik^c, S.K. Chen^d, S.A. Halim^e, W.T. Chong^f

Superconductor and Thin Film Laboratory, Department of Physics, Faculty of Science, Universiti Putra Malaysia, 43400 UPM Serdang, Selangor Darul Ehsan, Malaysia.

^alau7798@gmail.com, ^bamirahnatasha.ir@gmail.com, ^cmmak@upm.edu.my, ^dchensk@upm.edu.my, ^eahalim@upm.edu.my, ^fchristy0207_9@hotmail.com

Abstract. In this work, (1-x) (Nd_{0.67}Sr_{0.33}MnO₃): x (TiO₂) composites with x = 0, 0.1, 0.2, 0.3 and 0.4 have been prepared to investigate the structural and electrical properties. Nd_{0.67}Sr_{0.33}MnO₃ (NSMO) was synthesised via the solid-state reaction method before incorporated with TiO₂. The addition of TiO₂ as the secondary phase in manganite composite would favour the spin-polarized tunnelling near to the grain boundary and thus enhance the extrinsic magnetoresistance. The effect of the TiO₂ nanoparticle addition into NSMO composites has been examined by an X-ray diffractometer (XRD) and a four-point probe (4PP) system. From the thermogravimetric analysis (TGA), NSMO phase formation occurred in between 750 – 980 °C. XRD patterns show that there is no peak shift when the TiO₂ concentration increases. It can be deduced that TiO₂ was segregated at the NSMO grain boundary region and its grain surface. However, a small amount of Ti atoms are expected to replace the Mn atoms in NSMO crystal system and causing the increase in crystallite size. The electrical study shows that the presence of TiO₂ has weakened the double exchange (DE) mechanism in conducting ferromagnetic region and suppressed the metal-insulator transition temperature (T_{MI}). Besides, the insulating behaviour of TiO₂ has also caused the resistivity of composites to increase drastically.

ICSSST2019-019

Effect of Holmium Oxide on Optical Performance of Borotellurite Glass

Azlan M.N

Jabatan Fizik, Fakulti Sains dan Matematik, Universiti Pendidikan Sultan Idris, 35900, Tanjung Malim, Perak, Malaysia

Abstract. Borotellurite glass had been widely applied in the field of optical communications and devices. In this work, holmium oxide doped borotellurite glass had been fabricated by using melt-quenched technique. The structural properties of holmium oxide doped tellurite glass were found using fourier transform infrared studies and x-ray diffraction method. The results show that the inclusion of holmium oxide in borotellurite glass network leads to the formation of non-bridging oxygen (NBO) which indicates the long range of disorderness. The optical parameters of the glass system are determined by using UV-Vis spectrophotometers. The value of refractive index is enhanced with an increase of holmium oxide concentration, meanwhile, the optical band gap energy was decreased. The Urbach energy value shows that the glass system tends to be more fragile with increasing amount of holmium oxide.

ICSSST2019-022

Structural and Electrical Properties of Nd-Sr-Mn-O/CuO by Solid-state Reaction MethodAmirah Natasha Ishak, K.P. Lim^a, L.N. Lau^b, M.M. Awang Kechik^c, S.K. Chen^d, S.A. Halim^e, Y.X. Tneh^f

Superconductor and Thin Film Laboratory, Department of Physics, Faculty of Science, Universiti Putra Malaysia, 43400 UPM Serdang, Selangor Darul Ehsan, Malaysia.

^alimkp@upm.edu.my, ^blau7798@gmail.com, ^cmmak@upm.edu.my, ^dchensk@upm.edu.my, ^eahalim@upm.edu.my, ^fjsee-14@outlook.com

Abstract. Colossal magnetoresistive (CMR) effect in perovskite manganites has been taken a lot of interests among researches especially in thin films and its potential application in magnetic sensing industrial for the past few years. In this research, $(1-x)\text{Nd}_{0.67}\text{Sr}_{0.33}\text{MnO}_3$ samples were prepared by adding $x\text{CuO}$ where $x = 0.00, 0.05, 0.10, 0.15$ and 0.20 as the artificial barrier layer. Based on the previous research, it was proven that artificial barrier layer could enhance the extrinsic effect especially low-field magnetoresistance (LFMR). The $(1-x)\text{Nd}_{0.67}\text{Sr}_{0.33}\text{MnO}_3/x\text{CuO}$ composites were prepared using solid state reaction method. From the Thermogravimetric Analysis (TGA), NSMO phase was formed. Based on X-ray Diffraction (XRD) characterization, NSMO and CuO phases coexisted in the compound and did not react with each other. CuO acted as the artificial barrier layer and distributed on the surface of NSMO grains. Next, the electrical properties of the composites are measured using Four Point Probes (4PP) where the T_{MI} decreased as the CuO composition increased due to the double exchange (DE) mechanism that has been enhanced. CuO also acted as the insulating phase which caused the resistivity to increase. In conclusion, DE mechanism was dominant below T_{MI} value while Jahn-Teller (J-T) distortion took place above T_{MI} value which caused the resistivity to decrease as the temperature increased.

ICSSST2019-031

The Forming and Non-Forming Phases of LaZrTa₃O₁₁ Analogues

Fadhline Che Ros

Universiti Pertahanan Nasional Malaysia

Abstract. The synthesis of new ceramic oxides with structures based on stacking of $\alpha\text{-U}_3\text{O}_8$ type layers have shown that various rare earth cations can be accommodated at the A-site of $\text{A}_x\text{M}_{3n+1}\text{O}_{8n+3}$ ($n = 1, 2$). Attempts to investigate the possible substitution for A-site with a series of lanthanides and B-site with d^0 cation have led to the formation of eight (8) new phases which were prepared using solid state reactions and heated for different times at different temperatures of $1200 - 1500^\circ\text{C}$. The new phases are LaHfTa, LaHfNb, PrHfTa, NdHfTa, NdHfNb, NdZrNb, SmHfTa and GdHfTa which were indexed on a hexagonal space group $P6_322$ with the unit cell parameters and unit cell volume decrease with decreasing size of rare earth cation. Attempts to prepare another twelve (12) new phases were unsuccessful. Details of attained and unattainable LaZrTa₃O₁₁ analogues with different temperatures are included in this paper.

ICSSST2019-032

Fabrication of Silica (SiO₂) as-derived from Rice Husk Ash Foam via Polymeric Replication MethodR. Muda^a, H.A.Rahman^b, M.A.A. Azmi^c, S. Ahmad^d, S. Mahzan^e, H. Taib^f

Universiti Tun Hussein Onn Malaysia

^afirrizahaiza@gmail.com, ^bhamimah@uthm.edu.my, ^cazham@uthm.edu.my, ^dsufizar@uthm.edu.my, ^esharudin@uthm.edu.my, ^fhariati@uthm.edu.my

Abstract. Silica (SiO₂) foams have been widely applied in numerous fields, namely filters and catalysts supports, due to their characteristics of high permeability, high porosity and specific surface area. In this study, foams of as-derived from rice husk ash (RHA) was fabricated via polymeric sponge replication method. Polymeric foam initially was used as template and dipped into the SiO₂ slurry followed by drying and sintering to yield a replica of the original polymeric foam. Different solid loadings of SiO₂ as-derived from RHA (20 to 35 wt%) and sintering temperature of 1150°C were applied. Phase identification of the green and sintered foams were conducted using x-ray diffraction (XRD) analyses. Morphological observations were performed using scanning electron microscopy (SEM). Density and porosity of the SiO₂ foams were characterized using Archimedes method and compressive strengths were determined as per ASTM C773-88 (1999). It was found that the density of SiO₂ foams fabricated was in the range of 0.614 to 0.989 g/cm³, whereas the porosity values was in the range of 70% to 82%. Compressive strengths were found to increase from 0.05 to 0.30 MPa respectively, with the increased SiO₂ solid loading. Excellent properties of the SiO₂ foams definitely signifies that the polymeric replication method is indeed a promising technique for the SiO₂ foam fabrication.

ICSSST2019-039

Comparative Spectroscopic Studies on Luminescence Performance of Er³⁺ Doped Tellurite Glass Embedded with Nanoparticles at 0.55 μm EmissionS.N.S.Yaacob^a, M.R.Sahar^b, E.S.Sazali^c, P. Anigrahawati^d, N.A.M.Adnan^e, S.K.Md.Zain^f, Siti Maisarah Aziz^g
Advanced Optical Material Research Group, Department of Physics, Faculty of Science, Universiti Teknologi Malaysia, 81310 UTM Skudai, Johor Bahru, Johor, Malaysia^asyariffahnurathirah1593@gmail.com, ^bmrahim057@gmail.com, ^cezzasyuhada@utm.my, ^dnziluv18@gmail.com, ^eainaadnan2@gmail.com, ^fejakelly92@gmail.com, ^gsitimaisarahaziz@yahoo.com

Abstract. The spectroscopic performance of Er³⁺ doped glass at 0.55 μm emission contain different NPs have been comparatively evaluated. Glass containing 1.0 mol % of Er³⁺ doped with different NPs (Ag, Co and Fe) have been prepared using melt quenching technique. This paper discussed the influence of Ag, Co and Fe on the absorption and emission performance. X-Ray diffraction analysis reveals the all the prepared samples are amorphous. The UV-Vis absorption spectra of all the glasses shows several prominent peaks at 525 nm, 660 nm, 801nm, 982 nm and 959 nm due to transition from ground state ⁴I_{15/2} to different excited state such as ²H_{11/2}, ⁴F_{9/2}, ⁴I_{9/2}, ⁴I_{11/2}, and ⁴I_{13/2}. The emission of Er³⁺ at 0.55 μm for glass contain Ag NP shows significant enhancement about 3 folds up to 0.6 mol%. Meanwhile, the emission of Er³⁺ at 0.55 μm contain Fe NPs and Co NPs intensely quench due to the energy transfer from Er³⁺ ion to NPs and magnetic contributions.

ICSSST2019-043

Chemical and Mineralogical Characterization of Electric Arc Furnace (EAF) Steel Slag Waste: The Potential Green Resource for Geopolymer Ceramic ProductionPao Ter Teo, Nurulakmal Mohd Sharif^a, Anasyida Abu Seman^b, Julie Juliewatty Mohamed^c, Mahani Yusoff^d, Abdul Hafidz Yusoff^e

Advanced Materials Research Cluster, Faculty of Bioengineering and Technology, Universiti Malaysia Kelantan, Jeli Campus, Locked Bag 100, 17600 Jeli, Kelantan, Malaysia

^asrnurul@usm.my, ^banasyida@usm.my, ^cjuliewatty.m@umk.edu.my, ^dmahani@umk.edu.my, ^ehafidz.y@umk.edu.my

Abstract. Development of green ceramic tile from EAF steel slag waste receives wide attention from global material scientists. A ceramic tile is considered "GREEN" if it is made from industrial wastes, non-hazardous, recyclable and energy efficiency (embodied energy and carbon footprint). However, current conventional high temperature (1150°C to 1180°C) firing process of the ceramic tile incorporated with EAF slag is reported to merely meet criteria of industrial waste, non-hazardous and recyclable, without achieving the energy efficiency requirement. In addition, the high temperature firing causes drawbacks such as over-firing, surface defects and high closed porosity of the tile due to vigorous and hardly controlled fluxing action by the EAF slag. It is therefore, desirable to propose greener geopolymerization route to reduce energy inefficiency, as well as to minimize defects and improve final properties (lower water absorption and porosity, and higher modulus of rupture, MOR) of the ceramic tile incorporated with EAF slag. Prior to the geopolymerization, it is essential to characterize the EAF slag in terms of chemical composition, functional groups and mineral phases present to evaluate its suitability for the geopolymerization. Initially, the lump form of EAF slag was crushed into powder before the characterization tests. From X-ray fluorescence (XRF) chemical composition analysis, the slag mainly consisted of oxides such as Al₂O₃, CaO, MgO, SiO₂, FeO. Additionally, X-ray diffraction (XRD) analysis have revealed that CaO based minerals such as larnite (2CaO.SiO₂) and gehlenite (Al₂O₃.2CaO.SiO₂) were the major mineral phases in the slag while wustite (FeO) and magnetite (Fe₃O₄) were present as the minor mineral phases in the slag. More importantly, Fourier Transform Infrared Spectroscopy (FTIR) chemical analysis found that the slag consists of functional groups such as silico-aluminate (-Si-O-Al-O-) and ferro-silico-aluminate (-Fe-O-Si-O-Al-O-). Therefore, it is anticipated that the functional groups of slag will chemically react with typical functional group of clay (silico-oxide: -Si-O-Si-O) under alkaline medium (Na⁺ or K⁺) and forming amorphous polymeric 3-D network of geopolymer ceramic.

ICSSST2019-060

Elastic Properties of (80-x)B₂O₃-xTeO₂-10Li₂O-10Al₂O₃ Mixed Network Former Glass SystemNurul Ain Mohd Samsudin^{1,a}, Rosdiyana Hasham @ Hisam^{2,b*}, Ahmad Kamal Hayati Yahya^{3,c}¹School of Physics and Material Studies, Universiti Teknologi MARA, 40450 Shah Alam, Selangor, Malaysia²School of Physics and Material Studies, Universiti Teknologi MARA, 40450 Shah Alam, Selangor, Malaysia³School of Physics and Material Studies, Universiti Teknologi MARA, 40450 Shah Alam, Selangor, Malaysia^anurulain27.na@gmail.com, ^{b*}rosdiyana@salam.uitm.edu.my, ^cahmad191@salam.uitm.edu.my

Abstract. Mixed glass former (80-x)B₂O₃-xTeO₂-10Li₂O-10Al₂O₃ (x = 10 mol% to 60 mol%) glasses were prepared by melt-quenching technique to investigate the effects of mixing two glass formers on the elastic properties of the glass system. FTIR results revealed presence of BO₄, BO₃, TeO₄, TeO₃, and AlO₄ functional groups whereby beyond x = 40 mol% the only functional group that present are TeO₃, BO₃ and BO₄ units. Although at high TeO₂, N₄ (fraction of the four coordinated boron atoms) values seems to increase except at x = 20 mol% where a minimum was observed and at x = 40 mol% a drop in N₄ occurred. A less prominent decrease in N₄ values at x = 40 mol% occurred instead of a larger decrease which suggested to be due to a considerably high concentration of BO₄ units together with the presence of large NBOs concentration. Independent longitudinal (CL) modulus, shear (μ) modulus and related elastic modulus also exhibited non-linear behaviors whereby their values decreased to a minimum at x = 40 mol% due to the increase in NBO via TeO₃ and BO₃ units formation leading to less densely packed structure which deteriorates the rigidity of the glass. However, FTIR for the same glass system did not indicate a maximum increase in NBO formation in this region. Thus, this factor did not seem to be the only contribution to the elastic anomaly behavior in the region. Instead, MGFE phenomena is suggested to be the dominant factor for the minimum in elastic modulus in the region. Meanwhile, quantitative analysis of ultrasonic data using bulk compression model showed increased in K_b/K_e ratio at x ≤ 40 mol% which indicates decreased isotropic compression, whereas the decrease at x > 40 mol% demonstrated increased isotropic compression because reduction in ring deformation or bending. Meanwhile, the increase in average ring size l also followed the K_b/K_e behavior, thereby indicating the increase of ring deformation.

ICSSST2019-075

BiFeO₃ assisted with Different Weight Ratio of Polymer Chitosan: Structural, Optical and Photocatalytic Properties

Muhammad Safwan Bin Sazali, Dr. Muhamad Kamil Bin Yaakob, Dr. Mohamad Hafiz Bin Mamat, Prof. Madya. Dr. Oskar Hasdinor Hassan, Prof. Dr. Muhd Zu Azhan Bin Yahya

School of Physics and Materials Studies, Universiti Teknologi MARA 40450 Shah Alam, Selangor, Malaysia

Abstract. In this research work, different weight ratio (0.00g, 0.24g, 0.36g and 0.48g) of BiFeO₃ assist with Chitosan samples were prepared by hydrothermal method at 200°C for 6 hours. Potassium Hydroxide (KOH) was used as a mineralizer during the synthetization for the precipitation. The characterization of the samples was further analyzed in different properties such as structural, optical and photocatalytic. The result from the experiment shows that BiFeO₃ assist with Chitosan shows significant improvement in optical band gap where the obtained results show an increasing band gap. As for the structural properties, the size of the particles decreasing as the weight ratio of Chitosan increase where Chitosan will prevent the particles from agglomerates and this influence the photocatalytic properties where the efficiency is rapidly increasing.

ICSSST2019-102

Photoluminescence and Spectroscopic Properties of Erbium Doped Bio-Silica Borotellurite Glasses Containing Silver OxideHamza A. M^{1,2}., Halimah M. K¹., Muhammad F.D¹., Chan K.T¹.¹Glass and Dielectric Lab, Physics Department, Faculty of Science, Universiti Putra Malaysia.²National Agency for Science and Engineering Infrastructure, Idu, Abuja, Nigeria.^aelhamabdul2@yahoo.com, ^bhalimahmk@upm.edu.my, ^cfarahdiana@upm.edu.my, ^dchnkt@upm.edu.my

Abstract. In this paper, structural and spectroscopic properties of Er³⁺ doped bio-silica borotellurite [((TeO₂)_{0.8} (B₂O₃)_{0.2})_{0.8} (SiO₂)_{0.2}]_{0.99} (Ag₂O)_{0.01}]_{1-y} (Er₂O₃)_y where y = 0.01, 0.02, 0.03, 0.04 and 0.05 glasses were studied. The structural study was conducted using X-ray diffraction (XRD) and Fourier transform infrared (FTIR). Ultra violet visible (UV-Vis) spectrometer was used to measure the absorption spectrum and was analysed using Judd-Ofelt (J-O) and McCumber theory. Important parameters such as radiative lifetime, branching ratio, transition probability, gain band width and figure of merit are also determined from the analysis. The photoluminescence result showed that the optimum dopant concentration was achieved at 0.03 molar fraction. The gain band width and figure of merit are used to evaluate the future application of the glass in optical amplification and solid state laser.

v

ICSSST2019-104

The Effects of Tungsten Carbide WC-Co Thermal Spray Coating on Mechanical Properties of Carbon Steel

Mohamad Ariff Bin Moh Halmi, Ricardo Seta Anak Ripin, Mohd Azhar Bin Harimon

Universiti Tun Hussein Onn Malaysia

Abstract. Tungsten carbide cobalt (WC-Co) is a combination between a hard-ceramic phase tungsten carbide alloy (WC) and ductile metallic phase cobalt (Co). Both of these combinations are the main contributors in its impressive in strength, hardness, toughness and ductility. The method of using tungsten carbide WC-Co thermal spray coating on carbon steel is the main objective of this study by comparing to an uncoated carbon steel. In this HVOF process, oxygen and fuel (kerosene) are injected into a combustion nozzle with added spray powder. Tensile and hardness tests were conducted on coated specimens, and the fracture mechanism of the samples was observed by using Scanning Electron Microscope (SEM). The results show that hardness of the coated carbon steel is higher than the uncoated carbon steel. Meanwhile, uncoated carbon steel shows a higher elastic modulus, yield strength and tensile strength value compared to coated carbon steel. Using SEM, we can observe that some dimples and cleavage are present in both of the uncoated and coated carbon steel. This concluded that coated specimen lowers the tensile strength of the carbon steel due to its attribute to brittle characteristics of the coating. With the increasing of thickness, the tensile strength of carbon steel decrease. This also supports its high hardenability during hardness testing which due to its attribute to brittle characteristic.

ICSSST2019-118

Effect of SLS Glass Doping on ZnO Varistor Ceramics: Dry Milling ProcessNur Quratul Aini Ismail^{1,a}, Nor Kamilah Sa'at^{1,b*}, Mohd Hafiz Mohd Zaid^{1,c}¹Department of Physics, Faculty of Science, University Putra Malaysia, 43400 UPM Serdang, Selangor, Malaysia^anurquratulainiismail95@gmail.com, ^bkamilah@upm.edu.my, ^cmhmzaid@upm.edu.my

Abstract. There is lacking of study using dry milling process in the preparation of varistor based ceramics. Dry milling process is a good technique to produce fine and homogeneous sample powder. Soda lime silica (SLS) glass is used as dopants in ZnO varistor ceramics. This work focus on the effect of dry milling process on the microstructural and electrical properties of ZnO_{1-x} - SLS_x- CoO₂ using solid state method where x = 0.5, 1.0, 1.5 and 2.0 mol%. The XRD diffraction peaks detected Zn₂SiO₄ as secondary phase. The results show that the average grain size decreased from 0.028 to 0.023 and densities of the varistor samples increased as the SLS glass concentration increased. The varistor sintered at 1100°C and doped with 2 mol% showed good electrical properties with nonlinear coefficient, (α) 6.973, breakdown voltage 261.82 V/mm and leakage current (J_L) 4.463 $\mu\text{A}/\text{cm}^2$.

v

ICSSST2019-130

Nonlinearity Characteristics of ZnO Varistors Tailored by Perovskite-BaTiO₃ and Cobalt DopantsMuhamad Syaizwadi Shaifudin^a, Mohd Sabri Mohd Ghazali^b, Wan Mohamad Ikhmal Wan Mohamad Kamaruzzaman^c, Wan Rafizah Wan Abdullah^d, Syara Kassim^e, Nur Quratul Aini Ismail^f, Nor Kamilah Sa'at^g, Mohd Hafiz Mohd Zaid^h, Maria Fazira Mohd Fekeriⁱ, Khamirul Amin Matorij

Advanced Nano Materials (ANoMa) Research Group, Nano Research Team, School of Fundamental Science, Universiti Malaysia Terengganu, 21030 Kuala Nerus, Terengganu, Malaysia

^asyazwadi@gmail.com, ^bmohdsabri@umt.edu.my, ^cikhmal007@gmail.com, ^dwanrafizah@umt.edu.my, ^esyara.kassim@umt.edu.my, ^fnurquratulainiismail95@gmail.com, ^gkamilah@upm.edu.my, ^hmhmzaid@upm.edu.my, ⁱmariafazirafekeri@gmail.com, ^jkhamirul@upm.edu.my

Abstract. The nonlinearity characteristics of ZnO varistor ceramics were investigated for different contents of cobalt dopant at a given BaTiO₃ amount. The optimum value of nonlinear coefficient (α) equal to 4.8, which regard to the sample made with 12 wt.% BaTiO₃ additive. The nonlinear coefficient of the ceramics increased and then decreased with increasing concentration of Co₃O₄. Both the varistor voltage and leakage current density of the samples increased and then decreased as the cobalt doping level was increased at a given BaTiO₃ additive contents. The further Co₃O₄ doping caused the varistor voltage and leakage current density of the ZnO-BaTiO₃ ceramics to increase from 8.47 to 10.95 V/mm and 6.77 to 8.76 $\mu\text{A}/\text{cm}^2$ for up to 1.5 wt.%. The barrier height increased from 0.88 to 0.98 eV, whereas further doping caused it to decrease to 0.86 eV. The varistor ceramics with the highest nonlinear coefficient of 7.2 was obtained under an optimum Co content of 0.5 wt.%. The findings from this work could be helpful in the fabrication of high-quality varistor materials.

ICSSST2019-133

Effect of Heat Treatment to The Properties of Zinc Silicate Based Glass-Ceramics

Mohd Hafiz Mohd Zaid, Khamirul Amin Matori^a, Sidek Ab Aziz^b, Halimah Mohamed Kamari^c
Department of Physics, Faculty of Science, Universiti Putra Malaysia, 43000 UPM Serdang, Selangor,
Malaysia

^akhamirul@upm.edu.my, ^bsidek@upm.edu.my, ^chalimahmk@upm.edu.my

Abstract. Zinc silicate-based glass-ceramics were fabricated and synthesized using SLS glass bottle waste as a source of silicon. The series of precursor glass in the ZnO-B₂O₃-SLS glass system was prepared by the conventional melt-quench technique. Zinc silicate-based glass-ceramics were derived from the parent glass by a controlled heat-treatment process. The average density and linear shrinkage of glass and glass-ceramic samples were found increased with increasing of heat treatment temperatures. Besides, the structural properties of precursor glass and formation of zinc silicate crystal phase and bonding with the increase of heat-treatment temperatures were examined by X-ray diffraction (XRD) and Fourier transform infrared (FTIR) reflection spectroscopy. The appearance of SiO₂, ZnO and Zn-O-Si bands detected from FTIR measurements indicate that the formation of zinc-silicate crystal phase in the glass-matrix.

v

ICSSST2019-145

Gold Nanoparticles Activated Enhanced Photoluminescence of Samarium Ions Inside Tellurite Amorphous Host

Y. A. Tanko^{1,a}, M. R. Sahar^{2,b}, S. K. Ghoshal^{2,c*}, A. Shuaibu^{1,d} and S.G. Abdu^{1,e}

¹Department of Physics, Faculty of Science, Kaduna State University, Kaduna, Nigeria.

²Advanced Optical Materials Research Group, Department of Physics, Faculty of Science, Universiti Teknologi Malaysia, 81310 Skudai, Johor, Malaysia.

^aaatanko2000@gmail.com, ^bmrahim057@gmail.com, ^csibkrishna@gmail.com, ^dalhazikara@gmail.com,
^esgabdul@kasu.edu.ng

Abstract. Achieving enhanced photoluminescence of rare-earth inside oxide amorphous matrix by embedding metallic nanoparticles (NPs) of controlled sizes is a challenging task. We report the gold (Au) NPs activation of enhanced photoluminescence in samarium (Sm³⁺) ions doped tellurite amorphous matrix. Sm³⁺ doped zinc tellurite glasses containing Au NPs are synthesized by melt-quenching technique and spectroscopic characterization is made. X-ray diffraction (XRD) patterns confirm the amorphous nature of the prepared glass matrix. The transmission electron microscope (TEM) images manifest the growth of nearly spherical Au NPs with an average diameter of around ~17.12 nm. The selected area electron diffraction (SAED) results indicate that Au NPs are grown along [111] plane direction. UV-Vis-NIR spectra reveal ten absorption bands. The surface plasmon resonance (SPR) band is evidenced around 652 nm. The visible up-conversion (UC) emission for all samples under 945 nm excitation exhibits four bands centered at 562 (green), 600 (orange), 630 (intense red), and 646 (weak red) ascribed to ⁴G_{5/2} → ⁶H_{5/2}, ⁶H_{7/2}, ⁶H_{9/2}, and ⁶H_{11/2} transitions respectively. The proposed glass system may be potential as active lasing media.

ICSSST2019-163

Synthesis and Enhancement of Luminescence Properties of Co²⁺: Zn₂SiO₄ Willemite Based Glass Ceramic Derived for Potent Optoelectronic Applications

Siti Aisyah Abdul Wahab^{1,a}, Khamirul Amin Matori^{2,b*}, Mohd Hafiz Mohd Zaid^{2,c}, Mohd Mustafa Awang Kechik^{2,d}, Sidek Hj. Ab Aziz^{2,e}, Mohammad Zulhasif Ahmad Khiri^{1,f}, Nuraidayani Effendy^{2,g}

¹ Materials Synthesis and Characterization Laboratory, Institute of Advanced Technology, Universiti Putra Malaysia, 43400 UPM Serdang, Selangor, Malaysia.

² Department of Physics, Faculty of Science, Universiti Putra Malaysia, 43400 UPM Serdang, Selangor, Malaysia.

^aaisyahwahab94@gmail.com, ^{b*}khamirul@upm.edu.my, ^cmhmzaid@gmail.com, ^dmmak@upm.edu.my, ^esidek@upm.edu.my, ^fmzulhasif@gmail.com, ^gaidayanieffendy@gmail.com

Abstract. A series of zinc silicate glasses doped (Cobalt Oxide) Co₃O₄ based empirical formula [ZnO_{0.55} WRHA_{0.45}]_{1-x}[Co₃O₄]_x where x = 0, 0.01, 0.5 and 0.1 w.t.% was prepared by melt and quenching technique. Then, the alpha-willemite based glass ceramic doped Co₃O₄ were derived from this precursor glass by a controlled crystallization process. The samples were subjected to heat treatment process at 950 °C. The formation of the alpha-willemite phase and morphology with increase of dopant was examined by X-ray diffraction (XRD) and field emission scanning electron microscopy (FESEM) technique. The crystallinity of the willemite based glass ceramic doped Co₃O₄ was increased as the dopant increase. Besides, the optical absorption, optical bandgap and luminescence spectra of these glass ceramic also have been investigated. The absorption of alpha-willemite based glass ceramic doped Co₃O₄ was increase as the dopant increase due to enhancement of crystallinity. Meanwhile, the optical band gap decrease as the dopant increase. The photoluminescence spectra of alpha-willemite based glass ceramic doped Co₃O₄ exhibit blue emission. For these alpha-willemite based glass ceramic doped Co₃O₄ materials showing bright colours, their emission profiles have also been measured and these emissions are found to arise due to the occurrence of d-d transitions. Such luminescent properties of alpha-willemite based glass ceramic doped Co₃O₄ are expected to find potential in more optoelectronic applications.

ICSSST2019-172

Towards Dye Extraction using a Magnetic AerogelIng Kong^{1, a*}, Cin Kong², Wei Kong³, Zu Rong Ang⁴, Ai Bao Chai⁴, Oliver Buddrick⁵ and Win Kong⁶¹School of Engineering and Mathematical Sciences, La Trobe University, Bendigo, Victoria, 3552 Australia.²Division of Biomedical Sciences, University of Nottingham Malaysia Campus, Jalan Broga, Semenyih, Selangor, Malaysia.³Centre for Foundation and General Studies, Infrastructure University Kuala Lumpur, Jalan Ikram-Uniten, 43000 Kajang, Selangor, Malaysia.⁴Department of Mechanical, Materials and Manufacturing Engineering, University of Nottingham Malaysia Campus, Jalan Broga, Semenyih, Selangor, Malaysia.⁵William Angliss Institute, 555 La Trobe Street, Melbourne, Victoria 3000 Australia.⁶BASF Petronas Chemicals Sdn Bhd, Technical Office Building (TOB), Jalan Gebeng 2/1, Kawasan Perindustrian Gebeng, 26080 Kuantan, Malaysia.

a*.I.Kong@latrobe.edu.au

Abstract. We present a novel hybrid aerogel which can be magnetically extracted from water, so filtration is unnecessary, and the aerogel itself can be washed. Our three-dimensional magnetic graphene-based aerogel (3DmGT-PVA) consists of graphene oxide (GO), oxidised carbon nanotubes (O-CNT), nickel zinc ferrite ($\text{Ni}_{0.5}\text{Zn}_{0.5}\text{Fe}_2\text{O}_4$) and poly (vinyl alcohol) (PVA). The aerogel was characterized by using X-ray powder diffractometer (XRD), field emission scanning electron microscopy (FESEM), vibrating sample magnetometer (VSM) and thermogravimetric analysis (TGA) to study the microstructure, morphology, magnetic and thermal properties. It was found that a mass ratio of 12:1 iron (III) chloride hexahydrate ($\text{FeCl}_3 \cdot 6\text{H}_2\text{O}$) to graphene oxide (GO) and oxidised carbon nanotubes (O-CNT) mixture maximised adsorption capacity ($q_e = 3.77$ mg/g on methylene blue (MB)) and had a magnetic strength of $M_s = 3.519$ emu/g. 3DmGT-PVA was shown to adsorb the most common dyes, crystal violet (CV, $\eta = 8.9\%$), methyl orange (MO, $\eta = 4.2\%$) and mixture of MB, MO and CV (cocktail, $\eta = 11.1\%$). We also found that this aerogel can be reused for three regeneration cycles, with a regeneration efficiency of over 82%. Finally, we have proved that this aerogel is not toxic to living organism, strongly proposing that this 3DmGT-PVA shows great promise as a means of treating industrial wastewater.

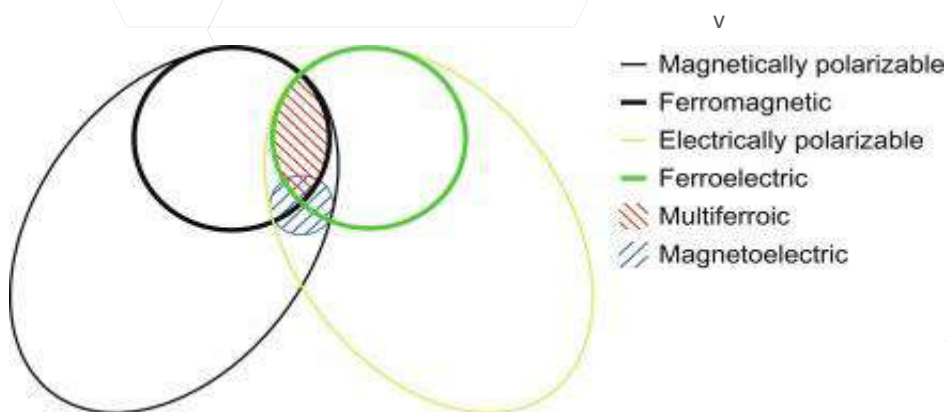
ICSSST2019-173

A Brief Review on the Fundamentals of Multiferroic Materials and their Possible Applications

Abdul Halim Shaari, Lim Kean Pah, Chen Soo Kien, Mohd. Mustafa Awang Kechik and Zainal Abidin Talib

Physics Dept., UPM

Abstract. Nowadays the term multiferroics is commonly used to indicate the materials that display ferroelectric and ferromagnetic, ferrimagnetic, or antiferromagnetic orders simultaneously in single or even in multiphase materials. Multiferroics belong to the family of multifunctional materials in which at least two of the ferroic orders, including ferromagnetism, ferroelectricity and ferroelasticity, exist concurrently. More specifically, in materials that simultaneously show ferromagnetism and ferroelectricity and the coupling between these two order parameters, the polarization can be handled by a magnetic field and the magnetization of the material by an electric field, and such materials are known as magnetoelectric multiferroics. The paper first introduces the basic physics behind perovskite multiferroics. Some of the fundamental aspects of solid-state multiferroic materials, followed by the detailed presentation of the latest and most interesting proposed applications of these multifunctional solid-state compounds driven by their fascinating physical properties and huge potential for technological applications will be addressed. The relationship between ferromagnetic, ferroelectric, multiferroic, and magnetoelectric materials are as shown in the Figure below by W. Eerenstein, N.D. Mathur, J.F. Scott, Nature 442 (2006) 759–765.



ICSSST2019-174

UV-Vis Spectroscopy of Samarium Doped Wollastonite - CaSiO₃:Sm³⁺

Sidek Ab Aziz, Karima AlMasri, Mohd Hafiz Mohd Zaid, Khamrul Amin Matori

Department of Physics, Faculty of Science, Universiti Putra Malaysia, 43400 UPM Serdang, Selangor

Abstract. This paper reports the UV-Vis studies on wollastonite doped samarium oxide, CaSiO₃:Sm³⁺ using recycled soda lime silica (SLS) glass bottles under the conventional melt-quenching method. A batch of prepared glass was mixed with CaO and Sm₂O₃ in a composition ratio of [(SLS)_{0.79}(CaO)_{0.21}]_{1-y}[Sm₂O₃]_y where y = (0, 1, 2, 3, 4, 5) wt.%. The UV-Visible spectroscopy was used to determine the absorbance spectra of the glass ceramic specimens and to gauge their optical band gap energy. Experimental result shows the absorption spectra of Sm³⁺ doped wollastonite based glass-ceramic specimen sintered at five varying temperatures was observed in the 250-500 nm region. The absorption curve in the glass and glass-ceramic systems shows that intensive absorption occurs between the 260-400 nm ranges. The higher intensity of the absorption spectra was observed with elevated sintering temperatures. Because at lower temperatures, the densification is low that results in significant light scattering and opaque samples, whereas higher temperatures produce additional absorption and scattering. The absorption spectra of undoped and Sm³⁺ doped wollastonite based glass-ceramic specimens sintered at five varying temperatures were observed in the 250-500 nm region. The absorption curve in the glass and glass-ceramic systems shows that intensive absorption occurs between the 260-400 nm ranges. It can be inferred that increasing the amount of Sm³⁺ resulted in increased intensity of the absorption spectra. This increase is because of the charge transfer state of the samarium-oxygen interactions ions, which overlaps with the absorption band of the host lattice and causes the charge transfer state.

ICSSST2019-175

Role of Sm³⁺ ions on the Optical Properties of Borotellurite Glass Under 480 nm Excitation WavelengthAzman Kasim^{1,a}, Siti Nasuha Mohd Rafien^{2,b}, Azhan Hashim^{1,c}, Wan Aizuddin Wan Razali^{1,d}, Syamsyir Akmal Senawi^{1,e}¹Faculty of Applied Sciences, Universiti Teknologi MARA Pahang, 26400 Jengka, Pahang, Malaysia²Faculty of Applied Sciences, Universiti Teknologi MARA, 40450 Shah Alam, Selangor, Malaysia^aazman615@uitm.edu.my, ^bnasuha_rafien@yahoo.com, ^cdazhan@uitm.edu.my,^dwanaizuddin@uitm.edu.my, ^esyamsyir@uitm.edu.my

Abstract. Incorporation of rare earth into borotellurite glass spearheads more research works on a development of optical devices application. In this work, melt-quenched technique has been used to prepare samarium doped borotellurite glass. From the results, the amorphous nature of the glasses were confirmed through XRD spectral analysis. Whereas, the FTIR spectral analysis confirmed the presence of BO₃, BO₄, TeO₃, TeO₄ and B – O⁻ structural units in the glasses. The absorption and emission spectra were analysed by UV-Vis and photoluminescence spectrophotometer in order to determine their optical properties. From the absorption spectra, three strong absorption peaks were observed and resolved in the ultra violet and visible regions due to transitions between the ground state and various excited state of Sm³⁺ ions. Meanwhile, from the luminescence spectra the upconversion emissions were found centered at 562 nm, 599 nm, 645 nm and 706 nm under the 480 nm excitation wavelength. The photoluminescence result reveal that 1.0 mol% of Samarium is the optimum concentration as shown by its most intense emission spectra. Some other results were also been analyzed, discussed and presented in this works.

Crystallography

ICSST2019-161

The Impact of Zr Substitution on the Crystal Structure of Yb doped BaCeO₃ Solid Solution Prepared by a Sol-gel MethodNafisah Osman^{1,2 a *}, Nurul Waheeda Mazlan^{2,b}, Oskar Hasdinor Hassan^{3,c} and Zakiah Mohamed^{4,d}¹Faculty of Applied Sciences, Universiti Teknologi MARA, 02600 Arau, Perlis, Malaysia.²Proton Conducting Fuel Cell Group, Universiti Teknologi MARA, 40450 Shah Alam, Selangor, Malaysia³Faculty of Art and Design, Universiti Teknologi MARA, 40450 Shah Alam, Selangor, Malaysia.⁴Faculty of Applied Sciences, Universiti Teknologi MARA, 40450 Shah Alam, Selangor, Malaysia^{a*}fisha@uitm.edu.my, ^bnurulwaheedamzln@gmail.com, ^coskar@uitm.edu.my, ^dzakiah626@uitm.edu.my

Abstract. A modified sol-gel method using metal nitrate salts was adopted to synthesis proton conductor of Ba(Ce_{1-x}Zr_x)_{0.95}Yb_{0.05}O_{2.975} where x=0, 0.2, 0.3, 0.4, 0.5 and 0.6 ceramic powders. The aim of this work is to study the crystal structure of Yb-doped barium cerate solid solution at different Zr concentrations. The powder was calcined at 1100°C for 12 hours and pressed at 5 tons to become a pellet by a dry pressing technique. The pellet was sintered at 1400°C in air for 6 hours and ground to powder form prior to the XRD measurement. XRD data of the sample at room temperature was analyzed using Rietveld refinement method in X'pert Highscore software. Two different crystal structures (orthorhombic and cubic), depending on Zr concentrations were observed by VESTA software with *goodness of fit*, GOF in average ~2.34. Phase formation, structure analysis and the empirical rule which holds the linear relation between lattice parameters at different Zr concentrations using Vegard's Law were also presented and discussed.

Defence and Security

ICSSST2019-010

Human Detection for Thermal and Visible ImagesMazlinda Ibrahim^{1,a},¹Department of Mathematics, Centre for Defence Foundation Studies, Universiti Pertahanan Nasional Malaysia, Kem Sungai Besi 57000 Kuala Lumpur^amazlinda@upnm.edu.my,

Abstract. Human detection and localization is one of the importance aspects in computer vision. It has broad applications in surveillance, robotic, driver assistance system, and for the military application. The task is difficult because its depends on various conditions such as illumination, distance, human pose and weather condition. This study aimed to investigate human detection methods for thermal and visible images. We have explored three methods which are histogram of oriented gradient, integral image and aggregate of channel features. Our result showed that histogram of oriented gradient outperformed the other two using the tested images. However, the method is only applicable when the human is on the standing or upright position and limited to a certain distance between the scene and the camera position.

v

ICSSST2019-023

Effects of Convective Boundary Conditions and Heat Transfer on MHD Stagnation Point Nanofluid Flow Past a Shrinking SheetNor Ain Azeany Mohd Nasir^{1,2, a}, Anuar Ishak^{2,b,*}, Ioan Pop^{3,c}, Fatin Amirah Ahmad Shukri^{1,d}, and Nurulhuda A. Manaf^{1,e}¹ Department of Mathematics, Centre for Defence Foundation Studies, Universiti Pertahanan Nasional Malaysia, Kem Sungai Besi 57000 Kuala Lumpur² School of Mathematical Sciences, Faculty of Science and Technology, Universiti Kebangsaan Malaysia, 43600 UKM Bangi, Selangor, Malaysia³ Department of Mathematics, Babeş-Bolyai University, 400084 Cluj-Napoca, Romania^anorainazeany@upnm.edu.my, ^banuarishak@yahoo.com, ^cpopm.ioan@yahoo.co.uk, ^dfatin@upnm.edu.my, ^enurulhuda@upnm.edu.my

Abstract. The steady flow of a nanofluid's stagnation point Magnetohydrodynamic (MHD) over a permeable shrinking sheet with convective boundary conditions and radiation effects is explored. The governing partial differential equations are converted using similarity transformation into a system of non-linear Ordinary Differential Equations (ODEs). The boundary value problem solver is selected in order to solve the ODEs. The roles of physical parameters such as the skin friction coefficient and local Nusselt number as well as velocity, temperature and nanoparticle volume fraction profiles are described in graphs and addressed in details. The findings showed that the suction strength improves the skin friction coefficient and the heat transfer rate as the sheet is shrunk. Meanwhile, the nanoparticle volume fraction and thermal boundary layer thickness are increased in the presence of radiation.

Electrochemical and Solid State

ICSSST2019-051

The Response of Ion Selective Electrode Based on Aryl Methyl Carbonylamino Thiazole Derivatives as IonophoreNoor Wahidah Zainol Jamil^{1, a}, Muhd Zu Azhan Yahya^{2, b}, Juliana Jumal^{3, c} and Noor Azilah Mohd Kasim^{4, d*}¹Department of Defence Sciences, Faculty of Defence Sciences and Technology, National Defence University of Malaysia, Kem Sungai Besi, 57000, Kuala Lumpur, Malaysia³Faculty of Science & Technology, University Sains Islam Malaysia (USIM), Bandar Baru Nilai, 71800 Nilai, Negeri Sembilan, Malaysia^awyda1992@gmail.com, ^bmzay@upnm.edu.my, ^cjuliana.j@usim.edu.my, ^ddrazilahkasim@upnm.edu.my

Abstract. Thiazole derivatives have been known to form a very stable complexes with metal ions. The properties of thiazole derivatives have made these compounds become a suitable ionophore which is a sensing material of Ion Selective Electrode (ISE). Ion Selective Electrode (ISE) based on ionophore is a liquid membrane sensor that having an attachable membrane on the bottom part of an electrode. This electrode is made up of four parts; body, silver electrode, internal filling solution and membrane. The membrane is consisting of four components, ionophore, polymeric membrane, ionic additive and plasticizer. This experiment is conducted to study the potential of aryl methyl carbonylamino thiazole derivatives as ionophore and its response in electrochemical set up. The response of ion selective electrode is depending on the compatibility of plasticizer and ionophore, and the composition of an ion selective membrane. The experiment conducted used the same plasticizer which is benzyl acetate (BA), and the same ratio of the component; 5.0:30.0:2.0:63.0 (Th:PVC:NaTPB:BA) by weight percentage; where Th is thiazole derivatives, PVC is polyvinyl chloride, NaTPB is sodium tetraphenylborate and BA is benzyl acetate. These components are acting as ionophore, polymeric matrix, ionic additive and plasticizer respectively. The Nernstian response for Cd²⁺ that obtained the best response with 26.96 mV/decade is when thiazole derivative of 2-chloroaniline is used as ionophore. The linear working range for this response is 1.0×10^{-6} to 1.0×10^{-3} .

ICSSST2019-073

Effect of Mechanical Agitation on Cr-Al₂O₃ Nanocomposite Coatings Fabricated from Trivalent Chromium ElectrodepositionEydar Tey^{1, a}, Zulkarnain Zainal^{1,2, b*}, Lim Kean Pah^{3, c} and Ismayadi Ismail^{1, c}¹Material Synthesis and Characterization Laboratory, Institute of Advanced Technology, Universiti Putra Malaysia, 43400 Serdang, Selangor, Malaysia.²Department of Chemistry, Faculty of Science, Universiti Putra Malaysia, 43400 Serdang, Selangor, Malaysia.³Department of Physics, Faculty of Science, Universiti Putra Malaysia, 43400 Serdang, Selangor, Malaysia.^aeydar0515@gmail.com email, ^bzulkar@upm.edu.my, ^climkp@upm.edu.my, ^dkayzen@gmail.com

Abstract. In the present work, Cr-Al₂O₃ nanocomposite coatings were electrodeposited onto copper substrate using a modified trivalent chromium electroplating bath with addition of 80nm Al₂O₃ powder. The effects of mechanical agitation of electrodeposition bath on Al₂O₃ particles dispersion and particles embedment were studied. The Cr-Al₂O₃ nanocomposite samples were subjected to different tests to characterize their surface morphology, crystalline structure and mechanical properties. The crystalline structure, composition and surface morphology of the deposits were studied by X-ray diffraction (XRD), energy-dispersive X-ray spectroscopy (EDX) and field emission scanning electron microscopy (FESEM). The corrosion resistance test was carried out by electrochemical polarization method. The microhardness was studied via Vickers Microhardness Test. The variation in the microhardness as a main property to achieve enhancement of Al₂O₃ incorporations with Cr matrix. The hardness results showed the Cr-Al₂O₃ composite coating has the best performance at 200 rpm stirring speed. The corrosion current density (i_{corr}) of Cr-Al₂O₃ coating revealed highest value at 200 rpm. This result indicated that the corrosion resistance performance of Cr-Al₂O₃ coating decreases with increasing Al₂O₃ particles content.

ICSSST2019-077

The Electrochemical Performance of Superconcentrated Na⁺ Salt in Ionic Liquid- Based Gel Electrolytes for Application in Sodium Rechargeable BatteriesN.C. Su^a, S.A.M. Noor^{b*}, N.S. Mohamed^c, A.Ahmad^e, M.Z.A Yahya^d,^aFaculty of Defence Science and Technology, National Defence University of Malaysia, 57000, Kuala Lumpur, Malaysia^bCentre for Defence Foundation Studies, National Defence University of Malaysia, 57000, Kuala Lumpur, Malaysia^cCentre for Foundation Studies in Science, University of Malaya, 50603, Kuala Lumpur, Malaysia^dSchool of Chemical Sciences and Food Technology, Faculty of Science and Technology, National University of Malaysia, 43600 Bangi Selangor, Malaysia

*s.aminah@upnm.edu.my

Abstract. Superconcentrated (highly concentrated) solutions are emerging as a new class of liquid electrolyte with various unusual functionalities beneficial for advanced sodium (Na) battery application. Herein, we reported the effect of high concentration of sodium fluorosulfonyl imide (NaFSI) in methylpropylpyrrolidinium (C₃mpyr) FSI ionic liquid (IL) with and without the presence of ethylene carbonate (EC) in gel state electrolyte for potential application in sodium secondary battery. NaFSI is highly soluble in the IL allowing the preparation of mixtures that contain 55 mol% of salt and the addition of 30 wt% of EC being studied for electrochemical performance. The ionic conductivity and thermal stability are evaluated through electrochemical impedance spectroscopy (EIS) and differential scanning calorimetry (DSC) respectively. FTIR showed the C-O-C stretching mode at 1060 cm⁻¹ in pure EC shift to higher wavenumber 1078 cm⁻¹ with the presence of EC as well as the C-O-C and C=O indicating that the oxygen lone pair of EC also provides coordination site for Na⁺. Stable gel electrolytes does not significantly affect the liquid-like ion dynamics in these materials. The ionic conductivity gel electrolyte at room temperature is slightly increase by 0.003 S cm⁻¹ with EC present. Despite of having lower conductivity compared to liquid state electrolyte, the gel electrolytes show high Na⁺ transference number and the deposition and dissolution of sodium metal were observed in cyclic voltammetry. The prepared gel electrolytes were verified in half- cells at room temperature using Na₃V₃(PO₄)₃ as a cathode.

ICSSST2019-109

Modification of Gold Electrodes using Reduced Graphene Oxide for Cortisol Electrochemical Biosensor

Ahmad Farid Mohd Azmi¹, Jahwarhar Izuan Abd Rashid¹, Vayithiswary Kannan², Muhammad Hafiz Ahmad², Ainsah Omar³ and Eme Marina Salleh^{1,2}

¹Department of Chemistry and Biology, Centre for Defence Foundation Studies, ²Faculty of Defence Science and Technology, ³Faculty of Medicine and Defence Health, National Defence University of Malaysia, Sungai Besi Camp, 57000 Kuala Lumpur, Malaysia.

Short Running Title: Modified SPGE using rGO as Cortisol Biosensor

Abstract. In this study, electrochemical sensor was developed for the determination of cortisol level using screen printed gold electrode (SPGE) modified with graphene oxide (GO) sheets. GO suspension was drop-casted then reduced electrochemically by cyclic voltammetry. Reduced GO modified gold electrode (rGO-SPGE) was characterized by cyclic voltammetry (CV) and Field Emission Scanning Electron Microscope (FESEM). The results indicated a successful deposition and distribution of rGO onto the SPGE. Cortisol monoclonal antibody (C-Mab) was immobilized by treating the modified SPGE using N-hydroxysuccinimide (NHS) and N-(3-dimethylaminopropyl)-N'-ethylcarbodiimide (EDC) solution to activate carboxyl group (COOH) on the rGO surface which then reacted with amines (NH₃) group of cortisol specific monoclonal antibody (C-Mab) to form an amide bond. The modified SPGE (C-Mab/rGO-SPGE) was then characterized for cortisol interaction using cyclic voltammetry (CV) techniques. A linear range was observed from 0.001 µg/mL to 10 µg/mL of hydrocortisone which is in the range of normal and stress human cortisol levels. The proposed procedure was observed to be providing good accuracy and precision.

ICSSST2019-112

Phase Formation and Morphology of NiO-BCZY Anode Functional Layer for Proton Conducting Fuel Cell

Lidayatty Abdul Malik^{1,a}, Nurul Waheeda Mazlan^{1,b}, Oskar Hardinor Hassan^{2,c}, Abdul Mutalib Md Jani^{3,5,d}, and Nafisah Osman^{4,5,e*}

¹Faculty of Applied Sciences, Universiti Teknologi MARA, 40450, Shah Alam, Selangor, Malaysia ²Faculty of Art and Design, Universiti Teknologi MARA, 40450, Shah Alam, Selangor, Malaysia ³Faculty of Applied Sciences, Universiti Teknologi MARA, 35400, Tapah Road, Perak, Malaysia ⁴Faculty of Applied Sciences, Universiti Teknologi MARA, 02600, Arau, Perlis, Malaysia

⁵Proton Conducting Fuel Cell Group, Faculty of Applied Sciences, Universiti Teknologi MARA, 40450, Shah Alam, Selangor, Malaysia

^alidayatty@gmail.com, ^bnurulwaheedamzln@gmail.com, ^coskar@salam.uitm.edu.my, ^dabdmusalib@uitm.edu.my, ^{e*}fisha@uitm.edu.my,

Abstract. Fabrication of anode functional layer (AFL) between porous anode support and dense thin film electrolyte can enhance the overall performance of proton conducting fuel cell (PCFC) in terms of physical strength, reducing diffusion of metal cation into electrolyte, and reducing thermal expansion mismatch between layers. One type of optimization for AFL is to create a gradient particle size between anode support and AFL to reduce mass transport resistance and increase the triple phase boundaries (TPB). In this work, the optimum formulation and particle size of AFL for a PCFC button cell was investigated and analyzed. The samples were mechanically mixed with different weight ratio of NiO commercial powder and in-house developed BCZY synthesized by sol gel method (NiO:BCZY = 10:90, 20:80, 30:70, 40:60, 50:50, 60:40). The samples were calcined at 1450° C for 5 hours and the phase formation and morphology of each samples were characterized using XRD and FESEM to extract the lattice parameter, crystallite size and particle size of AFL composite, respectively. The result shows that only NiO:BCZY = 10:90 exhibited a composite of NiO and BCZY phases and smaller particle size than others. Thus, this ratio has the potential to be used as AFL in the PCFC button cell.

ICSSST2019-116

Ionic Conductivity in Carboxymethyl cellulose (CMC) Biopolymer membrane incorporated with Ammonium Thiocyanate, NH₄SCNRosnah Zakaria^{1,2 a *}, Nor Kartini Jaafar^{1, b} and Nazli Ahmad Aini^{1, c}¹Faculty of Applied Sciences, Universiti Teknologi MARA, 40450 Shah Alam, Selangor, Malaysia²Institute of Sciences, Universiti Teknologi MARA, 40450 Shah Alam, Selangor, Malaysia^arosna593@uitm.edu.my, ^bnormka603@uitm.edu.my, ^cnazli2005@uitm.edu.my

Abstract. In recent years, scientists have been working together to inherent the strength and performance of biopolymer to produced new class of bio based composite due to the concern of the environment. Starch is an organic chemical that is produced by all green plant. It has been stored in chloroplast in the form of the granules and in certain organs of the plant like the root of tapioca plant, the tuber of potato plant, the stem pith of sago, the seed of wheat, corn, rice and etc (Ning, Xingxiang, Haihui & Benqiao, 2009; Ramesh, Liew & Arof, 2011). Cellulose is one of starch polymer found abundantly on Earth (Samsudin & Isa, 2013). The chemical formula (C₆ H₁₀ O₅), shows that the cellulose is a polysaccharide consisting of a linear chain of several hundred to many thousands of β(1→4) linked D-glucose units. Carboxymethyl cellulose (CMC) has attracted more attention as a representative water-soluble polysaccharide. As for now, chitosan leads to negative effect and very expensive material when pure chitosan can rarely be obtained from the suppliers due to difficulty in extracted material. However, in this study the carboxymethyl cellulose (CMC)^v was purchased from Sigma Aldrich. The film of biopolymer electrolyte (BPE) from CMC were prepared via solution casting method. Various amounts of ammonium thiocyanate, NH₄SCN ranging from 0 wt% to 50 wt% was added into the solution and stirred continuously for 24 hours to get homogenous solution which then poured into petri dish. It was left to dry for 24 hours again in an oven to form a thin film. The impedance of the samples was measured using the HIOKI 3531-01 LCR Hi-Tester interfaced to a computer with frequency ranging from 50 Hz to 1MHz at room temperature. While FTIR analysis is to see the occurrence of complexation and interaction of the polymer. The lowest conductivity of the sample is CMC-NH₄SCN (0 wt%) at 5.94 x 10⁻⁸ S cm⁻¹ while the highest is CMC-NH₄SCN (15 wt%) at 5.5 x 10⁻⁶ S cm⁻¹. After 15 wt%, the conductivity reduced which may due to agglomeration of polymer. It can be interpret through FTIR spectra when OH was stretching in plane at 1413 cm⁻¹ and new peak observed at 2065 cm⁻¹ which could be belong to thiocyanate (-S-C≡N) antisymmetric vibration of NH₄SCN. Hence, C=O also observed shifted to lower wavenumber upon dopant in CMC – NH₄SCN system at 1586 cm⁻¹ wavenumber.

ICSSST2019-158

Effect of pH and Immersion Time on the Corrosion Protection of SDBS-ZnSO₄ Pre-Treated Mild Steel in Sodium Chloride SolutionI. Ismail^{1, a *}, M.K. Harun^{2, b} and M.Z.A. Yahya^{3, c}¹Electrochemical and Corrosion Science Laboratory, Faculty of Applied Science, Universiti Teknologi Mara, 40450 Shah Alam Selangor, Malaysia²Electrochemical and Corrosion Science Laboratory, Faculty of Applied Science, Universiti Teknologi Mara, 40450 Shah Alam Selangor, Malaysia³Faculty of Defence Science & Technology, Universiti Pertahanan Nasional Malaysia, 57000 Kuala Lumpur, Malaysia*ismaliza@lgm.gov.my, ^bmohamadkamal@uitm.edu.my, ^cmzay@upnm.edu.my

Abstract. In this study, mild steel were treated with SDBS-ZnSO₄ compound by immersing the mild steel coupons in a SDBS-ZnSO₄ bath of varying pH. The effect of bath solution pH and immersion time on the corrosion protection properties of SDBS-ZnSO₄ pre-treated coupons in sodium chloride solution was investigated using electrochemical impedance spectroscopy (EIS) and polarization measurements. From the EIS results, it was found that the inhibition efficiency provided by the pre-treatment was significantly affected by the pH of the bath solution where inhibition was highest at pH 6. Increasing the immersion time from 1 h to 24 h increased the inhibition efficiency and it was maintained throughout the exposure period. From the polarization measurements, the current density was significantly reduced and the shift to a more positive corrosion potential value indicated a higher protection layer was formed on the metal surface during longer immersion. It has been found that longer pre-treatment immersion time allows a denser protective layer formed which prevented the diffusion of water towards the mild steel substrate that can lead to corrosion.

Laser and Optoelectronics

ICSSST2019-128

Generalized Function Projective Synchronization of 4D Chaotic Laser System for a Secure Communication

Nur Aisyah Abdul Fataf

Department of Mathematics, Centre for Defence Foundation Studies, National Defence University of Malaysia, Kem Sungai Besi, Kuala Lumpur, 57000 Malaysia

n.aisyah@upnm.edu.my

Abstract. In this paper, a new communication scheme based on generalized function projective synchronization (GFPS) of new 4D chaotic laser system studied by Natiq (2019) is proposed. The communication scheme is consist of the chaotic transmitter (drive system), the chaotic receiver (response system), the modulation and the demodulation technique. The modulation mechanism is to modulate the message signal into the system parameter. Hence, we check the system is still hyperchaotic after employing that system parameter. Then, the signal is sent to the receiver through public channel. We derived a controllers so that the response system can synchronize completely with the master system by using GFPS. Therefore, the receiver can extract the message signal successfully by the identifier parameter and the corresponding demodulation technique. Numerical results proved the effectiveness and the feasibility of the proposed communication scheme.

Material and Energy

ICSSST2019-003

Key Properties and Benefits of Clay in Environmental Protection

Muntari Mudi Yar' adua

Hassan Usman Katsina Polytechnic Katsina Nigeria

Abstract. This study examines the properties and benefits of clay and whether its use as a construction material enhances environmental protection. The rationale for this examination stems from the views held by scholars that clay bricks are more preferred as sustainable building materials; however there is limited research into whether the choice of clay materials is influenced only by its environmental benefits. The study undertook a systematic literature review and adopted a quantitative research methodology involving the survey of the selected building and civil construction companies in Katsina, Kano and Kaduna states of Nigeria. The research data collected on the economic, social and environmental properties of clay and its benefits in environmental protection, was analysed using descriptive statistical techniques. The study found that the economic aspects of clay make it more attractive as a building material that is useful in environmental protection. The study recommends further research into the improvement of clay as a building material that addresses the sustainable triple bottom line of economics, social and environmental requirements.

v

ICSSST2019-029

Effect of Gamma Radiation on Micromechanical Behaviour in Microelectronic Packaging

Noor Fadhilah Binti Rahmat

Universiti Pertahanan Nasional Malaysia

Abstract. Electronic packaging is the technology relating to the establishment of electrical interconnections and it is a major discipline within the field of electronics engineering. Packaging of an electronics system must consider the protection from mechanical damage, cooling, radio frequency noise emission and protection from electrostatic charge. Solder had been widely used as interconnection materials for microelectronic package. Nevertheless, solder joint in radiation need higher resistance to any damage caused by ionizing radiation. In this study a lead-free solder alloy 96.5Sn3.0Ag0.5Cu Wt.% (SAC305) was developed and subjected to various doses of gamma radiation and used Nano indentation approach in order to investigate the effect of the radiation to micromechanical properties of the solder. This paper presents the studies to determine hardness and elastic modulus of intermetallic compound (IMC) layers in lead-free solder joints using nanoindentation technique. The results showed that the hardness, H and elastic modulus, E of SAC solder changed when exposed to gamma rays. Highest mean hardness, 302.646 MPa was calculated on solder joint which was exposed to 5000 Gy dose of gamma radiation. This value indicates possible radiation hardening effect on irradiated solder. The hardness gradually decreased when exposed from dose of 5 Gy to 500 Gy. These value are also lower than the hardness of non-irradiated sample indicating possible radiation damage and needs further related atomic dislocation study.

ICSSST2019-037

Electrochemical Studies of Polymer Gel Electrolytes based on Agarose:LiBOB and P(VP-co-VAc):LiBOBM. S. Sak Ari^{1,b}, S. Z. Z. Abidin^{1,2,a*}, M. F. M. Taib^{1,2,c}, M. Z. A. Yahya^{3,d}¹Faculty of Applied Sciences, Universiti Teknologi MARA, 40450 Shah Alam, Selangor, Malaysia.²Ionic materials and Devices (iMADE) Research Laboratory, Institute of Science, Universiti Teknologi MARA, 40450 Shah Alam, Selangor, Malaysia.³Faculty of Defence Science and Technology, Universiti Pertahanan Nasional Malaysia, 57000 Kuala Lumpur, Malaysia.*szafirah@uitm.edu.my, ^bsyah3d@gmail.com, ^cmfariz@uitm.edu.my, ^dmzay@upnm.edu.my

Abstract. This study focuses on preparation and characterization of polymer gel electrolytes (PGEs) based on agarose:LiBOB:DMSO and poly(1-vinylpyrrolidone-co-vinyl acetate) [P(VP-co-VAc)]:LiBOB:DMSO. PGE were prepared by dissolving different amount (1-8 wt.%) of agarose and (1-8 wt.%) P(VP-co-VAc) in 0.8 M of LiBOB:DMSO solution. The addition of 1 wt.% of agarose and P(VP-co-VAc) into 0.8 M of LiBOB:DMSO solution will result an optimum conductivity which is $6.91 \times 10^{-3} \text{ S.cm}^{-1}$ for agarose:LiBOB:DMSO system and $7.83 \times 10^{-3} \text{ S.cm}^{-1}$ for P(VP-co-VAc):LiBOB:DMSO system. In the studied temperature range of conductivity discovered that the agarose:LiBOB:DMSO and P(VP-co-VAc):LiBOB:DMSO polymer gel electrolytes abide by Arrhenius rule indicating that this PGEs could run at elevated temperature conditions. Furthermore, transference number confirms that both electrolyte systems have a good ionic transport. And, linear sweep voltammetry (LSV) measurements demonstrate the both systems of agarose:LiBOB:DMSO and P(VP-co-VAc):LiBOB:DMSO are good in electrochemical stability.

ICSSST2019-050

Enhanced Mg Ion Transport in Cellulose Acetate based Gel Polymer Electrolytes: Effect of PlasticizerN. A. S. M. Azis^{1,b}, M. S. Sak Ari^{1,2,c}, M. Z. A. Yahya^{2,3,d}, S. Z. Z. Abidin^{1,2,a*},¹Faculty of Applied Sciences, Universiti Teknologi MARA, 40450 Shah Alam, Selangor, Malaysia.²Ionic materials and Devices (iMADE) Research Laboratory, Institute of Science, Universiti Teknologi MARA, 40450 Shah Alam, Selangor, Malaysia.³Faculty of Defence Science and Technology, Universiti Pertahanan Nasional Malaysia, 57000 Kuala Lumpur, Malaysia.*szafirah@uitm.edu.my, ^baidasyarmeen@gmail.com, ^csyah3d@gmail.com, ^dmzay@upnm.edu.my

Abstract. Plasticized gel polymer electrolytes (GPEs) are prepared using the mixture of 1.0 g of cellulose acetate (CA), 30 wt.% of magnesium triflate (MgTr) and 0-50 wt.% of ethylene carbonate (EC) plasticizer. The ionic conductivity of GPE showing the highest value at 40 wt.% EC with conductivity value of $2.44 \times 10^{-4} \text{ S.cm}^{-1}$. The increase in ionic conductivity of GPE is due to charge transporting ion leads to the increasing of the ionic mobility as confirmed by Fourier transform infrared (FTIR) analysis. The plots of temperature dependence conductivity shows an Arrhenius relationship. The complexation between CA and MgTr in FTIR are confirmed based on Mg^{2+} that form a coordination bond with the oxygen atom at functional group (C-O). FTIR also reveals that EC has been penetrated into the CA polymer chains and created more free volume without perturbing the CA:MgTr complexes. Analysis of x-ray diffraction (XRD) showing the addition of plasticizer has increased the amorphosity of CA:MgTr system thus enables ion to easily migrate and as a result the ionic conductivity will enhance. The enhancement of conductivity in this system can be confirmed by Field Emission Scanning Electron Microscopic (FESEM) analysis, where the amount of pores increase as the concentration of EC increases until 40 wt.%.

ICSSST2019-057

Influence of Surfactant on the Synthesis of NiO Nanoparticles by a Sol-gel MethodNoor Hidayah Aniza Zakaria^{1, a}, Hanani Yazid^{1, 2, b} and Nafisah Osman^{1, 2, c*}¹Proton Conducting Fuel Cell Research Group, Faculty of Applied Sciences, Universiti Teknologi MARA, 40450 Shah Alam, Selangor, Malaysia²Faculty of Applied Sciences, Universiti Teknologi MARA, 02600 Arau, Perlis, Malaysia^ahidayah_aniza@yahoo.com, ^b* hanani946@uitm.edu.my, ^c* fisha@uitm.edu.my

Abstract. Nickel oxide nanoparticles (NiO-Nps) has been widely used in many application due to its great properties. There are several synthesis methods that can be utilized to obtain nanosized NiO powder such as co-precipitation, hydrothermal decomposition, microwave assisted and sol-gel method. In this work, NiO nanoparticles were synthesized by a sol-gel method assisted with Triton X-100 as surfactant. The solution was controlled at pH 1, and then calcined at temperature of 450°C. The influence of surfactant Triton X-100 on physical properties of NiO nanoparticles were investigated by PSA, FESEM and XRD. Structural analysis confirmed that a cubic structure of NiO nanoparticle was obtained without any impurities for both NiO prepared with and without surfactant. Morphological observation showed that the NiO nanoparticles prepared with surfactant tends to form agglomerates compared to one prepared without surfactant. The average diameter of NiO nanoparticles with and without surfactant was approximately in the range of 20-100nm and 43.8nm, respectively.

ICSSST2019-083

Controlled Growth of Root-Free Ni₃Si₂ Nanowires for High Performance Supercapacitor ElectrodeMohammad Mukhlis Ramly^{1, a}, Fatin Saiha Omar², Zarina Aspanut¹, and Goh Boon Tong^{1, b*}¹Low Dimensional Materials Research Centre, Department of Physics, Faculty of Science, University of Malaya, 50603 Kuala Lumpur, Malaysia²Center for Ionics University of Malaya, Department of Physics, Faculty of Science, University of Malaya, Kuala Lumpur 50603, Malaysia^amukhlis.ramly88@gmail.com, ^bgohbt@um.edu.my

Abstract. One-dimensional based nanowire electrode has been recently attracting extensive interest in energy storage and conversion applications owing to its unique physical properties of extremely large surface areas and good electrochemical capability. In this work, the root-free nickel silicide nanowires (Ni₃Si₂ NWs) were grown by following a solid-phase diffusion control growth mechanism at different growth parameters. These NWs were mainly in a single crystalline structure with a preferred orientation of (100) plane. Moreover, the NWs exhibited excellence physical properties such as thin, straight, long, and root-free with their average length and diameter of the nanowires were 12.5 ± 0.5 μm and 13 ± 0.5 nm respectively, as well as a high aspect ratio of 923 and extremely large surface area of 5.184 × 10¹¹ NWs/cm². The fabricated Ni₃Si₂ NWs/activated carbon-based asymmetric supercapacitor demonstrated a maximum specific capacity of 578.3 C/g and energy density of 62.24 Wh/kg at 387.5 W/kg, and good cyclic stability with 76 % of capacity retention after 3, 000 cycles. The optimization of the growth parameters and the correlations of the electrochemical performances with the morphological, structural, and compositions properties of the Ni₃Si₂ NWs are comprehensively discussed.

ICSSST2019-085

Effect of Particles Size on Cu (II) Ion Removal from Aqueous Solutions using Fe₃O₄ Nanoparticles Adsorbents Synthesized from Mill Scale Waste

Syazana Sulaiman¹, Raba'ah Syahidah Azis^{1,2}, Ismayadi Ismail¹, Abdul Halim Shaari², Hasfalina Che Man³, Nur Asyikin Ahmad Nazri¹, Muhammad Syazwan Mustaffa and Nurshahiera Rosdi¹

¹ Materials Synthesis and Characterization Laboratory (MSCL), Institute of Advanced Technology (ITMA), 43400 Universiti Putra Malaysia, Serdang, Selangor, Malaysia.

² Department of Physics, Faculty of Science, 43400 Universiti Putra Malaysia, Serdang, Selangor.

³ Department of Biological and Agricultural Engineering, Faculty of Engineering, Universiti Putra Malaysia, 43400 Serdang, Selangor, Malaysia

Tel: +603-9269 6666, Fax: +603-8945 4454

rabaah@upm.edu.my, syazana2104@gmail.com

Abstract. The study investigates contaminant removal of Cu (II) ion and the efficiencies of Fe₃O₄ magnetite nanoparticles (MNP). The Fe₃O₄ were synthesized from mill scales waste. The micron-sized MNP were milled using the high energy ball mills (HEBM) for several milling hours (1,3,5,7 and 9 h) to produce nano-sized particles. The characterization methods of X-rays diffraction (XRD), vibrating sample magnetometer (VSM), transmission electron microscopy (TEM), Brunauer-Emmett-Teller (BET) and atomic adsorption spectrophotometer (AAS) were used to determine the crystal structure, hysteresis loop, particle size, specific surface area and adsorption capacity respectively. The effect of adsorbent dosage, initial ion concentration, contact time, temperature and pH value on the MNPs particles were investigated. The adsorption kinetics was relatively fast and equilibrium at about 30 minutes. The adsorption equilibrium data obeyed the Langmuir model and Pseudo-Second-Order for kinetic data. Thermodynamic analysis has indicated spontaneous endothermic adsorption of Cu (II) on MNP. The adsorption capacity of Cu (II) ion onto MNP are 6.18 mg/g at 7 hours milling hours. The experimental results reveal the technical feasibility of MNP, it is easy synthesis, economically, eco-friendly and a promising adsorbent for environmental pollution cleanup.

ICSSST2019-091

Screen Printing Methods for The Fabrication of Solid Oxide Fuel Cells (SOFCs): A Short Review

N.F.A. Rahman¹, P.L. Ying¹, H.A. Rahman^{1,*} and M.A. Azmi¹

¹Faculty of Mechanical and Manufacturing Engineering, Universiti Tun Hussein Onn Malaysia, 86400 Parit Raja, Batu Pahat, Johor, Malaysia.

*hamimah@uthm.edu.my

Abstract. A fuel cell is an electrochemical device which provides efficient and power generation. Due to the unique and performance characteristics of solid oxide fuel cells (SOFCs), this device is well suited and suitable for distributed on-site cogeneration of heat and power. The SOFCs, in particular is an electrochemical device that generates electrical energy and heat from a gaseous state of fuel with an oxidant. The SOFCs is a power generation technology that is has high efficiency and environmentally friendly to generate electrical energy from hydrogen gas, natural gas and other renewable fuel. SOFCs can be fabricated in many ways and the focus is on the methods that can achieve large production and cost saving methods. The method of using screen printing for the planar SOFC fabrication has acquired a great interest in industry. In this review, will focus more on the knowledge and provide information about fabrications of SOFC using screen printing methods.

ICSSST2019-098

Relationship Between Spectroscopic and Thermal Analysis of Poly(ethylene oxide) (PEO) - 50% Epoxidized Natural Rubber (ENR50) Complexed with Sodium Trifluoromethanesulfonate Based Polymer Electrolyte

Tian Khoon Lee, Wey Yih Heah; Kee Shyuan Loh; Nur Hasyareeda Hassan; Mohd Sukor Su'ait; Nuramylna Syafina Ahmad Nizam; Azizan Ahmad; Siti Aminah Mohd Noor

National Defence University of Malaysia

Abstract. High energy demand has driven the development of energy storage system worldwide. The success and implementation of lithium-ion batteries have raised the issue of lithium supplies to the industries. Series of polymer blend of poly(ethylene oxide) (PEO) -50% epoxidized natural rubber (ENR50) complexed with sodium trifluoromethanesulfonate (NaCF_3SO_3) based solid polymer electrolytes (SPEs) with different weight percentage of salts investigated for sodium-ion battery application. The maximum ionic conductivity obtained is $1.00 \times 10^{-5} \text{ S cm}^{-1}$ with 25 wt. % of NaCF_3SO_3 at room temperature and obeyed Arrhenius behaviour at two distinguish regions between 30°C to 60°C with activation energies (E_{a1}) at 1.27 eV and in second transition region between 60°C to 100°C with E_{a2} is 0.19 eV and pre-exponential factor, $\sigma_2 = 8.57 \times 10^{-2} \text{ S cm}^{-1}$. The conductivity transition at crossing point of these two linear regions has suggested that there is a correlation between temperature and solid-phase transition from a crystalline/semi-crystalline phase to a solid amorphous phase as proven by differential scanning calorimetry (DSC) investigation (T_m was found around $\sim 60^\circ\text{C} \pm 10^\circ\text{C}$). Higher sodium ion transference number was achieved at 0.23 in comparison to Li-based PEO-ENR50 electrolyte, 0.06. Whereas, both polymer electrolytes are ionically conducting with total ion transport of ca. 0.99 reflecting high ion dissociation of sodium salt in polymer electrolyte. Linear sweep voltammetry (LSV) indicated that Na-based polymer electrolyte has an electrochemical stability up to 5.0 V. Infrared analysis confirmed a polymer-salt interaction at ether functional group (1099 cm^{-1}) and thermal stability of SPE increase from 369°C and 503°C to 416°C and 522°C with addition of sodium salts due to the polymer-salt complexation. Above results suggested that PEO-ENR50- NaCF_3SO_3 has a promising potential to be applied as electrolyte in solid-state sodium ion battery.

ICSSST2019-110

The Effect of Sintering Temperature on Structural and Microwave Properties of Barium Hexaferrite Derived from Mill Scale

Nurshahiera Rosdi^{1,a}, Raba'ah Syahidah Azis^{1,2,b}, Ismayadi Ismail^{1,c}, Nurhidayat Mokhtar^{2,d}, Muhammad Misbah Zulkimi^{1,e}, Muhammad Syazwan Mustafa^{2,f}, Syazana Sulaiman^{1,g}

¹Materials Synthesis and Characterization Laboratory (MSCL), Institute of Advanced Technology (ITMA), Universiti Putra Malaysia, 43400 UPM Serdang, Selangor, Malaysia.

²Department of Physics, Faculty of Science, Universiti Putra Malaysia, 43400 UPM Serdang, Malaysia.

^anurshahierarosdi5243@gmail.com, ^brabaah@upm.edu.my, ^cismayadi@upm.edu.my,
^dhidayat@upm.edu.my, ^emuhammadmisbah1215@gmail.com, ^fmm_syazwan@upm.edu.my,
^gsyazana2104@gmail.com

Abstract. This project focused on the structural, magnetic and microwave properties of an M-type barium hexaferrite ($\text{BaFe}_{12}\text{O}_{19}$) derived from mill scale waste at a different sintering temperature (1000, 1100 and 1200 °C). The mill scale powder has been purified using impurity separation technique and magnetic separation technique, then oxidized at 500°C for 6 hours at 3°C/ mins to form hematite (Fe_2O_3). The comprise amount of BaCO_3 and Fe_2O_3 powder are ground mixing and the high-energy ball milling technique (HEBM) to prepare the barium hexaferrite ($\text{BaFe}_{12}\text{O}_{19}$). The as-prepared $\text{BaFe}_{12}\text{O}_{19}$ was characterized by several measurements such as X-ray Diffraction (XRD) and vibrating sample magnetometer (VSM) to observe their crystallography and the magnetic properties, respectively. The complex permittivity, permeability and the reflection loss ($RL\%$) were measured by a vector network analyzer in the range of 8–12 GHz (X-band). Samples morphology and the microstructure of samples was carried out using Field Emission Scanning Electron Microscope (FESEM) and found the average particles size of the sample was in the range of 160–177 nm. The results show that M-type barium hexaferrite sintered at 1200°C gives the best minimum reflection loss ($RL\%$) of -35.02 dB at the frequency 13.53 GHz with a bandwidth of 0.4 GHz for losses less than -10 dB at the thickness of 1 mm.

ICSSST2019-117

Acoustic Performance of Natural Fibres of Oil Palm Frond (OPF) and Empty Fruit Bunch (EFB)

R. Mageswaran^{1, a}, L.S. Ewe^{2, b*}, W.K. Yew^{3, c}, Zawawi Ibrahim^{4, d}

¹Collage of Engineering, Universiti Tenaga Nasional (UNITEN), Putrajaya Campus, Jalan IKRAM-UNITEN, 43000 Kajang, Selangor, Malaysia

²Collage of Engineering, Universiti Tenaga Nasional (UNITEN), Putrajaya Campus, Jalan IKRAM-UNITEN, 43000 Kajang, Selangor, Malaysia

³School of Engineering and Physical Science, Heriot-Watt University Malaysia, No 1, Jalan Venna P5/2, Precient 5, 62200, Putrajaya, Malaysia

⁴Engineering and Processing Division, Malaysian Palm Oil Board (MPOB), No 6, Persiaran Institusi Bnadar Baru Bangi, Kajang 43000, Selangor, Malaysia

^amageswaran1413@gmail.com, ^{b*}laysheng@uniten.edu.my, ^cw.yew@hw.ac.uk, ^dzawawi@mpob.gov.my

Abstract. The expansion of oil palm industry has affected the environment and the poor handling of oil palm waste has greatly endangered the habitat surrounds it. The oil palm natural fibre waste can be put to good use and used as sound absorber for its amazing acoustic properties. At the same time, the demand for natural fibre sound absorbing panel is increasing due to its low cost fabrication and its healthier than synthetic fibre. This research has studied the acoustic properties of mixing empty fruit bunch (EFB) and oil palm frond (OPF) in thickness of 12 mm, 14 mm, 16 mm and 18 mm. The fibreboard has been fabricated at density of 120 kg/m³. The sound absorption coefficient, SAC and morphologies of all the samples were examined using the Impedance Tube Method (ITM) and Scanning Electron Microscope, (SEM). The SAC values of all the samples increased with increasing in thickness. It is noteworthy that this combination percentage of natural fibres of EFB and OPF show good acoustic performance where the SAC values above 0.8 at wide frequency range of 3000 to 6400 Hz. Sample thickness 14 mm and 18 mm achieved unity (1.0) at frequency range of 4000 Hz to 5500 Hz. In addition, all the samples were found to exceed 90% of absorption rate in the range of 4500 Hz to 6400 Hz. The morphology content of EFB and OPF help in enhancing the absorption rate.

ICSSST2019-121

Band Structure and Thermoelectric Properties of Ni_(x)Zn_(1-x)Fe₂O₄

Lim Joon Hoong^{1, a*}

¹School of Engineering, Faculty of Built Environment, Engineering, Technology & Design, Taylor's University, Subang Jaya, Selangor, Malaysia

^{a*}JoonHoong.Lim@taylors.edu.my

Abstract. The band structure and thermoelectric properties of Ni_(x)Zn_(1-x)Fe₂O₄ have been investigated. The bulk pellets were prepared by appropriate amounts of analytical grade ZnO, NiO and Fe₂O₃ powder through solid-state method. It was possible to obtain high thermoelectric properties of Ni_(x)Zn_(1-x)Fe₂O₄ by controlling the ratios of dopant added and the temperature of the heat treatments. XRD analysis showed that the fabricated samples have a single phase formation of cubic spinel structure. The thermoelectric properties of Ni_(x)Zn_(1-x)Fe₂O₄ were improved when increasing Zn due to its high Seebeck coefficient and low thermal conductivity. It was found that the band gap of Ni_(x)Zn_(1-x)Fe₂O₄ becomes smaller with increasing Zn content and thus the electrical conductivity showed the highest electrical conductivity. The conductivity of the samples was found to be increased with increasing Zn content may due to presence of Fe³⁺ ions as Zn was added. Finally, it was reported that the electrical conductivity of ZnFe₂O₄ was higher than the conductivity of the NiFe₂O₄.

ICSSST2019-125

Photocatalyst Degradation of Methylene Blue by Using TiO₂-Graphene Composite

Mohd Fairul Sharin Bin Abdul Razak, Ong Soon Hin

UniMAP

Abstract. Inappropriate treatments of discharge wastewater from high colouring of concentrated dye in paint and textile industries are dangerous to the human and aquatic life due to the carcinogenic effect and chemicals toxicity. Therefore, by using a suitable treatment such as Advance Oxidation Process (AOP) of TiO₂ photocatalysis may reduce or even could fully treated of the polluted water into clean water. Moreover, with addition of graphene into TiO₂ system had increased the efficiency of TiO₂ photocatalysis by improving the amount of oxide radicals react with the dye radicals and eliminates the possibility any chances of recombination of photons and electrons during photodegradation process. Graphene/TiO₂ immobilized system was prepared by coated onto the glass supported by PVA/PVC binder. The adhesion of the immobilized system was fixed at ratio 1:0.025 of PVA/PVC binders. As a result, graphene/oxide immobilized system had improved the decolorization rate of methylene blue dye and by prolong the process treatment may improve the quality of treated dye with high sustainability photocatalytic process under good adhesion strength with lower cost. Indeed, the addition of binders also provides better surfaces and denser flat structure.

ICSSST2019-146

Development of a Computer-based Data Acquisition and Performance Analysis of Fuzzy-PID Hybrid Temperature Control for TorrefactionH.S. Chua^{1,a*}, Lee Pui Min^{1,b}, Ahmed.O.MohamedZain^{2,c}, J. Jamaludin^{1,d}, Alireza Zourmand^{1,e}, Yap. K. M^{2,f}, Momamed J.K.Bashir^{3,g} and K.T. Tan^{3,h}¹School of Engineering KDU University College, Selangor, Malaysia²School of Science and Technology, Sunway University Bandar Sunway, Malaysia³Faculty of Engineering and Green Technology (FEGT), Universiti Tunku Abdul Rahman, Kampar, Perak*hs.chua@kdu.edu.my, ^bjackson961@hotmail.com, ^cahmedalzain90@hotmail.com, ^djailani.j@kdu.edu.my, ^ea.zourmand@kdu.edu.my, ^fkmyap@sunway.edu.my, ^gjkbashir@utar.edu.my, ^htankt@utar.edu.my

Abstract. Malaysia produces on average 30,000 tonnes municipal solid waste (MSW) daily to these saturated disposal landfill. Therefore, Malaysia has initiated a Waste-To-Energy (WtE) treatment system project to be implemented near to sanitary landfills. But, pre-treatment of the MSW plays an important role before incineration. Unfortunately, MSW in its natural state is not an efficient method approach hence, processing treatments which enhance the properties such as moisture content (MC) and higher heating value (HHV) of the MSW are rising to attention. One of the processing treatments is known as torrefaction process which is a thermal decomposition process of MSW at a temperature between 130°C to 300°C. The main objective of this study is to compare and study the performance of hybrid fuzzy-PWM and PID controller on regulating the temperature level on the torrefaction process during the thermal decomposition. Each controller has its own downside effects in output response such as long rise time, high overshoot percentage and long settling time. This research aims to study the effect of PID and Fuzzy-PWM hybrid controller for temperature control during the torrefaction process. The PID controller is manually tuned resulting in 7 different forms of tuning parameters. The most suitable PID tuning is chosen based on shortest rise time, lowest percentage overshoot and lowest peak temperature. As for fuzzy controller, there are 5 different forms of rule bases established for fuzzy controller. The most suitable fuzzy controller is chosen based on shortest settling time, lowest overshoot percentage and lowest peak temperature. The best PID and fuzzy controllers are used to develop the hybrid controller. As a conclusion, the hybrid controller has the ability to perform temperature control at 130°C and 150°C by exhibiting shorter rise time by 30%, shorter settling time by 14% and lower overshoot percentage by 94% as compared to conventional PID or fuzzy controllers in the industry.

ICSSST2019-147

Structural and Conductivity Properties of Na₂ZnSiO₄-Py₁₄TFSI Hybrid Solid Electrolyte for Sodium-ion BatteriesJohari NSM^{1,a} and Adnan SBR^{*2,b}¹Institute of Advanced Studies, University of Malaya, 50603 Kuala Lumpur, Malaysia²Centre for Foundation Studies in Science, University of Malaya, 50603 Kuala Lumpur, Malaysia^asofina.johari@gmail.com, ^bsyed_bahari@um.edu.my

Abstract. Sodium-Ion Batteries has emerged as a potential alternative to the conventional Lithium-Ion Batteries, with current research focusing mainly on realising an all-solid-state battery system. In building a highly conducting hybrid electrolyte, Na₂ZnSiO₄ was synthesized using sol-gel method and then infused with ionic liquid Py₁₄TFSI. Crystal structure of hybrid Na₂ZnSiO₄ electrolyte was characterized by X-ray diffraction and refined by Rietveld method, showing phase purity at almost 100%. FTIR and FESEM-EDX measurements indicated that Py₁₄TFSI did not change the Na₂ZnSiO₄ structure and fill up the pores within the crystalline pellet. Highest conductivity value obtained by the hybrid solid electrolyte system of Na₂ZnSiO₄-Py₁₄TFSI is 5.0 x 10⁻³ Scm⁻¹ at 498 K.

v

ICSSST2019-160

Improved Performance of Inverted Type Organic Solar Cell Using Copper Iodide-doped P3HT:PCBM as Active LayerFarah Liyana Khairulaman^a, Chi Chin Yap^{b*}, Mohammad Hafizuddin Hj Jumali^c

School of Applied Physics, Faculty of Science and Technology, Universiti Kebangsaan Malaysia, 43600 UKM Bangi, Selangor, Malaysia.

^afarahbbs@gmail.com, ^bccyap@ukm.edu.my, ^chafizhj@ukm.edu.my

Abstract. Solution-dispersed copper iodide (CuI) anode buffer layer has been reported previously to improve the photovoltaic performance of inverted type organic solar cell. In this work, instead of being deposited as separate layer, CuI was doped directly into an active layer of poly(3-hexylthiophene) (P3HT):(6,6)-phenyl-C61-butyric acid methyl ester (PCBM). Zinc oxide (ZnO) thin film, serving as cathode buffer layer, was spin coated on cleaned fluorine-doped tin oxide (FTO) glass substrates. The undoped and 6 wt% CuI-doped P3HT:PCBM layers were then spin coated on top of ZnO and silver (Ag), acting as the top electrode, was deposited via thermal evaporation method. It was found that the solar cell with CuI doping achieved a better power conversion efficiency of 2.10% compared to the reference device with undoped P3HT:PCBM active layer (1.86%).

ICSSST2019-170

Effect of Vanadium Doping on Thermoelectric Properties of CaMnO_3 using First Principle CalculationsAbdullah Chik^{1,a}, Ruhiyuddin Mohd Zaki^b; Akeem Adekunle Adewale^c; Faizul Che Pa^d; Yeoh Cheow Keat^e^bruhiyuddin@unimap.edu.my, ^cadewaleakeem12@gmail.com, ^dfaizul@unimap.edu.my, ^ekyeoh@unimap.edu.my

Abstract. The study of thermoelectric materials that can convert heat to electricity is due to the search for clean energy conversion technologies. The dimensionless figure of merit (ZT) is a parameter for comparing thermoelectric materials and any materials display ZT more than or equal to 1, that is indicator for the materials to be useful for practical applications. Currently there are materials that exceed these value, however oxides with low ZT are considered promising due to less toxicity and stability at high temperature. In this paper, the electronic structure and thermoelectric properties of CaMnO_3 doped with 17% d block transition metal V using first principles calculations and semi-classic Boltzmann theory on Ca site as well as Mn sites. The G-type AFM phase is most stable among five phases for V doped CaMnO_3 a Mn site while V doped CaMnO_3 at Ca site displayed a stable A type AFM phase. The calculated band structure of V doped at Ca site shown the sample exhibit metallic behavior while V doped at Mn site sample shows a semi metallic behavior. The calculated partial density of states plot for V doped at A site shows that V d orbital electrons density of states has a highest peak and situated close to Fermi level at valence band and conduction band. The density of states of V d orbital electrons for V doped at Mn site has highest peak at the conduction band closed also to the Fermi level. However, the band gap is still there but V doping has brought the Fermi level to the conduction band to change the CaMnO_3 from semiconducting behavior to the semi metallic behavior. Thermoelectric property calculations show that the magnitude of Seebeck coefficient decreased with V doping at both sites with V doping at Mn sites has the lowest magnitude of Seebeck coefficient. All samples show the negative Seebeck coefficient indicating n type behavior. The magnitude of conductivity increases with V doping with the highest magnitude belong to V doped at Mn site. The magnitude of thermal conductivity also increased with V doping at Mn site, but shows a reduction for V doping at Ca site. The figure of merit ZT for V doping at Ca site shows a significant improvement over pure CaMnO_3 at 0.57 at 800 K. However, V doping at Mn site sample shows a reduction of ZT, lower than pure CaMnO_3 at 0.002 at 800 K compare to 0.007 for CaMnO_3 at 800 K.

ICSSST2019-176

Fabrication of Porous ZnO:Al Nanostructures Using Microwave Assisted Hydrothermal MethodNoor J. Ridha^{1, a *}, Firas K. Mohamad Alosfur¹ and Mohammad Hafizuddin Haji Jumali^{2, b}¹Department of Physics, College of Science, University of Kerbala, Iraq.²School of Applied Physics, Faculty of Science and Technology, Universiti Kebangsaan Malaysia, 43600 UKM Bangi, Malaysia.^anoor.jawad@uokerbala.edu.iq, ^bhafizhj@ukm.edu.my

Abstract. The aim this work is to investigate the effect of Al layer thickness on the formation of ZnO nanostructures synthesized using microwave assisted hydrothermal method. Five different Al thicknesses (0, 10, 30, 50, and 150 nm) were deposited on the Si substrates. Subsequently, ZnO seeds were spincoated on the layer followed by immersion in ZnO growth solution. The microwave power and the growth period were fixed at 10% and 30 min, respectively. Without Al layer, common ZnO nanorods with length and diameter of 350 nm and 50 nm respectively were observed. By comparison, all samples with Al layer exhibited the formation of flaky structures with thickness between 10 nm and 20 nm. The height of the nanoflakes was directly dependent on the thickness of Al layer. These thin nanoflakes are linked together producing large scale porous nanostructures. Thin film XRD confirmed the formation of ZnO wurtzite based structure without any secondary crystalline phase. The steady increment in I_{002}/I_{101} with thicker Al layer represented strong c-direction growth of the crystal. Although all samples with Al layer exhibited continuous improvement in ethanol vapor detection sensitivity, lowering the operating temperature remains as the major challenge. The possible construction mechanism of the unique ZnO nanoflakes grown using the present approach will also be presented.

Metal and Alloys

ICSSST2019-080

The Effect of Blast Exposure Distance on Hardness and Reduced Modulus Properties of Lead Free Solder

Wan Yusmawati Wan Yusoff^{1,a*}, Nur Shafiqah Safee^{1,b}, Ariffin Ismail^{1,c}, Norliza Ismail^{2,d}, Maria Abu Bakar^{2,e} and Azman Jalar^{2,f}

¹Centre for Defence Foundation Studies, Universiti Pertahanan Nasional Malaysia, Kem Sungai Besi, 57000 Kuala Lumpur, Malaysia.

²Institute Microengineering and Nanoelectronics, Universiti Kebangsaan Malaysia, 43600 Bangi, Selangor, Malaysia.

*ayusmawati@upnm.edu.my

Abstract. The effect of blast exposure distance of lead free solder towards micromechanical properties has been investigated. Sn-Ag-Cu (SAC) solder exposed to 1000 g of Plastic Explosive. The soldered sample were place at 1 m, 2 m and 4m at distance from the blast source. The nanoindentation test was used in order to evaluate the distance of blast exposure effect on solder sample in more details and localized. Prior to nanoindentation test, the specimens were cross-sectioned diagonally. The constant load nanoindentation was performed at the center of solder to investigate the hardness and reduced modulus. The load-depth curve of nanoindentation for the blast exposure at 1 m distance has apparent the discontinuity during loading compared to control sample. The hardness value decreased as the distance from blast source increased. However, the hardness increased when the distance increased to 4 m. The results obtained from nanoindentation is important in assessing the effect of sample's distance from blast source.

ICSSST2019-139

The Effect of Cooling Rate at the Cooling Bed Step on the Volume Fraction of the Constituent Phases of the Tempcore Steel Rebar

Mohamed K. El-Fawkhry^{1,a}, A. Fathy^{2,b}, *A. El-Sherbiny^{3,c}

¹Central Metallurgical R&D Institute (CMRDI), Cairo, Egypt.

²Al Ezz Steel Rebars S.A.E., Cairo, Egypt.

³Mechanical design & Production Department, Faculty of Engineering, Cairo University, Cairo, Egypt.

^amohamed.elfawkhry@gmail.com, ^ba.fathy@ezzsteel.com, ^ca.elsherbiny@cu.edu.eg

Abstract. The tempcore process considers as the most widely process that is being used in the production of reinforced steel rebar. The normal tempcore process is fundamentally dependent on the amount of latent heat in the core of the steel rebar, and the cooling rate of the rebar cross section. Cooled water box and the cooling bed have a powerful effect on the cooling rate of the steel rebar. This research has been designed to monitor the continuous cooling transformation CCT diagram of steel rebar with different two contents of residual elements. Moreover, the effect of cooling bed's conditions has been simulated to identify the effect of cooling rate at the cooling bed step on the microstructure, as well as the hardness value of the produced steel rebar. It was found that the cooling rate at the cooling bed step has a great powerful effect on the produced steel rebar in term of bainite phase increment, and the hardness value as well.

Nanoscience and Nanotechnology

ICSSST2019-009

Synthesis, Characterization and Catalytic Activity of Pd Nanoparticles Supported on Anatase (Pd/TiO₂)Norli Abdullah^{1*}, Hasliza Bahruji²¹Department of Chemistry & Biology, Centre for Defence Foundation Studies, National Defence University of Malaysia, Malaysia.²Centre of Advanced Material and Energy Science, University Brunei Darussalam, Jalan Tungku Link, BE 1410, Brunei Darussalam.

*norli.abdullah@upnm.edu.my

Abstract. Palladium nanoparticles immobilized onto anatase phase of TiO₂ were successfully synthesized by simple colloidal method. This catalyst was highly active and selective for the hydrogenation of cinnamaldehyde to hydrocinnamaldehyde at 50°C under low hydrogen pressure. The trend for conversion and selectivity in this liquid phase hydrogenation demonstrated the influenced of particle size diameter of the catalysts. Smaller diameter provide more active size thus results in 48% conversion and 60% selectivity to hydrocinnamaldehyde. Whereas larger particle size of 5.5 nm gives lower conversion and selectivity.

ICSSST2019-020

Synthesis and Controlled Release Properties of Nanohybrid Zinc-Aluminium Layered Double Hydroxide -CaptoprilZaemah binti Jubri^{1*}, Anissa Azlan¹, Siti Halimah Sarijo², Monica Limau Anak Jadam²¹College of Engineering, Universiti Tenaga Nasional, 43000 Kajang, Selangor, Malaysia.²Faculty of Applied Sciences, Universiti Teknologi MARA, 40450 Shah Alam, Selangor, Malaysia.

*zaemah@uniten.edu.my

Abstract. An anti-hypertensive drug, captopril (CPL) was successfully intercalated into the interlayer spaces of zinc-aluminium-layered double hydroxide (ZLDH) for the formation of ZCPL hybrid nanocomposite by self-assembly method. The concentration of CPL used was 0.08 M and pH 7 in a constant 3:1 molar ratio of Zn:Al in the mother liquor. The intercalation of CPL was confirmed as the powder X-ray diffraction pattern (PXRD) showed an increased in the basal spacing from 8.91 Å in ZLDH to 9.69Å in the ZCPL hybrid nanocomposite. FTIR study showed the intercalated compound of ZCPL resembled the spectra of ZLDH and CPL thus indicating the presence of both functional groups in ZCPL spectra. CHNS analysis showed the ZCPL nanocomposite contains 30.63% (w/w) of CPL calculated based on the percentage of carbon in the sample. It was also found that the BET surface area increased from 1.7 m²/g to 10.9 m²/g for ZLDH and ZCPL, respectively. The release of CPL from the interlayer spaces of ZCPL was done in 0.0001 M phosphate, carbonate, nitrate, and normal saline solutions with percentage released of 48, 30, 24 and 19%, respectively. This study suggests that ZLDH can be used as a carrier for drugs that allow safe and controlled delivery of various bio agents into target with high efficiency.

ICSSST2019-028

Study on the Impact of pH Adjustment to Remove Metallic Ions using MembranesN. Kasim^{1*}, A.W. Mohammad^{2,3}, S.R.S.Rozaimah²

¹Department of Chemistry and Biology, Centre for Defence Foundation Studies, National Defence University of Malaysia, 57000 Kuala Lumpur.

²Research Centre for Sustainable Process Technology (CESPRO), Faculty of Engineering and Built Environment, Universiti Kebangsaan Malaysia, 43600 UKM Bangi, Selangor, Malaysia.

³Department of Chemistry, Centre for Defence Foundation Studies, National Defence University of Malaysia, Kem Sg. Besi, 57000 Kuala Lumpur, Malaysia.

*herdawati@upnm.edu.my

Abstract. Iron and manganese occur naturally in groundwater. Both metallic ions at excessive amounts normally contribute to rusty taste and reddish color to the water. Membrane technology may improve the conventional groundwater treatment method which commonly requires a large area and a lot of manpower. The present experimental work focused on membrane filtration of iron and manganese in order to study the influence of pH adjustment to the prepared artificial groundwater on permeates quality and membrane performance. In this study, two commercially available NF/UF membranes (TFC-SR3, GHSP) and a fabricated polysulfone UF membrane (GOS) are tested to examine their capabilities in treating groundwater for drinking water resources. In order to achieve WHO drinking water standard, permeate quality of the artificial groundwater is considered satisfy if iron and manganese have reached 0.3 and 0.1 ppm, respectively. Experimental results showed that pH at range of 3 to 11 have significantly improved membrane performance in terms of their rejection. Rejection of iron at feed concentration of 100 ppm increased as pH of feed solution increased for all tested membranes. However, the manganese rejection with feed concentration at 50 ppm showed different performance for each membrane. The solution pH played an important role in changing the membrane surface properties. This concludes that solute-membrane interaction mechanism has improved the performance of the tested membranes.

ICSSST2019-033

Enhanced Optical Efficiency of Graphene Oxide-coated Tellurite Glasses Doped with Erbium for Advanced Fiber Optics

Azlina Yahya^{1,2,a}, Muhammad Noorazlan Abd Azis^{1,2,b*}, Suriani Abu Bakar^{1,2}

¹Physics Department, Faculty of Science and Mathematics, Universiti Pendidikan Sultan Idris, 35900 Tanjung Malim, Perak, Malaysia.

²Nanotechnology Research Centre, Faculty of Science and Mathematics, Universiti Pendidikan Sultan Idris, 35900 Tanjung Malim, Perak, Malaysia.

^aazlinayahya15@gmail.com, ^bazlanmn@fsmt.upsi.edu.my

Abstract. Graphene oxide (GO) is a two-dimensional (2D) nanomaterials, which currently captured particular interest for optoelectronics and biotechnology applications. In this work, we experimentally utilize the coatings of GO for a single and double sides on the tellurite glass surface using the spray coating method, which can significantly enhance its optical characteristics. Due to an existence of a large amount of oxygen-containing functional groups, GO can readily make it possible to hold a great potential for the use of a coating layer on erbium oxide doped tellurite glass which has been successfully prepared via melt-quenching technique. The results of characterization through Field Emission Scanning Electron Microscopy (FESEM), X-ray Diffraction (XRD) and Fourier Transform Infrared (FT-IR) analyses of graphene oxide-coated tellurite glasses has been presented and the optical band gap energy was analyzed to be improved on the glass system. The structural analysis determined by XRD pattern proved the amorphous nature of the glass system and also the surface morphological of GO deposited on the glass surface was examined. The refractive index and electronic polarizability were calculated for the fabricated glasses. The experimental results reveal that the tellurite glasses coated with graphene oxide gives better performance compared to the uncoated glasses by its ability to enhance the band gap energy, considering its potential use for fiber optics applications.

ICSSST2019-036

Effect of Different Drying Method on the Morphology of Nanocellulose

Muhammad Syukri Mohamad Misenan^{1,a}, Nurjahirah Janudin^{1,b}, Mohd Faiz Norrrahim^{1,c}, Siti Hasnawati Jamal^{2,d}, Noor Aisyah Ahmad Shah^{2,e}, Norherdawati Kasim^{2,f}, Wan Yusmawati Wan Yusof^{2,g}, Wan Md Zin Wan Yunus^{3,h}, Victor Feizal Knight Victor Ernest^{1,i} and Noor Azilah Mohd Kasim^{1,j}

¹Centre for Chemical Defence, Universiti Pertahanan Nasional Malaysia, Kem Sg. Besi, 57000, Kuala Lumpur, Malaysia.

² Centre for Defence Foundation Studies, Universiti Pertahanan Nasional Malaysia, Kem Sg. Besi, 57000, Kuala Lumpur, Malaysia.

³ Centre for Tropicalisation (CENTROP), Universiti Pertahanan Nasional Malaysia, Kem Sg. Besi, 57000, Kuala Lumpur, Malaysia.

^asyukrimisenan@gmail.com, ^bnurjahirahjanudin@gmail.com, ^cfaiznorrrahim@gmail.com, ^dhasnawati@upnm.edu.my, ^eaisyah@upnm.edu.my, ^fherdawati@upnm.edu.my, ^gyusmawati@upnm.edu.my, ^hwanmdzin@upnm.edu.my, ⁱvictor.feizal@upnm.edu.my, ^jazilah@upnm.edu.my

Abstract. The effect of drying method on selected material properties of nanocellulose was investigated. Samples of nanofibrillated cellulose (NFC) and bacterial nano cellulose (BNC) were each subjected to two distinct drying methods: freeze drying and oven drying. The morphology of both nano cellulose were scanned by Field Emission Scanning Electron Microscopy (FESEM). The thermal stability and crystallinity of the dried nanocellulose were evaluated using thermogravimetric analysis (TGA) and X-ray diffraction.

ICSSST2019-045

Nanocellulose-based Filters as Novel Barrier Systems for Chemical Warfare Agents

Mohd Nor Faiz Norrahim^{1,a}, Wan Md Zin Wan Yunus^{2,b}, Victor Feizal Knight Victor Ernest @ Abd Shatar^{1,c}, Noor Aisyah Ahmad Shah^{2,d}, Wan Yusmawati Wan Yusoff^{2,e}, Siti Hasnawati Jamal^{2,f}, Norherdawati Kasim^{2,g}
Noor Azilah Mohd Kasim^{2,h*}

¹Research Centre for Chemical Defence, Universiti Pertahanan Nasional Malaysia, Kem Sungai Besi, 57000 Kuala Lumpur, Malaysia.

²Centre for Defence Foundation Studies, National Defence University of Malaysia, Kem Sungai Besi, 57000 Kuala Lumpur, Malaysia.

^afaiznorrahim@gmail.com, ^bwanmdzin@upnm.edu.my, ^cvictor.feizal@upnm.edu.my, ^daisyah@upnm.edu.my, ^eyusmawati@upnm.edu.my, ^fhasnawati@upnm.edu.my, ^gherdawati@upnm.edu.my, ^{h*}azilah@upnm.edu.my

Abstract. Current world events have made several countries as a target for terrorism. Chemical weapons are like nuclear weapons, which commonly referred to as weapons of mass destruction. Organophosphorus compounds have long been used as pesticides and have been developed into warfare nerve agents such as tabun, soman, sarin, VX, and others. They are highly toxic and considered to be the most dangerous chemical weapons. Development on protection material against of these weapons are gained interest among researcher. Nanocellulose is a renewable material that combines a high adsorption capacity, large surface area, high strength, chemical inertness, and versatile surface chemistry which make nanocellulose a very promising material for high-performance filters. Nanocellulose is expected could excellently remove chemicals agents in military. Therefore, the evaluation on the chemical interaction between nanocellulose and organophosphorus are important. The analyses of fourier-transform infrared spectroscopy (FT-IR), gas chromatography–mass spectrometry (GC-MS) and scanning electron microscopy - energy dispersive X-ray (SEM-EDX) were carried out in this study. This is the initial step to develop the nanocellulose as potential material for the military protection mask.

ICSSST2019-046

Synthesis of Calcium/Aluminium-Ciprofloxacin-Layered Double Hydroxide for A New Antibacterial Drug Formulation

Monica Limau Jadam^{1,a}, Siti Halimah Sarijo^{2,b*}

^{1,2}Faculty of Applied Sciences, Universiti Teknologi MARA, 40000 Shah Alam, Selangor, Malaysia.

^amonica.jadam@gmail.com, ^{b*}siti_halimah_404@yahoo.com

Abstract. An antibacterial drug, Ciprofloxacin (CP) was successfully encapsulated into Ca/Al-layered double hydroxide (CLDH) by anion exchange method at optimum condition of 0.2 M CP and molar ratio of Ca:Al = 3. The pH of the synthesis of Ca/Al-CP-LDH (CCPLDH) was kept constant at pH11. This successfully intercalation confirmed by patterns analysis from Powder X-Ray Diffraction (PXRD), Fourier Transform Infrared Spectroscopy (FTIR), Elemental Analysis (CHNS), Accelerated Surface Area and Porosity (ASAP) and Thermogravimetric and Derivative Thermo Gravimetric (TGA/DTG). Basal spacing of CLDH synthesized in this study observed from PXRD is 8.68 Å. Due to the inclusion of CP into the layered material, basal spacing expanded to 16.22 Å in CCPLDH. The FTIR spectra of the hybrid nanocomposite show resemblance peaks of the layered double hydroxide (LDH) and CP, indicating the inclusion of the drug anion into the LDH interlamellae. The percentage loading of CP calculated from the data obtained from CHNS analyzer is 75.85% (w/w) in CLDH. The physicochemical properties of the new formulation of drug, CCPLDH was significantly enhanced compared with the pure form, CP. This shows that the drug-inorganic layered material, CLDH has prospective application as the potential host of a novel drug delivery system.

ICSSST2019-089

Multi-walled Carbon Nanotubes Functionalized with Amide for Acetone Detection in VENUE Temperature

Nurjahirah Janudin^{1, a}, Norli Abdullah^{2, b}, Faizah Md Yasin^{3, c}, Mohd Hanif Yaacob^{4, d}, Muhammad Zamharir Ahmad^{5, e} and Noor Azilah Mohd Kasim^{2, f*}

¹Department of Defence Science, Faculty of Science and Defense Technology, National Defence University of Malaysia, Kem Sg. Besi, 57000, Kuala Lumpur, Malaysia.

²Department of Chemistry/Biology, Centre for Defence Foundation Studies, National Defence University of Malaysia, Kem Sg. Besi, 57000, Kuala Lumpur, Malaysia.

³Department of Chemical and Environmental Engineering, Faculty of Engineering, Putra University of Malaysia, Serdang, 43400, Malaysia.

⁴Wireless and Photonic Research Centre (WiPNET), Faculty of Engineering, Universiti Putra Malaysia, Serdang, 43400, Selangor, Malaysia.

⁵Biotechnology and Nanotechnology Research Centre, Malaysia Agricultural Research and Development Institute, Persiaran MARDI-UPM, Serdang, 43400, Selangor, Malaysia.

^anurjahirahjanudin@gmail.com, ^bnorli.abdullah@upnm.edu.my, ^cfmy@upm.edu.my, ^dhanif@upm.edu.my, ^ezamharir@mardi.gov.my, ^fazilah@upnm.edu.my

Abstract. The functionalization of multi-walled carbon nanotubes (CNT) with amide group is reported as an alternative to enhance response time, recovery time and sensitivity of detecting acetone gas. We have fabricated an interdigitated transducer (IDT) deposited with amide-functionalized CNT. The elemental compositional analysis was characterized using Energy Dispersion X-ray spectroscopy and CHNOS elemental analyzer. The detection of acetone gas was performed in room temperature and digital multimeter was employed to record the changes of resistivity of IDT upon exposure of acetone. Results showed that amide functional group increases sensitivity, shortens the response time as well as recovery time of the sensor.

ICSSST2019-094

Synthesis and Controlled Release Properties of Nanohybrid Zinc-Aluminium Layered Double Hydroxide – Captopril

Zaemah binti Jubri^{1*}, Anissa Azlan¹, Siti Halimah Sarijo², Monica Limau Anak Jadam²

¹College of Engineering, Universiti Tenaga Nasional, 43000 Kajang, Selangor, Malaysia

²Faculty of Applied Sciences, Universiti Teknologi MARA, 40450 Shah Alam, Selangor, Malaysia

*zaemah@uniten.edu.my

Abstract. An anti-hypertensive drug, captopril (CPL) was successfully intercalated into the interlayer spaces of zinc-aluminium-layered double hydroxide (ZLDH) for the formation of ZCPL hybrid nanocomposite by self-assembly method. The concentration of CPL used was 0.08 M and pH 7 in a constant 3:1 molar ratio of Zn:Al in the mother liquor. The intercalation of CPL was confirmed as the powder X-ray diffraction pattern (PXRD) showed an increased in the basal spacing from 8.91 Å in ZLDH to 9.69Å in the ZCPL hybrid nanocomposite. FTIR study showed the intercalated compound of ZCPL resembled the spectra of ZLDH and CPL thus indicating the presence of both functional groups in ZCPL spectra. CHNS analysis showed the ZCPL nanocomposite contains 30.63% (w/w) of CPL calculated based on the percentage of carbon in the sample. It was also found that the BET surface area increased from 1.7 m²/g to 10.9 m²/g for ZLDH and ZCPL, respectively. The release of CPL from the interlayer spaces of ZCPL was done in 0.0001 M phosphate, carbonate, nitrate, and normal saline solutions with percentage released of 48, 30, 24 and 19%, respectively. This study suggests that ZLDH can be used as a carrier for drugs that allow safe and controlled delivery of various bio agents into target with high efficiency.

ICSSST2019-123

Supramolecular Interactions in Aromatic Structural Units for Non-Optical and Optical DetectionJuan Matmin^{1,a*}, Nur Fatiha Ghazalli^{2,b}, Fazira Ilyana Abdul Razak^{1,c} and Mohamad Azani Jalani^{3,d}¹Department of Chemistry, Faculty of Science, Universiti Teknologi Malaysia, 81310 Johor Bahru, Johor, Malaysia.²School of Dental Sciences, Health Campus, Universiti Sains Malaysia, Kubang Kerian, 16150, Kota Bharu, Kelantan, Malaysia.³Kolej GENIUS Insan, Universiti Sains Islam Malaysia, Bandar Baru Nilai, 71800 Nilai, Negeri Sembilan, Malaysia.^{a*}juanmatmin@utm.my, ^bfatiha85@usm.my, ^cfazirailyana@utm.my, ^dmazanijalani@usim.edu.my

Abstract. The scientific investigation based on the molecular design of aromatic compounds for high-performance chemosensor is challenging. This is because their multiplex interactions at the molecular level should be precisely determined before the desired compounds can be successfully employed as sensing materials. Here we report on the molecular design of chemosensors based on aromatic structural units of benzene as the organic motif of benzene-1,3,5-tricarboxamides (BTA) and as the side-chains of benzyl pyrazolate complexes (BPz), respectively. In the case of BTA, the aromatic benzene act as the core to enables the formation of π - π stacking for one-dimensional materials having rod-like arrangements stabilized by threefold hydrogen bonding. We found that on the addition of nitrate the rod-like BTA spontaneously turned into random aggregate due to deformation of their hydrogen bonding to form inactive nitroso groups for non-optical detection capability. For optical detection, the aromatic benzene is placed as the side-chain of BPz ensuring cage-shaped molecules and benefiting the most from their central metal-metal interactions for fluorescence-based sensing materials. In particular, on benzene exposure, the Cu-BPz demonstrate blue-shift of its original emission band from 616 to 572 nm ($\Delta\lambda = 44$ nm) and emitted bright orange to green emission colours. We also observe a different mode of fluorescence-based sensing materials for Au-BPz that shows a specific quenching mechanism resulting 81% loss of its original intensity on benzene exposure to give less emissive of red-orange colour ($\lambda = 612$ nm). These synthesized compounds of BTA and BPz are promising materials for high-performance supramolecular chemosensor based on non-optical and optical detection of a particular interest analyte.

Optical and Dielectric Materials

ICSSST2019-035

High Dielectric Permittivity of La_{0.88}Bi_{0.12}Mn_{0.80}Ni_{0.20}O₃ CompositeAaliyawani Ezzerin Sinin^a, Walter Charles Primus^b, Zainal Abidin Talib^c, Chen Soo Kien^d, Abdul Halim Shaari^e, Sinin Hamdan^f^aaaliyawanisinin@gmail.com, ^bwalter@upm.edu.my, ^czainalat@upm.edu.my, ^dchensk@upm.edu.my, ^eahalim@upm.edu.my, ^fhsinin@unimas.my

Abstract. Composite La_{0.88}Bi_{0.12}Mn_{0.80}Ni_{0.20}O₃ was synthesized using the conventional solid-state reaction method with sintering temperature of 1200 °C for 12 hours and the dielectric properties investigated. The X-ray diffraction result shows that the composite has a rhombohedral $R\bar{3}C$ structure with lattice parameter of $a = 5.52 \text{ \AA}$, $b = 5.52 \text{ \AA}$, $c = 13.37 \text{ \AA}$. Scanning electron microscope shows grains with approximately 2.22 μm in size with presence of voids of 1.60 μm . The dielectric permittivity and dielectric loss was measured in the range of 298 K to 473 K and are both temperature and frequency dependent. At 1000 Hz to 100000 Hz, the ϵ' is around 10000 and the dielectric loss tangent, $\tan \delta$ is below 1.5 which can serve as a capacitor. Further analysis using circuit model reveals that the high ϵ' is due to the grain properties. The electric behavior of this composite is best represented by Quasi-dc model which consist of two universal capacitors in parallel. From the fitting, the value parameters obtained indicates high correlation of electrons between inter and intra-clusters. The activation energy, E_a calculated from the conductivity of the sample gives a value of 0.116 eV.

ICSSST2019-063

Dielectric and ac Conductivity Studies of SrXLiTeO₆ (X=La, Nd) Double PerovskitesMZM Halizan^{1a}, AK Yahya¹, Z. Mohamed^{1b*}¹Faculty of Applied Sciences, Universiti Teknologi MARA, 40450, Shah Alam, Selangor, Malaysia.^ahalizanzharfan@yahoo.com, ^{b*}zakiah626@salam.uitm.edu.my

Abstract. SrXLiTeO₆ (X=La, Nd) double perovskites were synthesized using solid-state reaction method to investigate the effects of different ion substitutions on structural, dielectric and ac conductivity properties using x-ray diffraction and electrical impedance spectroscopy measurements. The X-ray diffraction patterns at room temperature confirm both SrLaLiTeO₆ and SrNdLiTeO₆ compounds crystallize in monoclinic symmetry ($P2_1/n$ space group). Dielectric properties were evaluated using dielectric constant, ϵ' and dielectric tangent losses, $\tan \delta$. The compound shows significant frequency dispersion in its dielectric properties with non-Debye type plot with ϵ' and $\tan \delta$ shows enhancement and decrement with temperature, respectively for both compounds. At 1 MHz of all studied temperatures, X=Nd shows higher ϵ' values compared to X=La. The frequency dependent conductivity spectra follow the universal power law at all frequencies. The ac conductivity, σ_{ac} at 1MHz varies from $1.75 \times 10^{-4} \text{ Sm}^{-1}$ to $7.24 \times 10^{-3} \text{ Sm}^{-1}$ for compounds with X=La and Nd, respectively. Electrical measurements were influenced the contribution from the lattice at high frequencies. The σ_{ac} behaviour is due to the hopping of oxygen vacancies. Modulus analysis was performed to understand the mechanism of electrical transport process where it exhibits dispersion at both low and high frequencies, whereas non-Debye type relaxation was determined from variation in imaginary parts of modulus, M'' which shows dispersion at high frequencies.

ICSSST2019-177

High-Sensitivity Single/Double Layer Coating Side Polished Optical Fiber Refractive Index Sensor Based on Surface Plasmon Resonance

Rozalina Zakaria

Photonics Research Centre, Faculty Science, University of Malaya, 50603 Kuala Lumpur

rozalina@um.edu.my

Abstract. Here we propose a rigorous configuration of using surface plasmon resonance properties on a side polished optical fiber in various sensor applications. The used of Au, Ag, Co, Pt with combination of several materials like TiO₂ and 2D-material like graphene oxide, MoS₂ and WS₂ are our motivation. The experimental technique is mainly focused on using side-polished or D-shape optical fiber. The process starts from polishing single mode fiber (SMF) with diameter of 125/85 microns. The power loss will be deliberately obtained from the polish optical fiber with record of loss of each sample. The samples were then undergone coating process in the evacuated chamber in the electron beam machine. Variation of thicknesses has been set in order to observed the effects of Surface Plasmon waves (SPs) acting on the optical fiber. This talk will generally describe potential application based on the respective SPR own by certain materials from different aspects of fabrication namely thickness layer, annealing process, size distribution, size of particles and spacing of the particles. The properties of these materials will be studied from tunability of the wavelength for specific aspect of sensor. The characteristics own were then been combined with various materials such as TiO₂ and 2D materials to observed their performance. Thickness on titanium (Ti) surface plasmon resonance (SPR) optical fiber sensor. The present configuration is included side-polished optical fiber sensor, titanium (Ti) coating, MoS₂ and sensing medium. We perform the performance of the design sensor in terms of sensitivity, detection accuracy and quality factor. Addition of MoS₂ layer on the Ti for example; will increase overall sensitivity of the device. The polishing region is covered by metallic layer acted as active sensing medium as the interaction between the SPW, fiber mode and consequently the fiber mode attenuation depend strongly on the refractive index of analytes. Variations of analytes used such as water, 60% alcohol, sodium chloride, glucose and sucrose can be determined by monitoring changes in the wavelength at which the resonant attenuation of the fiber mode occurs.

ICSSST2019-183

Study of Dielectric Properties of Polycrystalline Ex situ Magnesium DiborideSoo Kien Chen^{1,3,a*}, Kwee Yong Tan^{1,b}, Kar Ban Tan^{2,c}, Kean Pah Lim^{1,d}, Mohd Mustafa Awang Kechik^{1,e} and Abdul Halim Shaari^{1,f}¹Department of Physics, Faculty of Science, Universiti Putra Malaysia, 43400, Serdang, Selangor, Malaysia²Department of Chemistry, Faculty of Science, Universiti Putra Malaysia, 43400, Serdang, Selangor, Malaysia³Institute of Advanced Technology (ITMA), Universiti Putra Malaysia, 43400, Serdang, Selangor, Malaysia*chensk@upm.edu.my, ^bkweeyong@gmail.com, ^ctankarban@upm.edu.my, ^dlimkp@upm.edu.my, ^emmak@upm.edu.my, ^fahalim@upm.edu.my

Abstract. In this work, dielectric properties of ex situ polycrystalline Magnesium Diboride (MgB₂) were investigated. The samples were obtained after sintering at 650 – 850 °C for an hour in argon gas flow. Measurements of dielectric permittivity, dielectric loss and alternating current conductivity were conducted in the frequency range of 100 Hz – 10 MHz at room temperature. X-ray diffraction (XRD) revealed the presence of dominant MgB₂ phase in the samples. However, phases of Mg-O and B-O were also observed. It was found that the unit cell volume increased with increasing sintering temperature. For the samples sintered at higher temperature, higher AC conductivity and dielectric loss were measured indicative of improved grain connectivity. The semicircle observed in the complex impedance plots together with the combined spectroscopy plots suggests that the electrical behavior of the samples is mainly due to the bulk and grain boundary responses. This is likely to be due to the presence of the insulating oxides at the grain boundaries as opposed to the conductive intragains.

ICSSST2019-187

Structural and Optical Properties of Europium Doped and Dysprosium Co-Doped with Yttrium Aluminium Garnet Nanocrystalline Powders Prepared by Combustion SynthesisAbd Rahman Tamuri^{1,a*}, Nurliyana Nabilah Ghazali^{1,b}, & Rosli Husin^{1,c}¹Physics Department, Universiti Teknologi Malaysia, 81310 Johor Bahru, Malaysia.*rahmantamuri@utm.my, ^bnabilahghazali@yahoo.com, ^croslihusin@utm.my

Abstract. This paper presents the study on synthesized the yttrium aluminium garnet (YAG), Europium-doped YAG (YAG:Eu) and, Europium and Dysprosium co-doped YAG (YAG:Eu,Dy) phosphors prepared by a Solution Combustion Synthesis (SCS) using a mixture of fuel (urea). The effects of Eu³⁺ and Dy³⁺ ions concentration and annealing temperature were studied by X-ray diffraction (XRD) and photoluminescence (PL). The YAG nanocrystalline powders were calcined in the temperature range of 900 °C to 1200 °C for 4 hours. The Europium and Dysprosium were added in different concentrations in the range of 0.1 at.% to 1.0 at.% to the coarsened pure YAG particles in order to understand its influences on the optical properties and sintered microstructure. The doping of YAG:Eu and co-doped of YAG:Eu,Dy were calcined at temperature of 1100 °C for 4h. The X-ray diffraction results show that the phosphors are single phase YAG with crystalline size ranging from 30 to 40 nm. The room temperature photoluminescence results confirmed the introduction of the ion in the host lattice and its optical activation for all the the Eu³⁺ and Dy³⁺ ions concentrations. The CIE1931 color coordinates shows that the samples emission lays in the near red region for Eu³⁺ ions concentration and near white region for addition of Eu³⁺ and Dy³⁺ ions concentration. The highest emission spectra intensity was achieved for a Eu³⁺ ions concentration of 1.0 at.% while 0.5 at.% for Dy³⁺ ions concentration and the ions luminescence were preferential excited with 395 nm for YAG:Eu while, 353 nm for YAG:Eu,Dy wavelength photons.

Organic Materials and Application

ICSSST2019-012

Corrosion and Microbial Inhibition Characteristic of Local Herb (Petai Belalang) on Stainless Steel (316L) in Seawater

Wan Mohamad Ikhmal Wan Mohamad Kamaruzzaman, Maria Fazira Mohd Fekeri^a, Wan Rafizah Wan Abdullah^b, Wan Mohd Norsani Wan Nik^c, Mohd Sabri Mohd Ghazali^d

Advanced Nano Materials (ANoMa) Research Group, School of Fundamental Science, Universiti Malaysia Terengganu, 21030 Kuala Nerus, Terengganu, Malaysia.

^amariafaziarafekeri@gmail.com, ^bwanrafizah@umt.edu.my, ^cniksani@umt.edu.my, ^dmohdsabri@umt.edu.my

Abstract: Corrosion is a phenomenal problem which affects most industries globally. The consequences of neglecting the issue may yield to catastrophic incidents such as the collapse of a structure and loss of human lives. Hence, the needs of an eco-friendly solution to counter the rising situation is essential. In this study, a green approach of utilizing the beneficial properties of *Leucaena leucocephala* leaves extract (LLE) as additive to a newly formulated coating to prevent localized corrosion on stainless steel 316L (SS316L) is introduced. The performance of coatings with LLE is studied by varying the additive concentration according to the weight percentage (wt.%) and tested against two different medium, i.e., artificial seawater and real environment for 60 days. Multiple characterizations were executed including Fourier Transform Infrared spectroscopy (FTIR), Ultraviolet-Visible spectroscopy (UV-Vis), X-Ray Diffraction (XRD), antimicrobial assay (well-diffusion method), Electrochemical Impedance spectroscopy (EIS), potentiodynamic polarization and Scanning Electron Microscope with Energy Dispersive X-Ray (SEM/EDX) to investigate the inhibitive properties of LLE and the stability of the new coatings in protecting the substrates. The presence of functional groups like carboxylic acid and carbonyl increase the strength of the coating and contribute to reducing the corrosion rate on SS316L. As an evidence, coating with the incorporation of 3% LLE possessed the optimum protection values for artificial seawater (60th day, $R_{ct} = 5.25 \times 10^3 \Omega \cdot \text{cm}^2$ and $CR = 3.21 \times 10^{-3} \text{ mm/year}$) and real environment (60th day, $R_{ct} = 14.50 \times 10^3 \Omega \cdot \text{cm}^2$ and $CR = 1.39 \times 10^{-2} \text{ mm/year}$). Moreover, it is also identified that the coatings with LLE decrease the corrosion current density, i_{corr} exponentially, implying that the inhibitive action is mixed-type. Based on the antimicrobial screening, coatings with LLE showed a good ability to stop the growth of both *S. aureus* and *P. aeruginosa* when compares with the commercialized antibiotic, gentamicin. Additionally, the morphological study is also in agreement with the electrochemical result of optimum LLE concentration. Thus, it can be concluded that the addition of 3% LLE in rosin-based coating can enhance the anticorrosive and antimicrobial properties of coating to protect SS316L from the surrounding aggressive nature.

ICSSST2019-027

Biosynthesis of Silver Particles Using *Citrus Microcarpa* Peel's ExtractGong Wee Jie^{1, a}, Masrina Mohd Nadzir^{1, b*} and Kalaivani Rangasamy^{1, c}¹School of Chemical Engineering, Engineering Campus, Universiti Sains Malaysia, 14300 Nibong Tebal, Penang, Malaysia.^awjgong10@gmail.com, ^{b*}chmasrina@usm.my, ^ckalai.eicc@gmail.com

Abstract. Biosynthesis of particles involves the use of safe biological agents as an eco-friendly and cost effective alternative to chemical synthesis. In this study, silver particles were biosynthesized by using silver nitrate and aqueous *Citrus Microcarpa* peel's extract as the reducing and stabilizing agent. The biosynthesized silver particles were confirmed and characterized by UV-Vis Spectroscopy, Scanning Electron Microscopy (SEM), Energy Dispersive X-ray Spectroscopy (EDX), and Dynamic Light Scattering (DLS). The UV-vis spectrum showed surface plasmon resonance (SPR) with maximum peak intensity around 450 nm. Images taken using SEM suggests that the silver particles were spherical in shape. The DLS studies show that silver particles have an average Z-diameter value of 235 nm with a polydispersity index of 0.363, which indicates the presence of agglomeration. The reaction parameters have a significant effect on the formation of silver particles. The highest absorbance recorded was 1.42 obtained under conditions of 72 hours reaction time, using 5 wt% peel extract to react with 8 mM silver nitrate solution in ratio of 1:5 (volume of 5 wt% peel extract to volume of 8 mM silver nitrate solution). Silver particles can be successfully synthesized by *Citrus Microcarpa* peel's extract, which has potential to replace chemical method.

v

ICSSST2019-030

Conductivity Mapping of SWCNT Dispersed in Conducting PolymerNurul Syahirah Nasuha Sa'aya^{1, a}, Norhana Abdul Halim^{2, b*}, Siti Zulaikha Ngah Demon², Norli Abdullah², Victor Feizal Victor Ernest@Abd Shatar^{3, c}, Muhammad Zamharir Ahmad^{4, d}¹Faculty of Defence Science and Technology, National Defence University of Malaysia, Sungai Besi Camp, 57000 Kuala Lumpur.²Centre for Defence Foundation Studies, National Defence University of Malaysia, Sungai Besi Camp, 57000 Kuala Lumpur.³Research Centre for Chemical Defence, National Defence University of Malaysia, Sungai Besi Camp, 57000 Kuala Lumpur.⁴Biotechnology & Nanotechnology Research Centre, Malaysian Agricultural Research & Development Institute, MARDI Headquarters, 43400 Serdang, Selangor.^a3181097@alfateh.upnm.edu.my, ^bnorhana@upnm.edu.my, ^cvictor.feizal@upnm.edu.my, ^dzamharir@mardi.gov.my

Abstract. Currently, Scanning Electron Microscopy (SEM) and High-resolution Transmission Electron Microscopy (HR-TEM) instruments were employed to characterize the state of carbon nanotube (CNT) dispersion in a polymer matrix. In our technique, conductivity mapping were obtained simultaneously with nanostructure surface mapping method to study first hand electrical properties of single walled carbon nanotubes and poly(3-hexylthiophene-2,5-diyl). Morphology and conductivity mapping of the nanocomposites characterized by Atomic Force Microscope PeakForce Tunneling (AFM-PF-TUNA) will be less time and cost consuming. Highest conductivity measured from our film is 3 nA from the lowest point of the film. FTIR and Raman vibrational modes spectra were obtained of the polymer after SWCNT incorporation.

ICSSST2019-034

Feasibility of Irradiated Corn-Based Bioplastics as Packaging Material

Nur Nadia Nasir and Siti Amira Othman*

Department of Physics and Chemistry, Faculty of Applied Sciences and Technology, Universiti Tun Hussein Onn Malaysia, 84600, Panchor, Johor.

*sitiamira@uthm.edu.my

Abstract. There is hot debate about using irradiated corn based bioplastic as packaging material. This review paper will be discussing and also to provide information on influence of radiation on the properties corn based bioplastic and its feasibility as packaging material. By using radiation, the properties of corn based bioplastic will be improve and also acceptable to use as packaging material. Irradiated corn based bioplastic also have wide range of technology, the availability, less harmful to environment and the most important is the potential to use as packaging material.

ICSSST2019-040

Synthesis of Antidote Conjugation with Oximes for Chemical Warfare AgentsMas Amira Idayu Abdul Razak^{1,a*}, Noor Azilah Mohd Kasim^{2,b*}, Noor Aisyah Ahmad Shah², Mohd Nor Faiz Norrahim², Feizal Victor Ernest@Abd Shatar^{3,c*} and Wan Md. Zin Wan Yunus³

¹Faculty of Defence Science and Technology, National Defence University of Malaysia, Sungai Besi Camp, 57000 Kuala Lumpur.

²Centre for Defence Foundation Studies, National Defence University of Malaysia, Sungai Besi Camp, 57000 Kuala Lumpur.

³Research Centre for Chemical Defence, National Defence University of Malaysia, Sungai Besi Camp, 57000 Kuala Lumpur.

*^amasamira920724@gmail.com, ^bazilah@upnm.edu.my, ^cvictor.feizal@upnm.edu.my

Abstract. Organophosphate compounds (OPs) are widely used as pesticides, softening agents, lubricant additives and therapeutic agents. Some OPs are declared as nerve agents. OPs compounds act by inhibiting the enzyme acetylcholinesterase (AChE), which is fundamental for the control of nervous impulses transmission. It is well known that oximes are effective for the reactivation of OPsinhibited AChE. 2-pyridinealdoxime (2-PAM) is one of the most favoured reactivator of inhibited AChE. However, AChE activity in the central nervous system (CNS) was not significant. 2-PAM cannot penetrate into the CNS because of the blood brain barrier (BBB). The BBB only allows free diffusion of small lipophilic and uncharged molecules. It was reported that, the BBB penetration of 2-PAM was approximately only 10%. Therefore, it was deemed necessary to develop a new reactivator that can easily penetrate the BBB. Novel conjugation of glucose-oximes is a great approach to increase the BBB penetration. This is because, the presence of the sugar moiety would be recognised by the facilitative glucose transporter located at BBB. Thus, higher reactivation potency of inhibited AChE could be achieved. This glucose-oxime conjugate will be characterised and identified by ¹H and ¹³C Nuclear Magnetic Resonance (NMR). The relatively high reactivation activities will be examined by in-vitro and in-vivo study by using rat. The limit of detection, quantification range and linearity of the calibration curve of the 2-PAM reactivator will also be determined. This glucose-oxime conjugate holds great promise for the medical treatment of OPs poisoning in CNS.

ICSSST2019-048

Synthesis of Carbide Lime Derived Solid Superbase Catalyst for Biodiesel ProductionHong Hua, Lim^{1, a}, Fei Ling, Pua^{1,2, b*}, Rohaya Othman^{3, c}, Yun Hin Taufiq-Yap^{4, d} and Sharifah Nabihah^{5, e}¹Department of Mechanical Engineering, College of Engineering, Universiti Tenaga Nasional, 43000 Kajang, Selangor, Malaysia.² Institute of Sustainable Engineering (ISE), Universiti Tenaga Nasional, 43000 Kajang, Selangor, Malaysia.³ Mineral Research Centre, Department of Mineral and Geoscience Malaysia, Jalan Sultan Azlan Shah, 31400, Ipoh, Perak.⁴ Catalysis Science and Technology Research Centre, Faculty of Science, Universiti Putra Malaysia, 43400 UPM Serdang, Selangor, Malaysia.^alimhonghua115@gmail.com, ^{b*}gracepua@uniten.edu.my, ^crohaya@jmg.gov.my; ^dtaufiq@upm.edu.my

Abstract. Nowadays, huge amounts of industrial waste are being generated around the world. Without proper disposal of the industrial waste, it can be harmful to the environment. However, the disposal of the waste could lead to very high costs. The rising rate carbide lime waste (CLW) which is known as lime slurry produced as a by-product of acetylene production, has warranted the need for the repurposing. Carbide lime composed mainly of calcium hydroxide with minor parts of calcium carbonate. Although calcium based catalyst being studied as one of the efficient heterogeneous catalyst to produce the methyl ester but the properties of the catalyst still can be improved by transforming it into superbase catalyst with stronger basic strength. In this study, calcium rich solid superbase catalyst was synthesized by mixing the CaO with ammonium carbonate. Production of biodiesel by using carbide lime derived solid superbase catalyst was studied. The new catalyst was prepared via two-step calcination and impregnation process. All the catalysts were characterized by X-ray diffraction, CO₂ temperature programmed desorption, Brunauer-Emmet-Teller isotherm and scanning electron microscope. The effect of different catalyst loading on transesterification reaction was studied by and Fourier Transform Infrared Spectroscopy (FTIR) analysis and comparing the biodiesel yield produced. Fatty acid methyl ester (FAME) was successfully synthesized with the presence of carbide lime waste derived solid superbase catalyst.

ICSSST2019-099

Discovering Picrocrocine from the Extraction of *Crocus* Species

Wan Nurin Nurjeha Wan Mohd Nazif, Hannis Fadzillah Mohsin, Syed Adnan Ali Shah and Ibtisam Abdul Wahab*

Faculty of Pharmacy, Universiti Teknologi MARA Selangor, Puncak Alam Campus, 42300 Bandar Puncak Alam, Selangor Darul Ehsan, Malaysia.

*ibtisam@uitm.edu.my

Abstract. The saffron or Azza'faran is one of the Islamic medicinal herbs. It is botanically known as *Crocus sativus* and classified in the iris family (Iridaceae). This plant is historically used as a food colouring and flavouring agent. It is actually among the most expensive spice in the world. In this study, the phytochemicals and the biological properties of *Crocus* species were reviewed. From the literatures, the extracts exhibited anti-Parkinson, anti-Alzheimer, antidepressant and antihyperlipidemic activities. The extracts were investigated to detect the biomolecules. Major organic constituents such as the crocin, picrocrocine and safranal could be acquired from this miracle herb. In the methodology, the dried stigmas of *Crocus sativus* were extracted through maceration with methanol. Liquid chromatography was used to differentiate the natural compositions of the *Crocus* plant. In conclusion, picrocrocine could be successfully detected from the spectroscopic analysis.

ICSSST2019-134

Green Approach in Anti-Corrosion Coating by using *Andrographis paniculata* Leaves Extract as Additives of Stainless Steel 316L in SeawaterMaria Fazira Mohd Fekeri^{1,2, a}, Wan Mohamad Ikhmal Wan Mohamad Kamaruzzaman^{1,2,b}, Azila Adnan¹ and , Mohd Sabri Mohd Ghazali^{1,2,3,c*}¹Advanced Nano Materials (ANoMa) Research Group, School of Fundamental Science, Universiti Malaysia Terengganu, 21030 Kuala Nerus, Terengganu, Malaysia.²Materials and Corrosion Research Group, Universiti Malaysia Terengganu, 21030 Kuala Nerus, Terengganu, Malaysia.³Institute of Biodiversity and Sustainable Development, Universiti Malaysia Terengganu, 21030 Kuala Nerus, Terengganu, Malaysia.^amariafazirafekeri@gmail.com, ^bikhmal007@gmail.com, ^cmohdsabri@umt.edu.my

Abstract. The analysis of anticorrosion coating by using *Andrographis paniculata* (kalmegh) leaves extract (KLE) as an additive to protect stainless steel 316L that immersed in seawater environment was successfully carried out. The anti-corrosive coating is the combination of selected binder, pigment, solvent, and additive. *Andrographis paniculata* leaves extract was selected as an additive due to excellent antioxidant properties. There are five types of coating with different concentration which are C1 (0 wt.%), C1 (3 wt.%), C1 (6 wt.%), C1 (9 wt.%) and C1 (12 wt.%). The coated substrate the immersed in seawater for 30 days and taken out for each subsequent 10 days for analysis. The analysis involves optical, electrochemical, and morphology studies. A few techniques involve including of Fourier transform infrared spectroscopy (FTIR), ultraviolet-visible spectroscopy (UV-Vis), electrochemical impedance spectroscopy (EIS), potentiodynamic polarization (PP) and scanning electron microscope with energy-dispersive x-ray spectroscopy (SEM/EDS). The result of FTIR shows several functional group presence in the KLE that can enhance anti-oxidation properties such as phenol, carboxylic acid, carbonyl, and amide. The presence of andrographolide compound obtained from UV-vis analysis at peak absorption spectrum 229 nm. Electrochemical analysis result from EIS, the most efficiency coating was predicted at C3. Hence, it has higher R_{ct} value and low C_{dl} value. The result in EIS is corresponding to PP; hence the result of corrosion rate at C3 is the lowest value, which is 0.00211 mm/year at 30th day immersion. The observation on the surface morphology of the coating also shows that C3 that has a smooth surface with less pitting, cracks, and salt precipitate when compared to another coating. The addition of KLE increases the efficiency of anticorrosion coating with optimum concentration, which is 6 wt.%.

Other Solid State Research

ICSSST2019-004

Computational Insights of Some Ruthenium Complexes with Azobenzene Derivatives for Non-Linear Optic ApplicationFazira Ilyana Abdul Razak^{1, a*}, and Pang Siew Woon^{2, b}¹ Chemistry Department, Faculty of Science, Universiti Teknologi Malaysia, Malaysia² Chemistry Department, Faculty of Science, Universiti Teknologi Malaysia, Malaysia^{a*}fazirailyana@utm.my, ^bsiewwoonyu@gmail.com

Abstract. Metal complexes containing different azobenzene derivatives with different substituents provide different nonlinear optic (NLO) property. However, investigative of NLO property through experimental study may consume time and cost. Hence, computational study through Hartree-Fock (HF) based on a 3-21G level and density functional theory (DFT) methods based on LANL2DZ/6-31G level were used to investigate the NLO property for three complexes; Complex A, B and C. It was discovered that DFT-based calculations were more accurate than HF in providing the best geometry structure based on the result of bond length and bond angle. The investigation through DFT method revealed that the three complexes possess a high NLO property based on the value of total frequency-dependent first hyperpolarizability, β_{tot} obtained at the wavelength of 1064 nm. It was revealed that Complex C possesses the highest NLO property with a value β_{tot} of 12414.87×10^{-30} esu, followed by Complex A (11828.63×10^{-30} esu) and Complex B (3372.10×10^{-30} esu) at 1064 nm. The high NLO property of Complex C as compared to others is due to the presence of strong electron donating and withdrawing group from the azobenzene derivatives, which promotes higher electron delocalization effect. Their NLO property studies also supported by the dipole moment and HOMO-LUMO energy gap calculation.

ICSSST2019-061

Optimum Lasing Cavity for Erbium Doped Zinc Tellurite Glass Doped with Ag Nanoparticles

Nur Aina Mardia Binti Adnan

rahimsahar@utm.my; ezzasyuhada@utm.my

Abstract. A laser cavity was constructed for excitation of Erbium Doped Zinc Tellurite Glass rods embedded with various concentration of Ag nanoparticles (TZEA). Central to the system is a Xenon flashlamp for optical pumping, and mirrors to amplify the light waves. The beams were made visible by detection using a phosphor card. The output of TZEA laser was characterized via spectrum analyser and was found that the spectrum dominated at line of 835 nm. The diameter of the beam spot on burn paper remains constant to rod diameter (6 mm) at high energy but linearly increases at low energy.

ICSSST2019-065

Microwave Absorption Properties of Monovalent Doped $\text{La}_{0.85}\text{Ag}_{0.15}\text{MnO}_3$ Manganite Prepared by Solid State Method

N.A.A. Apandi^{1,a}, N.Ibrahim^{1,b*}, Z.Awang^{2,c}, R.S.Azis^{3,d}, M.M. Syazwan^{3,e}, A.K. Yahya^{1,f}

¹ School of Physics and Materials Studies, Universiti Teknologi Mara, 40450 Shah Alam, Selangor, Malaysia

² Microwave Research Institute, Universiti Teknologi Mara, 40450 Shah Alam, Selangor, Malaysia

³Department of Physics, Faculty of Science, Universiti Putra Malaysia, UPM, 43400 Serdang, Selangor, Malaysia

^aaintrah@gmail.com, ^{b*}noraz954@salam.uitm.edu.my, ^czaiki437@salam.uitm.edu.my, ^drabaah@upm.edu.my, ^emm_syazwan@upm.edu.my, ^fahmad191@salam.uitm.edu.my

Abstract. The microwave absorption of $\text{La}_{0.85}\text{Ag}_{0.15}\text{MnO}_3$ which prepared by solid state method was investigated. An analysis on X-ray diffraction measured data using refinement technique confirmed the rhombohedral structure of the sample. The microstructure of the sample which characterized from field emission scanning electron microscope, FESEM micrograph shown an irregular shape. Electrical resistivity measurement of $\text{La}_{0.85}\text{Ag}_{0.15}\text{MnO}_3$ showed transitions from metallic behavior to insulating behavior with two peaks were observed at 230 K and 242 K. Magnetic susceptibility versus temperature measurement showed the sample exhibit ferromagnetic at room temperature. The real and imaginary parts of permittivity, permeability as well as microwave reflection loss were measured by vector network analyzer in the 8-18 GHz of frequency range. The reflection loss of $\text{La}_{0.85}\text{Ag}_{0.15}\text{MnO}_3$ sample reached -57.2 dB at 16.41 GHz and the bandwidth corresponding to reflection loss below -10 dB (90% absorption) was 2.67 GHz.

ICSSST2019-067

Electroresistance Effect Due to Mo Substitution at Mn-site in $\text{La}_{0.85}\text{Ag}_{0.15}\text{Mn}_{1-x}\text{Mo}_x\text{O}_3$ ($x = 0.00$ and 0.05) Monovalent doped Manganites

Muhammad Syazwan Bin Mohd Sabri^{1, a}, Nor Ain Athirah Binti Apandi^{2, b} and Norazila Binti Ibrahim^{3, c*}

^{1,2,3} Faculty of Applied Sciences, Universiti Teknologi MARA, 40450, Shah Alam, Selangor, Malaysia

^asyazwanstar@gmail.com, ^bathirah@gmail.com, ^{c*}noraz954@salam.uitm.edu.my

Abstract. The electroresistance, ER effect of $\text{La}_{0.85}\text{Ag}_{0.15}\text{Mn}_{1-x}\text{Mo}_x\text{O}_3$ ($x = 0.00$ and 0.05) samples which were prepared using solid method method have been investigated. Both samples showed transition from metallic behavior at low temperatures region to insulating behavior at high temperatures region under applied current of 5mA and 10mA. The metal-insulator transition temperatures, T_{MI} decreased from 284 K ($x = 0.00$) to 280 K ($x=0.05$) due to Mo^{6+} substitution at Mn-site under applied current of 5mA. The increased of applied current to 10 mA not much change the T_{MI} for both samples however decreased the resistivity in the temperature region from 20 K – 300 K. The ER effect which related to decreased of resistivity under increased of applied current was observed has a maximum value at the vicinity of T_{MI} with the value of 4355.07% ($x = 0.00$) and 1530% ($x = 0.05$). It is suggested that the decreased of resistivity at the vicinity of T_{MI} may possibly due to reduction of scattering effect of conduction electrons and also due to the growth of conductive filaments under increased of applied current. These results indicates the potential application of $\text{La}_{0.85}\text{Ag}_{0.15}\text{Mn}_{1-x}\text{Mo}_x\text{O}_3$ ($x = 0.00$ and 0.05) in spintronic devices.

ICSSST2019-078

Effect of Fe Partial Substitution at Mn-site on Electroresistance Behaviour in $\text{La}_{0.7}\text{Ba}_{0.3}\text{Mn}_{1-x}\text{Fe}_x\text{O}_3$ ($x = 0$ and 0.02) ManganitesM.S. Sazali^{1,2 a}, N. Ibrahim^{1,2 b *}, Z. Mohamed^{1,2 c}, R. Rajmi^{1,2 d}, A.K. Yahya^{1,2 e}¹Faculty of Applied Sciences, Universiti Teknologi MARA, 40450 Shah Alam, Malaysia²Superconductor Laboratory, Faculty of Applied Sciences, Universiti Teknologi MARA, 40450 Shah Alam, Malaysia^amuhammadsuffian93@yahoo.com, ^bnoraz954@uitm.edu.my, ^czakiah626@uitm.edu.my, ^drozilahrajmi@gmail.com, ^eahmad191@uitm.edu.my

Abstract. $\text{La}_{0.7}\text{Ba}_{0.3}\text{Mn}_{1-x}\text{Fe}_x\text{O}_3$ ($x = 0$ and 0.02) were prepared by using solid state synthesis method to investigate the effect of Fe^{3+} substitution at Mn-site on electrical behaviour and structural properties. An analysis of x-ray diffraction data using refinement method showed both $x = 0$ and $x = 0.02$ samples were in single phased and crystallized in rhombohedral R-3c structural. From p vs T curves shown resistivity decreased under increased of applied current of 10mA for both samples in the temperature range of 20K-300K. The electroresistance, ER effect was observed have a maximum value at the vicinity of metal-insulator transition temperature, TMI for both samples with the value of 18% ($x = 0$) and 20% ($x = 0.02$). The increased of ER max may related to development of filamentary conduction path under increased of applied current. It is suggested that Fe substitution favours the growth of magnetic inhomogeneity which contribute to the formation of conductive path under increased of applied current.

ICSSST2019-090

Green Approach of Rice (MR 219) Treatment using a 2-D Clinostat: Factorial Design AnalysisN.A. Zulkifli¹, C.C. Teoh², K.K. Ong^{3*}, Norliza A.B.⁴, U.F. Abdul Rauf⁵, W.M.Z. Wan Yunus⁶¹Department of Defence Science, Faculty of Defence Science and Technology, Universiti Pertahanan Nasional Malaysia, Kem Sungai Besi, 57000 Kuala Lumpur Malaysia²Engineering Research Centre, MARDI Headquarters, Persiaran MARDI-UPM, 43400 Serdang, Malaysia³Department of Chemistry and Biology, Centre for Defence Foundation Studies, Universiti Pertahanan Nasional Malaysia, Kem Sungai Besi, 57000 Kuala Lumpur, Malaysia⁴Biotechnology and Nanotechnology Research Centre, MARDI Headquarters, Persiaran MARDI-UPM, 43400 Serdang, Malaysia⁵Department of Mathematics, Centre for Defence Foundation Studies, Universiti Pertahanan Nasional Malaysia, Kem Sungai Besi, 57000 Kuala Lumpur, Malaysia⁶Centre for Tropicalisation, Universiti Pertahanan Nasional Malaysia, Kem Sungai Besi, 57000 Kuala Lumpur Malaysia

Abstract. A sustainable and green approach was applied to treat rice (MR 219) in order to improve the rice yield (1000-grain weight) using a 2-D clinostat. A 2³ full factorial experimental design technique was used to investigate the effects of distances of rice seeds from the center of clinostat (1.5 and 2.5 cm), rotation speeds (2 and 10 rpm) and periods (5 and 10 days) on 1000-grain weight of rice (variety of MR 219) at low and high levels. The results were analysed using the Student's t -test, analysis of variance and F -test by Minitab software to determine the significant factors that affected the yield. Main effects and interaction effects of the factors were also analysed statistically. The most significant variable was thus found to be distance of rice seeds from the center of clinostat followed by two interaction effects of rotation period and distance of rice seeds from the center of clinostat. Higher rice yield (28.96 g of 1000-grain weight) was achieved by the rice seeds treated with the clinorotation compared to that of control (23.06 g).

ICSSST2019-120

Effect of Fe Doping on the Structural, Electrical and Magnetic Properties of $\text{La}_{0.7}\text{Ca}_{0.3}\text{Mn}_{1-x}\text{Fe}_x\text{O}_3$ ($x = 0, 0.01, 0.03$ and 0.05) Perovskite Manganite Materials

Nor Azah Nik-Jaafar^{1,a*}, R. Abd-Shukor^{2,b} and K. Muhammad-Aizat^{2,c}

¹Pusat GENIUS@Pintar Negara, Universiti Kebangsaan Malaysia, 43600 UKM Bangi, Selangor, Malaysia

²School of Applied Physics, Faculty of Science and Technology, Universiti Kebangsaan Malaysia, 43600 UKM Bangi, Selangor, Malaysia

^{a*}norazah_nj@ukm.edu.my, ^bras@ukm.edu.my, ^caizatkamarudin1@gmail.com

Abstract. The effect of Fe-substitution at the Mn-site in $\text{La}_{0.7}\text{Ca}_{0.3}\text{Mn}_{1-x}\text{Fe}_x\text{O}_3$ ($x = 0, 0.01, 0.03$ and 0.05) on its structural, electrical and magnetic properties has been studied. These properties were investigated via X-ray diffraction (XRD) analysis, temperature-dependent resistance measurements and temperature dependent ac magnetic susceptibility measurements. XRD analysis showed all samples are single phase materials. Temperature dependent resistance measurements between 30–290 K showed all samples to undergo insulator-metal transition as temperature decreases. Increase in Fe doping for $x = 0, 0.01, 0.03$ and 0.05 causes the transition temperature T_{IM} to decrease from 257 K, 244 K, 205 K and 162 K respectively. The magnetic susceptibility measurements showed the samples to exhibit paramagnetic to ferromagnetic transition where the amount of Fe doping x progressively decrease the Curie temperature T_{C} from 230 K at $x = 0$ to 155 K at $x = 0.05$.

ICSSST2019-137

Synthesis and Characterization Barium M-Hexaferrites ($\text{BaFe}_{12-2x}\text{Co}_x\text{Mn}_x\text{Ni}_x\text{O}_{19}$) as a Microwave Absorbent Material

Susilawati^{1, a *} and Aris.Doyan^{2, b}

^{1,2}Master of Science Education Program, University of Mataram, Lombok, West Nusa Tenggara, Indonesia.

^{a*}susilawatihambali@unram.ac.id, ^baris_doyan@unram.ac.id

Abstract. This study aims to synthesis microwave absorbent material from barium M-hexaferrites which doped Co-Mn-Ni ions ($\text{BaFe}_{12-2x}\text{Co}_x\text{Mn}_x\text{Ni}_x\text{O}_{19}$) using co-precipitation method with varying concentrations ($x = 0.2, 0.4, 0.6, 0.8,$ and 1.0) and calcination temperatures at 200 to 800°C. Sample characterization was conducted to investigate the effect of doping concentration variations on the electrical, magnetic and microwave absorption properties using X-Ray Diffraction (XRD), Scanning Electron Microscope (SEM-EDX), Transmission Electron Microscope (TEM), Vibrating Sample Magnetometer (VSM), and Network Vector Analyzer (VNA). The results from XRD characterization showed that the sample formed the barium iron oxide ($\text{BaFe}_{12}\text{O}_{19}$) phase with $a = b = 4.35 \text{ \AA}$ and $c = 13.803 \text{ \AA}$. The results of SEM-EDX and TEM samples of $\text{BaFe}_{9.6}\text{Co}_{0.8}\text{Mn}_{0.8}\text{Ni}_{0.8}\text{O}_{19}$ showed that the sample size ranged from 79 - 165 nm and the hexagonal crystal structure was formed. The magnetic properties with VSM indicate that the sample coercivity value decreases significantly from 0.413 T at $x = 0.0$ to 0.097 T at $x = 0.8$, indicating that the sample is soft magnetic. The value of electrical conductivity is in the range of 0.5×10^{-4} to $13.81 \times 10^{-4} \text{ S/cm}$ which shows that the sample is semiconductor. Analysis of the absorption properties of microwaves with VNA produced maximum permittivity and permeability values of 28.4 and 54.4 at 10.3 GHz, and a maximum Reflection Loss (RL) value of -20.20 dB at a frequency of 15 GHz with an absorption coefficient of 99.05% at concentration $x = 0.6$. The high permittivity, permeability, RL, and absorption coefficients indicate that the $\text{BaFe}_{12-2x}\text{Co}_x\text{Mn}_x\text{Ni}_x\text{O}_{19}$ sample has the potential to be a microwave absorbent material on X-band to Ku-band frequency.

ICSSST2019-150

Solid State Synthesis and Characterization of Cu(II) and Ni(II) Polynuclear Metal Complexes With Ligand Derived from 3-Methoxy-4-Hydroxy Benzaldehyde and L-LeucineZainab Sulaiman^{1,2, a*} and Junaid Na'aliya^{2, b}¹Department of Science Laboratory Technology, College of Science and Technology, Hussaini Adamu Federal Polytechnic, Kazaure, Jigawa, Nigeria²Department of Pure and Industrial Chemistry, Bayero University, P. M. B. 3011, Kano, Nigeria^{a*}zsjahun@yahoo.com, ^bJna'aliya@yahoo.com

Abstract. Two polynuclear metal complexes with general formula $[M^{II}_3L_4(H_2O)_9].4.5H_2O$ and $[M^{II}_3L_3(H_2O)_9].5H_2O$ for Cu(II) and Ni(II) ions respectively, have been synthesized via the one step solid state synthesis with ligand derived from 3-methoxy-4-hydroxy benzaldehyde and L-Leucine. The compounds were characterized by elemental analysis, ESI-Mass spectrometry, infrared spectroscopy, thermogravimetric analysis (TGA) and conductivity measurements. Data from experimental results showed that the ligand binds to two metal centers in a Tridentate (O N O) manner through the imine nitrogen, phenolic and carboxylic oxygen respectively. Antimicrobial activities of the ligand and the coordination polymers were investigated and found active against some selected bacterial and fungal species.

v

ICSSST2019-178

Computational Designing of Energy Materials for Futuristic Technological ApplicationsRashid Ahmed^{1,2*}, Ali Hassan Tahir¹, Saira Shabbir², Bakhtiar Ul Haq³, Amiruddin Shaari², Maqsood Ahmed¹¹Center for High Energy Physics, University of the Punjab, Quaid-e-Azam Campus 54590-Lahore, Pakistan²Department of Physics, Faculty of Science, Universiti Teknologi Malaysia, 81310 Johor Bahru, Johor, Malaysia³Advanced Functional Materials & Optoelectronics Laboratory (AFMOL), Department of Physics, Faculty of Science, King Khalid University, P.O. Box 9004, Abha, Saudi Arabia

*rashidahmed.pu2@gmail.com

Abstract. The imperative need for more efficient, robust, non-toxic and cheaper energy materials has led to an increasing focus on more resourceful materials along with the devolvement of methods to characterize these materials. In the past, most of the innovation in material science was accomplished through exhausting laboratory experimentation. However, in the present era, this trend is rapidly transferring to quantum mechanically numerical modeling techniques for better understanding and tuning the materials electronic structure at atomistic level to achieve their required physical properties for advanced technological applications. Among these, first-principles approaches structured within density functional theory (DFT) are comprehensively employed to design and predict novel materials and tuning their properties accordingly. In this research work, very precise, robust, widely used state of the art full-potential (FP) linearized (L) augmented plane wave plus local orbital (APW+lo) method is applied to simulate, and then for the computation of the properties of the orthorhombic phase of tin monosulfide (SnS). To investigate electronic properties, FP-L(APW+lo) method is used in conjunction with modified approximations such as mBJ-GGA. Obtained results of structural, electronic and optical properties of the orthorhombic phase of SnS are presented. Moreover, our obtained results are also compared with the previous computational and experimental results on other phases of these important materials as well. The results of the presented work seem to be of fundamental importance and endorse the potential of its different phases for the fabrication of optoelectronics and photovoltaic applications.

ICSSST2019-179

GPU Based Computing For Application In Material Physics

Maqsood Ahmed*, Tariq Mahmood

Centre for High Energy Physics, University of the Punjab, Lahore-PAKISTAN

*maqssod1162@gmail.com

Abstract. With the advent of Graphical Processing Unit (GPU) it has now become possible to solve complex problems by using parallel processing techniques. The massively parallel nature GPU has made it capable of giving a performance in the range of Giga to Tera Flops as compared with traditional CPUs. GPUs are now extensively used in modern high-performance computing systems for their vast applications in the study of various properties of materials. We have studied the performance of Nvidia's GTX 640 GPU for QUANTUM ESPRESSO freeware software used to study electronic properties and material modeling.

Polymers and Composites

v

ICSSST2019-024

Mechanical Properties and Thermal Behavior of Poly(lactic acid) Composites Reinforced with TiO₂ NanofillerNur Ain Syafiqah Sudin^{1,a}, I.R.Mustapa^{1,b*}, Norlinda Daud^{2,c} and Mohammed Zorah¹¹Department of Physics, Faculty of Science and Mathematics, Universiti Pendidikan Sultan Idris, 35900, Tanjong Malim, Perak, Malaysia²Department of Chemistry, Faculty of Science and Mathematics, Universiti Pendidikan Sultan Idris, 35900, Tanjong Malim, Perak, Malaysia^aainpikah94@gmail.com, ^bizan.mustapa@gmail.com, ^cnorlinda@fsmpt.upsi.edu.my

Abstract. The reinforcement effect of nanofiller in polymer enhance the thermal stability, physical and mechanical properties of poly(lactic acid) (PLA) composites with good reinforcing capabilities for bio-based polymers. In this paper, the effect of reinforcement of titanium dioxide (TiO₂) nanofiller on the mechanical properties and thermal behavior of PLA matrix are reported. PLA/TiO₂ nanocomposites with different percentages of 2.0, 3.5, 5.0 and 7.0 %·w/w were prepared by using solvent casting method. TiO₂ were dispersed in PLA matrix using mechanical mixer and ultrasonication technique. The mechanical properties and thermal behavior of PLA nanocomposites were characterized using dynamic mechanical analysis (DMA) and differential scanning calorimeter (DSC). The increased in storage modulus by the addition of nanofiller with the highest increment provided by 2.0 %·w/w TiO₂ indicating a strong influence and better interfacial bonding between nanofiller and PLA matrix. An increase in storage modulus started at 100°C that linked to the cold crystallization (T_{cc}) of PLA composites is in agreement with DSC result. The T_{cc} shifted to higher temperature as the content of nanofiller increased and this result were observed at 2.0%·w/w of the nanofiller content. Reinforcement of nanofiller increased the melting temperature from lower filler loading until 5.0 %·w/w. The incorporation of TiO₂ nanofiller as the reinforcement agent for PLA has a potential in biopolymer medical engineering and packaging industry, a highly competitive application with a great demands of cost and performance.

ICSSST2019-038

Fatigue Crack Growth of Natural Rubber/Butadiene Rubber Blend Containing Waste Tyre Rubber PowdersDayang Habibah Abang Ismawi Hassim^{1, a*}, Frank Abraham^{2, b}, John Summerscales^{3, c}, Paul Brown^{4, d}¹Malaysian Rubber Board, RRIM Experiment Station, 47000, Sg.Buloh, Selangor, Malaysia^{2,3}School of Engineering, University of Plymouth, Plymouth PL4 8AA, United Kingdom⁴Tun Abdul Razak Research Centre (TARRC), Malaysian Rubber Board, Brickendonbury, SG13 8 NL Hertford, United Kingdom^{a*}dyghabibah@gmail.com, ^bfrank.abraham@plymouth.ac.uk, ^cJ.Summerscales@plymouth.ac.uk, ^dpbrown@tarrc.co.uk

Abstract. Mechanical properties such as tensile strength, abrasion and tear resistance give simple and quick information which are often used for quality control of rubber compounds. However, these tests do not describe rubber performance in dynamic conditions. Wear loss in tyres or cracking in rubber mountings is usually associated with crack growth due to repeated cyclic stress. Therefore, crack growth resistance is of great importance in determining the strength and durability of rubber products. Fatigue crack growth in NR/BR compound and the effect of two different types of recycled rubber powder (RRP) were studied using fracture mechanics approach. Absolute and relative hysteresis losses using single-edge notch tensile (SENT) specimens were determined with a displacement controlled strain compensating for permanent set of the samples throughout the Fatigue Crack Growth (FCG) experiments. Differences in relative hysteresis loss showed that additional energy dissipation, due to multiple new crack surfaces at the crack tip, contributes to the FCG of the RRP compounds. At higher tearing energy, beside other factors affecting the FCG performance of the RRP compounds, both higher absolute and relative hysteresis loss are slightly detrimental to the crack growth rates.

ICSSST2019-053

Enhancement of Heat Ageing Properties of Epoxidised Natural Rubber Blend for Automotive Application

Dr. Mazlina Mustafa Kamal

Abstract. In recent years, automotive hose and belt specifications have changed, requiring longer product life in terms of swelling, wear and heat ageing. Diene-based rubbers, such as natural rubber (NR) and styrene-butadiene rubber (SBR), have been widely used in diverse industries. However, some apparent defects such as limited ageing resistance and large compression set, have been demonstrated in some rubbers cured by sulfur or peroxides. In the making of general and industrial rubber goods, short production and sufficient scorch time is crucial especially by using an injection moulding. In this work, blend of Epoxidised Natural Rubber (ENR 25) and Butadiene was developed with two types of curing systems namely Conventional and Efficient Vulcanisation system. The aim of the study is to produce a satisfactory heat resistance rubber compounds and adequate process safety for rubber manufacturing. Results showed that curing system applied significantly affected thermal stability property of the compounds. Modulus and hardness of the blends appeared to decrease progressively with ageing. However, greater thermal stability especially ageing at 100°C for 200h was observed with compound containing efficient curing system compared to conventional curing system which corresponded to the cross link density attributed by the torque value and dynamic mechanical analysis.

ICSSST2019-054

Physical and Electrical Studies of High Molecular Weight Poly(Methyl Methacrylate) Based Solid Polymer ElectrolytesN Azhar^{1,a}, R Zakaria^{1,4,b}, M F M Taib^{1,c}, O H Hassan^{2,d}, M Z AYahya^{3,e} and A M M Ali^{1,4,f*}¹Faculty of Applied Sciences, Universiti Teknologi MARA, 40450 Shah Alam, Selangor, Malaysia²Faculty of Art & Design, Universiti Teknologi MARA, 40450 Shah Alam, Selangor, Malaysia³Faculty of Defence Science & Technology, Universiti Pertahanan Nasional Malaysia, 57000 Kuala Lumpur, Malaysia⁴Institute of Science, Universiti Teknologi MARA, 40450 Shah Alam, Selangor, Malaysia^afarlinaazhar@gmail.com, ^brosnah@uitm.edu.my, ^cmfariz@uitm.edu.my, ^doskar@uitm.edu.my, ^emzay@upnm.edu.my, ^{f*}ammali@uitm.edu.my

Abstract. In this work, a film contained a mixture of PMMA, salt, and plasticizer was prepared. PMMA is a host polymer, ammonium trifluoromethane sulphonate of ammonium triflate ($\text{NH}_4\text{CF}_3\text{SO}_3$) as a doping salt, and ethylene carbonate (EC) as a plasticizer was used in this present study. PMMA salt complexes system and plasticized PMMA salt complexes system were prepared by solution cast technique at room temperature. FTIR was used to study the interaction between polymer and salt, and between polymer-salt and plasticizer. The C=O band stretching mode observed was broadened and shifted to lower wavenumber when ammonium triflate was added into PMMA. The broadening, shifting and reduction in wavenumbers of FTIR spectra show that the complexation has occurred between the polymer and salt. EIS was used to measure the electrical conductivity of the system prepared at ambient temperature. The electrical conductivity of film containing 1.0g of PMMA – 35 wt% $\text{NH}_4\text{CF}_3\text{SO}_3$ – 16 wt% EC exhibit the highest electrical conductivity with the value is $2.461 \times 10^{-4} \text{ S/cm}^2$. XRD was used to study the pattern of pure PMMA, PMMA – $\text{NH}_4\text{CF}_3\text{SO}_3$ and PMMA – $\text{NH}_4\text{CF}_3\text{SO}_3$ – EC. The addition of plasticizer to the polymer electrolytes increase the amorphous region of the polymer host and reduce its crystallinity. The conductivity increases with the increase of amorphous.

ICSSST2019-062

A Study on Milling Time and Composition of Mechanical Milled Graphite Powder Effect as Filler in MDPE Composite to Physical and Tensile PropertiesCheah Woi Leong^{1,a}, Engku Abd Ghapur Engku Ali^{2,b*} and Mohd Aidil Adhha Abdullah^{3,c}¹School of Fundamental Science, Universiti Malaysia Terengganu, 21030 Kuala Nerus, Terengganu, Malaysia²Advanced Nano Materials (ANoMa) Research Group, School of Fundamental Science, Universiti Malaysia Terengganu, 21030 Kuala Nerus, Terengganu, Malaysia^arain_tly@yahoo.com, ^{b*}engku_ghapur@umt.edu.my, ^caidil@umt.edu.my

Abstract. Effects of milled graphite composition on the physical and tensile properties of medium density polyethylene (MDPE)/graphite composite were investigated. The milled graphite powders were mixed with the MDPE by using the melt blending process. The addition of graphite content did not change much on surface chemistry of MDPE. Graphite that was milled for 50 hours still in crystalline phase but the crystallite size decreased with the increment of the milling time. For MDPE/graphite composite with 4 wt% of 50 hours milled graphite mixed with MDPE, the value of the young's modulus was 872.44 N/mm^2 which was 34% higher than the MDPE-graphite composite with 1 wt% of unmilled graphite mixed with MDPE showing the value of young's modulus of 651.91 N/mm^2 . SEM micrograph shows that when milling time increased, the decreased in particle size of graphite was observed. When this smaller size particle mixed with MDPE, the better mechanical properties of composites were obtained.

ICSSST2019-071

Thermomechanical Study and Thermal Behavior of Plasticized Poly(lactic Acid) CompositesMohammed Zorah^{1,a}, I. R. Mustapa^{1,b*}, Norlinda Daud^{1,c}, Nahida J.H.^{2,d} and N. A. S. Sudin^{1,e}¹Department of Physics, Faculty of Science and Mathematics, Universiti Pendidikan Sultan Idris, 35900, Tanjung Malim, Perak, Malaysia²Applied Science Department, University of Technology, Baghdad, Iraq^a Mohamed.n224@yahoo.com, ^{b*} izan.mustapa@gmail.com, ^c norlinda@fsmt.upsi.edu.my, ^d nahidajoumaa61@yahoo.com, ^e ainpikah94@gmail.com.

Abstract: Poly(lactic acid) (PLA) is a biodegradable aliphatic polyester well suited for various applications. PLA was plasticized with tributyl citrate (TBC) as plasticizer in PLA to modify PLA properties. The efficiency of varying TBC contents on the morphology, thermomechanical properties and thermal behavior of PLA/TBC composites were evaluated. FESEM images of plasticized PLA revealed homogeneous fractured surfaces. The polycrystallinity of PLA/TBC composites was increased with the rise in the plasticizer content without altering its transparency significantly. With the increase of TBC contents the temperatures for glass transition, the cold crystallization as well as the melting was discerned to be lowered. Furthermore, the dynamic mechanical analysis disclosed a drop in the storage modulus as much as 2.2 GPa at 7% of TBC inclusion wherein the peak value of $\tan \delta$ was increased, indicating an enhanced flexibility of TBC modified PLA. It was asserted that the inflexibility and brittleness associated with pristine PLA can considerably be improved by activating it with the additive plasticizer TBC.

ICSSST2019-108

Investigation of Chemical and Optical Properties of Polystyrene/Silver NanocompositesJibrin Alhaji Yabagi^{1,a}, Mohammed Isah Kimpa³, Babakatcha Ndanusa¹, Embong Zaidi² Mohd Arif Agam^{2,b}¹Department of Physics Ibrahim Badamasi Babangida University Niger State Nigeria Lapai²Department of Science, University Tun Hussein Onn Malaysia, 84600 Pagoh, Johor Malaysia.³Department of Physics Federal University of Technology Minna Niger State Nigeria Bosso^a jibrinyabagi@ibbu.edu.ng, ^b arif@uthm.edu.my

Abstract. Nanocomposites are materials that combine the unique properties of both constituents in one material that are found to have diverse applications such as optical device, diamond-like carbon, sensors and microwave absorbance materials. Polymer nanocomposites consisted of different ratio of silver (Ag) nanoparticles incorporated in a polystyrene (PS) matrix were prepared by ultrasonic solution mixing method. The chemical and optical properties of the polystyrene films before and after incorporation of Ag nanoparticles were investigated using Fourier transformation infrared spectrophotometer (FT-IR), Raman spectroscopy and UV-Vis spectrophotometer. The Raman spectra revealed that the degree of graphitization of the PS/Ag films increased with increasing of silver content and decreases with increasing time of exposure. The relative Raman intensity was found to decrease with the possibility of sp^3/sp^2 ratio decreasing in the films. The optical study revealed that energy band gap for nanocomposites was found to increase with increasing filler concentration. The potential applications of resultant nanocomposites are various fields, e.g. optoelectronics, microwave absorbance, electronics.

ICSSST2019-127

Influence of Hydroxymethylated Lignin on Mechanical Properties and Payne Effect of NR/BR CompoundsNor Anizah Mohamad Aini^{1, a}, Nadras Othman^{1, b*}, M.Hazwan Hussin^{2, c}, Kannika Sahakaro^{3, d} and Nabil Hayeemasae^{3, e}¹School of Material and Mineral Resources Engineering, Engineering Campus, Universiti Sains Malaysia, 14300 Nibong Tebal, Penang, Malaysia²School of Chemical Science, Universiti Sains Malaysia, 11800 Minden, Penang, Malaysia³Department of Rubber Technology and Polymer Science, Faculty of Science and Technology, Prince of Songkla University, Pattani Campus, Pattani, 94000 Thailand^anoranizah.ma@gmail.com, ^{b*}srnadras@usm.my, ^cmhh@usm.my, ^dkannika.sah@psu.ac.th, ^enabil.h@psu.ac.th

Abstract. The aim of this work is to study the relationship between hydroxymethylated lignin and its behavior in natural rubber (NR) / butadiene rubber (BR) compounds, in focusing on Payne effect and mechanical properties. Two types lignins from kenaf biomass, organosolv lignin (OL) and soda lignin (SL) were modified by using hydroxymethylation modification process and named as hydroxymethylated organosolv lignin (HMOL) and hydroxymethylated soda lignin (HMSL). All lignins were characterized in terms of particle size, molecular weight distribution (Gel Permeation Chromatography, GPC), Nuclear Magnetic Resonance (NMR) and Fourier Transform Infrared (FTIR). Then, the modified and unmodified lignins were incorporated in NR/BR blends by dry-mixing approach method. Payne effect and mechanical properties of lignin – filled NR/BR blends were investigated in both masterbatches and vulcanized compounds. The rubber process analyzer (RPA) was used to determine the Payne effect of the hydroxymethylated lignin-filled NR/BR masterbatches, while tensile properties of the compounds were evaluated after vulcanization. It was found that differences in the chemical characteristics of HMOL and HMSL influenced its filler-filler interaction and reinforcement capability. In conclusion, the addition of modified lignin to vulcanized compounds demonstrated the possibility to improve the mechanical properties of the rubber compounds.

ICSSST2019-135

Thermomechanical, Crystallization and Melting Behavior of Plasticized Poly (lactic acid) NanocompositesNur Ain Syafiqah Sudin^{1,a}, I.R. Mustapa^{1,b*}, Norlinda Daud^{2,c} and Mohammed Zorah^{1,d}¹Department of Physics, Faculty of Science and Mathematics, Universiti Pendidikan Sultan Idris, 35900, Tanjong Malim, Perak, Malaysia² Department of Chemistry, Faculty of Science and Mathematics, Universiti Pendidikan Sultan Idris, 35900, Tanjong Malim, Perak, Malaysia^aainpikah94@gmail.com, ^bizan.mustapa@gmail.com, ^cnorlinda@fsmt.upsi.edu.my, ^dmohamed.n224@yahoo.com

Abstract. The incorporation of filler and plasticizer provides effective nucleation and mechanical reinforcement in polymer composites to impart flexibility, toughness, thermal stability and tensile strength of PLA composites that can be used in the development of packaging applications. In this paper, the inclusion of plasticizer and reinforcement of nanofiller in PLA matrix aims to improve the thermomechanical properties that consequently alter the crystallization and melting behavior of PLA composites. Plasticized PLA with different percentages of TiO₂ at 2.0, 3.5, 5.0 and 7.0 %·w/w were dispersed in PLA solution using mechanical mixer and ultrasonication technique to introduce a matrix reinforcing nanophase within the composite. TiO₂ nanofiller were adopted along with tetrahydrofuran by using solvent casting method. The thermomechanical properties and thermal behavior of PLA nanocomposites were characterized using dynamic mechanical analysis (DMA) and differential scanning calorimeter (DSC). DSC cooling curves at low scanning rate of 2.0 K·min⁻¹ proved that the presence of TBC in PLA matrix increased the crystallinity of plasticized PLA nanocomposites that initiated the formation of perfect spherulites. TBC increased the crystallization activity during cooling, which in turn reduced the recrystallization effect on heating in parallel with DMA results that revealed no crystallization activity on PLA nanocomposites with the addition of plasticizer observed at temperature range of 40°C to 70°C. Nanofiller induced nucleation for crystallization of PLA matrix and plasticizer accelerated the overall crystallization process. Considerable adjustments of plasticizer and nanofiller in PLA matrix in having a good balance of stiffness and flexibility are a practical strategy that has a potential in biopolymer medical engineering and can be used in the development of packaging applications.

ICSSST2019-162

Localized Deep and Shallow Traps of α -Peaks from Thermally Stimulated Current (TSC) Measurement on Thermoplastic Polymers

Norhana Abdul Halim ^{1,a*}, Zul Hazrin Zainal Abidin, Siti Zulaikha Ngah Demon¹, Norli Abdullah¹, Abu Bakar Ahmad^{2,b} and Zainol Abidin Ibrahim³

¹Centre for Defence foundation Studies, National Defence University of Malaysia, Kem Sungai Besi, 57000 Kuala Lumpur, Malaysia

²Centre of Ionics, Department of Physics, Faculty of Science, University of Malaya, 50603, Kuala Lumpur, Malaysia

³Department of Physics, Faculty of Science, University of Malaya, 50603, Kuala Lumpur, Malaysia

^{a*}norhana@upnm.edu.my

Abstract. In this paper, trap levels around the glass transition temperature (T_g) of polymers have been characterized using Thermally Stimulated Current (TSC) technique. Deconvolution on α -peaks of the T_g for PE (-104°C), plasticized PVC (-35°C), PMMA (90°C) and PET (96°C) were carried out based on the first-order kinetic theory for non-Debye relaxation. Using temperature, T from TSC experimental data, we have successfully separated the α -peaks of the thermoplastic polymers. It is found that the complex curve of α -peaks can be composed of four (4) to eight (8) sub peaks. Dominant sub peaks were identified at $T_{max} = -105^\circ\text{C}$, -34°C , 89°C and 92°C for PE, plasticized PVC, PMMA and PET, respectively. These peaks show activation energy, E_a of shallow and deep trap centers ranged from 0.6 eV to 4.6 eV. Where they represent the depolarization of localized dipoles and space charges relaxations in the polymers.

Semiconductors and Devices

ICSSST2019-159

Nonlinearity Characteristics of Zn-Bi-Ti-O Varistor Ceramics Doped with Sb₂O₃ Prepared by Co-Precipitation Method

Mohd Sabri Mohd Ghazali^{1,2,a*}, Azmi Zakaria^{3,b}, Halimah Mohamed Kamari^{3,c}, Zahid Rizwan^{4,d}, Mohd Hafiz Mohd Zaid^{3,e} and Wan Rafizah Wan Abdullah^{2,5,f}

¹Advanced Nano Materials (ANoMa) Research Group, Nano Research Team, Faculty of Science and Marine Environment, Universiti Malaysia Terengganu, 21030 Kuala Nerus, Terengganu, Malaysia

²Materials Synthesis & Characterization Laboratory (MSCL), Institute of Advanced Technology (ITMA), Universiti Putra Malaysia, 43400 UPM Serdang, Selangor Darul Ehsan, Malaysia;

³Department of Physics, Faculty of Science, Universiti Putra Malaysia, 43400 UPM Serdang, Selangor, Malaysia

⁴Faculty of Science, Convener Purchase, National Textile University, Faisalabad (37610), Pakistan

⁵Faculty of Ocean Engineering Technology and Informatics, Universiti Malaysia Terengganu, 21030 Kuala Nerus, Terengganu, Malaysia

^{a*}mohdsabri@umt.edu.my, ^bazmizak@gmail.com, ^chalimah@upm.edu.my, ^dzahidrizwan64@gmail.com, ^emhmzaid@upm.edu.my, ^fwanrafizah@umt.edu.my

Abstract. There were few reports of fabrication of varistor ceramics that used as a protective device for electrical equipments from transient voltage surges, using other method than conventional solid-state. Hence, it is useful to characterize in terms of morphology and electrical non-linearity characteristics by using wet chemical processing. This processing promised a fine and homogenous powder. The effect of Sb₂O₃ dopant in ZnO based varistor fabricated by using co-precipitation method was investigated. For the methodology, the prepared samples from co-precipitation was examined with EDX microanalysis for chemical and physical examinations, SEM and FESEM for morphological examinations, XRD and the *I-V* measurements for non-linearity characteristic. In this study, with the use of different additives, secondary phases are developed and coexisted in the varistor ceramics that are Bi₄Ti₃O₁₂, Zn₂TiO₄, and Zn₇Sb₂O₁₂ as a grain inhibitor and segregated at the grain boundaries and the triple point junctions. The development of these secondary phases influences the varistor ceramics performances in electrical properties. The additive of Sb₂O₃ is a strong grain inhibitor which produces secondary phases, Zn₂Bi₃Sb₃O₁₄ at low and Zn₇Sb₂O₁₂ at high doping concentrations. The α value of co-precipitation method samples is optimum at 10.48.

Superconductors

ICSSST2019-058

Effect of Cr₂O₃ on the T_c and Phase Formation of Tl_{2-x}Cr_xBa₂CaCu₂O_{8-δ} SuperconductorSyahrul Humaidi^{1,a*} and Roslan Abd-Shukor^{2,b}¹Department of Physics, FMIPA, Universitas Sumatera Utara, Jln Bioteknologi 1 Medan 20155, Indonesia²School of Applied Physics, Universiti Kebangsaan Malaysia, 43600 Bangi, Selangor, Malaysia^{a*}syahrul1@usu.ac.id, ^bbras@ukm.edu.my

Abstract. The Tl-based (Tl2212) high T_c superconductor, Tl_{2-x}Cr_xBa₂CaCu₂O_{8-δ} has been prepared via solid state reaction method. The substitution of Cr to the Tl-site was aimed to investigate the role of Cr on the critical transition temperature and phase stability of Tl2212 superconductor. The samples were prepared in two stages: the first, Ba₂CaCu₂O_y precursor material was synthesized using BaCO₃ (99.9%, Aldrich), CaO (99.99%, Alfa Aesar) and CuO (99.9%, Alfa Aesar) powder as starting compound. These compounds were mixed in an appropriate ratio and sintered at 900°C for 24 h followed by cooled to room temperature. The second step: precursor was then ground for about 1 h and mixed with Tl₂O₃ (99.9%, Alfa Aesar) and Cr₂O₃ (99.9%, Merck) powders to produce Tl_{2-x}Cr_xBa₂CaCu₂O₈. The pellets were heated at 900°C in a preheated tube furnace with oxygen flow for 4 min. The critical temperature, T_c was determined using the standard four point probe technique in a closed cycled cryogenic system from 50K to 300K with constant current of 20 mA. The phase was determined by X-Ray (powder method) using X-ray CuK_α source with λ = 1.5418 Å. The samples were in the 14/mmm space group. It was found that the maximum zero-resistance temperature, T_{c zero} was 96 K and onset temperature, T_{c onset} was 116 K for composition Tl_{1.8}Cr_{0.2}Ba₂CaCu₂O_{8-δ}. The volume fraction of the Tl2212 phase in this composition was 88% with c-lattice parameter = 29.3880 Å. The results showed that the phase formation of the Tl2212 phase affected the critical temperature.

ICSSST2019-113

Structural and Electronic Properties of Ag-doped in Ba-site of YBa_{2-x}Cu₃O₇ using Density Functional Theory via First Principle StudySiti Fatimah Saipuddin^{a*}, Azhan Hashim^b and Mohamad Fariz Mohamad Taib^c¹Faculty of Applied Sciences, Universiti Teknologi MARA (UiTM) Pahang, 26400, Jengka, Pahang, Malaysia²Faculty of Applied Sciences, Universiti Teknologi MARA (UiTM), 40450 Shah Alam, Selangor, Malaysia^{a*}sitifatihmah7020@uitm.edu.my, ^bdazhan@uitm.edu.my, ^cmfariz@uitm.edu.my

Abstract. This study reports on the First Principle Study with Density Functional Theory (DFT) used to determine the structural and electronic properties of Ag-dopant in Ba-site of YBa_{2-x}Cu₃O₇ superconductor. The computational method adopting CASTEP computational code was used to calculate the electronic properties for Ag-dopant in range of x = 0.0 to 0.5 in Ba-site of YBa_{2-x}Cu₃O₇ ceramic superconductor. The structural changes in terms of lattice parameters also compared as the percentage of dopant increase to seek variance of orthorhombicity (Pmmm space group) of the structure. The crystal structure constructed and calculated using Visual Crystal Approximation (VCA) applying the local density approximation (LDA) and ultrasoft pseudopotential. Geometry optimization shown energy converged at 400 eV with k-point sampling of 4x4x1. The structural properties of YBa_{2-x}Cu₃O₇ are observed to be approximately close to the experimental data obtained by other researches. The electronic properties was determined via energy band gap and density of states visualisation and was used to further enhance the experimental findings.

ICSSST2019-142

**AC Susceptibility and Superconducting Properties of Low Density
Bi_{1.6}Pb_{0.4}Sr₂(Ca_{2-x}Yb_x)₂Cu₃O_y Superconductor**H. Azhan^a, L. N. F. Syahira^b, E. S. Nurbaisyatul^c, K. Azman^d

Faculty of Applied Sciences, Universiti Teknologi MARA Pahang, 26400 Bandar Tun Abdul Razak, Jengka, Pahang, Malaysia

^adazhan@uitm.edu.my, ^bfarahiyahsyahira@gmail.com, ^cersyamiza@gmail.com, ^dazman615@uitm.edu.my

Abstract. A systematic study on the effects of Ytterbium (Yb) oxide nano-particle doped with BSCCO-2223 on the ac susceptibility (ACS) and superconducting properties was carried out. All samples were synthesized using solid state reaction method. Yb concentration was varied from $x = 0.0$ up to 0.08 mol% in a general stoichiometry of $\text{Bi}_{1.6}\text{Pb}_{0.4}\text{Sr}_2\text{Ca}_{1-x}\text{Yb}_x\text{Cu}_3\text{O}_y$. The samples were characterized via X-Ray Diffraction (XRD), four-point probe method and ACS. XRD analysis shows that both (Bi,Pb)-2212 and (Bi,Pb)-2223 phases coexist in the samples having tetragonal crystal structure but changed to orthorhombic Yb-doped samples. The values of critical transition temperature, T_C of the samples decreased with the increase of Yb concentration. ACS measurement showed the onset critical temperature, T_C -onset (< 1 K) decreases toward Yb concentration. Both intra and intergranular peaks, T_P appeared in Yb-free sample but diminished in Yb-doped samples. The possible reasons for the degradation in superconducting and structural properties of Bi-2223 due to Yb nanoparticles addition were discussed.

v

ICSSST2019-143

Rare-Earths, Alkali and Transition Metals Effects on the TI-1212 Type Phase Superconductors

R. Abd-Shukor, A.B.P. Ilhamsyah, M. S. Mohd-Syahmi, J. Nur-Akasyah

School of Applied Physics, Universiti Kebangsaan Malaysia, 43600 Bangi, Selangor, Malaysia

Abstract. In this paper we report the effects of rare-earth elements (R), alkali metals (A) and transition metals (M) effects of the superconducting properties of the (TI-1212) phase. The elements were $R = \text{Gd, Er, La}$, $A = \text{Li, Na, K and Rb}$ and $M = \text{Cr, Pb, and Bi}$. The samples were prepared using the solid state reaction method. The samples were characterized using X-ray diffraction method, scanning electron microscopy, resistance versus temperature measurements and ac susceptibility. The results were analyzed using the effect of the ionic radius of the elements on the formation of the TI-1212 phase and the transition temperatures. This work showed that Rb greatly enhanced the TI-1212 phase formation due to the proximity of the Rb^{+1} and Ti^{+1} ionic radius. Na and Rb improved the transition temperature. Li, Na and Rb improved the inter-grain critical current density and increased the grain size of the samples. Rare-earth elements improved the transition temperature and inter-grain coupling of TI-1212 superconductors.

ICSSST2019-148

Ferrimagnetic Cr₂S₃ Effect on (Bi,Pb)-Sr-Ca-Cu-O SuperconductorMasnita Mat Jusoh^{1,2}, Nurul Raihan Mohd Suib^{1,2}, Madihah Mujaini² and R. Abd-Shukor²¹Fakulti Sains Gunaan, Universiti Teknologi MARA, 40450 Shah Alam, Selangor, Malaysia²School of Applied Physics, Universiti Kebangsaan Malaysia, 43600 Bangi, Selangor, Malaysia

Abstract. We report the effect of ferrimagnetic Cr₂S₃ on (Bi,Pb)-Sr-Ca-Cu-O superconductor. Samples with composition (Bi,Pb)-Sr-Ca-Cu-O (Cr₂S₃)_x for $x = 0$ to 0.3 wt. % were prepared via the co-precipitation method. The structure, electrical resistance and AC susceptibility were determined. The critical transition temperature, T_c was suppressed as the amount of Cr₂S₃ were increased. The transport critical current density, J_c , was measured using the 1 μ V/cm criterion. The $x = 0.1$ wt% sample sintered for 48 h ($T_{c-zero} = 103$ K) showed the highest J_c of 8.37 Acm⁻² at 30 K. The peak temperature of the imaginary part of the complex susceptibility, T_p , increased with addition of Cr₂S₃, indicating full flux penetration occurred at higher temperature and improved intergrain coupling. Cr₂S₃ suppressed the transition temperature but it improved the transport critical current density by more than two times indicating that its enhanced flux pinning and connectivity between grains.

ICSSST2019-169

Impact of Zinc Ferrite Nanoparticles on Transport and Superconducting Properties of (Ti_{0.85}Cr_{0.15})Sr₂CaCu₂O_{7- δ} Bulk SuperconductorsNurul Auni Khalid^{1, a*}, Wei Kong^{2, b}, Mohd Mustafa Awang Kechik^{1, c}, Ing Kong^{3, d}, Eng Hwa Yap^{4, e} and Roslan Abd-Shukor^{5, f}¹Faculty of Science, Universiti Putra Malaysia, 43400 Serdang, Selangor, Malaysia.² Centre for Foundation and General Studies, Infrastructure University Kuala Lumpur, Jalan Ikram-Uniten, 43000 Kajang, Selangor, Malaysia.³School of Engineering and Mathematical Sciences, La Trobe University, Bendigo VIC 3552, Australia.⁴Faculty of Transdisciplinary Innovation, University of Technology Sydney, Broadway NSW 2007, Australia.⁵School of Applied Physics, Faculty of Science and Technology, Universiti Kebangsaan Malaysia, 43600 Bangi, Selangor, Malaysia.

^{a*}nurulauni2412@gmail.com, ^bkwei@iukl.edu.my, ^cmmak@upm.edu.my, ^dI.Kong@latrobe.edu.au, ^eEngHwa.Yap@uts.edu.au, ^fras@ukm.edu.my

Abstract. High temperature superconductor (Ti_{0.85}Cr_{0.15})Sr₂CaCu₂O_{7- δ} (TI-1212) with addition of zinc ferrite (ZnFe₂O₄) nanoparticles were synthesized using high purity oxide powders through a solid state reaction method. ZnFe₂O₄ nanoparticles with composition of 0.01 wt.%, 0.02 wt.%, 0.05 wt.%, 0.10 wt.%, and 0.15 wt.% were added to the TI-1212 superconductor. These TI-1212 samples were characterized using scanning electron microscopy (SEM), powder X-ray diffraction method (XRD), energy dispersive X-Ray analysis (EDX), electrical resistance measurement, and transport critical current density measurement. All samples indicated a dominant TI-1212 phase of a tetragonal structure with a minor phase of TI-1201. The transition temperatures (T_{c-zero} and $T_{c-onset}$) were measured using a four-point probe method. The highest T_{c-zero} recorded was 97 K, which was exhibited by the pure TI-1212 sample. The onset critical temperature ($T_{c-onset}$) recorded was between 97 K and 105 K. The transport critical current, I_c , all samples were found through the 1 μ V/cm criterion with temperature ranging from 30 K to 77 K. The introduction of ZnFe₂O₄ nanoparticles has enhanced T1-1212 superconductor's flux pinning effects and increased its transport critical current density (J_c).

Thin Films and Nanostructures

ICSSST2019-015

Solution process growth of Co, Bi and Mn Doped Zinc Oxide Nanowires by Hydrothermal MethodSyed Jamal Ahmed Kazmi^{1,a}, Mohd Farhanulhakim Mohd Razip Wee^{2,b} and Mohd Ambri Mohamed^{3,c*}

Institute of Microengineering and Nanoelectronics (IMEN), Universiti Kebangsaan Malaysia (UKM), 43600 Bangi, Selangor, Malaysia

^aajamal_physics@outlook.com, ^bm.farhanulhakim@ukm.edu.my, ^{c*}ambri@ukm.edu.my

Abstract. Defects in ZnO, a large bandgap semiconductor, result in unpaired electrons which induces ferromagnetism, but this induced ferromagnetism is not stable because the sample can be oxidized with passage of time. In present studies pristine/undoped Bismuth (Bi), Cobalt (CO) and Manganese (Mn) doped ZnO nanowire (NW) having different concentration based thin film are grown on a seeded glass substrate by hydrothermal method. XRD spectra have one main and very well pronounced 0002 peak which is related to top hexagonal face which shows that the NWs are predominantly vertically grown or c-axis growth only. The XRD peaks found to be shifted a little bit after doping which is also a confirmation of doping. The XRD peak broadening was used to estimates stress and strain. Recently it has been predicted theoretically that heavy metal ions like Bi can induce stable ferromagnetism at room temperature due to the strong spin-orbit coupling between valence band and heavy ion Bi and a stabilized ferromagnetic phase is expected. The magnetization curve (M-H curve) of undoped and Bi, Co and Mn doped ZnO NWs shown ferromagnetic behavior at room temperature. Field Emission Scanning Electron Microscopy (FE-SEM) images shown the hexagonal top face of the NWs and the average diameter was calculated for undoped and doped NWs using ImageJ Software. The band gap was estimated from UV-Vis absorption spectra and for Bi: ZnO, Co: ZnO and Mn: ZnO and there was an increase in bandgap in all cases. From the study above, this kind of ferromagnetism and excellent optical tunability because of doping will be the potential materials for future magneto-optoelectronic devices.

ICSSST2019-049

Impact of Ba/Fe Molar Ratio on the Structural and Magnetic Properties of BaFe₁₂O₁₉ Film Synthesized by a Sol-gel MethodN.B. Ibrahim^{1,a*}, Noratiqah. Y^{1,b}, M.F.A. Jailani^{1,c}, E.R. Iruthayaraj^{1,d}¹ School of Applied Physics, Faculty of Science and Technology, Universiti Kebangsaan Malaysia, 43600, Bangi, Selangor, Malaysia.^{a*}baayah@ukm.edu.my, ^bnoratiqah.yusop@gmail.com, ^cmfaremir72@gmail.com, ^dedwinjar16@gmail.com

Abstract. The effect of different Ba/Fe molar ratio (1:2, 1:4, 1:6, 1:8, 1:10 and 1:12) on the structural and magnetic properties of barium hexaferrite film has been studied. The films were prepared by a sol-gel method followed by an annealing process at 800°C in air. The XRD analysis for microstructural properties revealed sample with ratio 1:4, 1:6 and 1:8 crystallized into single phase of BaFe₁₂O₁₉, while the rest of sample crystallized into mixed phase with hematite as the major phase. The size of crystallite increased as the content of Fe increased. The microstructure analysis using a field emission scanning electron microscope showed the grains have mixed acicular and hexagonal shape, where sample with molar ratio of 1:4 and 1:6 have the most grain shape of hexagon. The magnetic measurement using a vibrating sample magnetometer at room temperature showed film with molar ratio of 2 has the lowest coercivity value (149.0 Oe), while film with molar ratio of 6 has the highest value of coercivity (5111.1 Oe). Film with molar ratio of 4 and 12 exhibit the highest and the lowest saturation magnetization with respective value of 327.9 emu/cm³ and 52.93 emu/cm³.

ICSSST2019-064

Synthesis and Characterization of Polyaniline Thin Film: The Effect of pH and ConcentrationN. A. Shaari^{1,a}, N. A. Abdul-Manaf^{1,b*}¹Physics Department, Centre for Defence Foundation Studies, National Defence University of Malaysia, Kem Sungai Besi, 57000 Kuala Lumpur, Malaysia^a3181102@alfateh.upnm.edu.my, ^{b*}azlian@upnm.edu.my

Abstract. Polyaniline (PANI) thin films have been successfully prepared from an aqueous electrolyte bath containing aniline and sulphuric acid, (H₂SO₄) using electrodeposition method. The study demonstrates that the properties of PANI thin film depends on the variation of pH and aniline concentration in prepared precursor. The optical and structural of PANI thin films have been characterized using UV-Visible spectrometer (UV-Vis), X-ray diffraction spectrometer (XRD), Fourier Transform Infra-Red spectrometer (FTIR) and Raman spectrometer. PANI layer grown at pH 2.00 shows green colour layer which denoted as emeraldine base (half oxidized state of PANI) while at pH 3.80 the colour of PANI layer was yellow that represent the leucoemeraldine base (fully reduced state of PANI). Optical analysis using UV-Vis demonstrated the smallest energy band gap, E_g of PANI is 3.54 eV for sample with 0.50 M aniline concentration and pH 2.00. The trend shows that the bandgap of PANI is increased as the pH increased from 2.00 to 3.40. Structural characterizations were carried out by XRD, FTIR and Raman spectrometer. XRD result shows that all the deposited PANI layers are amorphous. Results obtained from FTIR confirmed the footprint of PANI and Raman spectrometer confirmed the half oxidized emeraldine base of PANI. Full characterization of this material is providing new information on PANI behavior due to pH and concentration in the prepared precursor. v

ICSSST2019-070

Influence of Applied Potential on Electrodeposited ZnSe/ZnO Nanostructured Films for Photoelectrochemical CellLaimy Mohd Fudzi^{1,a}, Zulkarnain Zainal^{1,2,b*}, Hong Ngee Lim^{1,2,c}, Suhaidi Shafie^{2,3,d} and Sook-Keng Chang^{1,2,e}¹Department of Chemistry, Faculty of Science, Universiti Putra Malaysia, 43400 UPM Serdang, Selangor, Malaysia²Materials Synthesis and Characterization Laboratory, Institute of Advanced Technology, Universiti Putra Malaysia, 43400 UPM Serdang, Selangor, Malaysia³Department of Electronic Engineering, Universiti Putra Malaysia, Serdang 43400, Malaysia^alaimy93@yahoo.com, ^{b*}zulkar@upm.edu.my, ^chongnglee@upm.edu.my, ^dsuhaidi@upm.edu.my, ^eskchang28@hotmail.com

Abstract. Zinc oxide (ZnO) nanorods is widely investigated due to its high photoelectrochemical conversion performance. Further enhancement may be afforded by introducing a metal chalcogenide sensitization layer such as zinc selenide (ZnSe). In this study, ZnO nanorods were electrodeposited with ZnSe at potential range from -0.5 V to -0.9 V vs Ag/AgCl reference electrode. Structural, morphological and composition of ZnSe electrodeposited were investigated as a function applied potential by using X-ray diffractometry (XRD), field emission scanning electron microscopy (FESEM), and ultraviolet-visible spectroscopy (UV-Vis). ZnSe electrodeposited for 15 minutes at -0.7 V showed crystallite size of 22.8 nm. Besides, the size of electrodeposited ZnSe particles of 41.8 nm on vertically aligned ZnO nanorods with average diameter and length of 80.6 nm and 1931 nm respectively, were evidenced from FESEM images. The photocurrent density generated by samples were measured in a three-electrodes cell incorporated with halogen lamp. The photocurrent generated increased between -0.5 V to -0.7 V before dropped at higher applied potential due to hydrogen evolution process which affected the thin film quality, ultimately affecting photoconversion performance. The highest photocurrent density of 0.2621 mAcm⁻² was recorded for samples prepared at -0.7 V vs Ag/AgCl.

ICSSST2019-076

Sol Precursor Concentration Effect on Synthesis and Characterization of ZnO Nanoparticles FilmHuey Jing Tan^{1,a}, Zulkarnain Zainal^{1,3,b*}, Zainal Abidin Talib^{2,c}, Hong Ngee Lim^{1,3,d} and Suhaidi Shafie^{4,e}¹Department of Chemistry, Faculty of Science, Universiti Putra Malaysia, 43400 UPM Serdang, Selangor, Malaysia²Department of Physics, Faculty of Science, Universiti Putra Malaysia, 43400 UPM Serdang, Selangor, Malaysia³Materials Synthesis and Characterization Laboratory, Institute of Advanced Technology, Universiti Putra Malaysia, 43400 UPM Serdang, Selangor, Malaysia⁴Functional Device Laboratory, Institute of Advanced Technology, Universiti Putra Malaysia, 43400 UPM Serdang, Selangor, Malaysia^ags52626@student.upm.edu.my, ^{b*}zulkar@upm.edu.my, ^czainalat@upm.edu.my, ^dhongngel@upm.edu.my, ^esuhaidi@upm.edu.my

Abstract. Zinc oxide nanorod arrays (ZnO NRs) are known to be one of the intensive-studied materials for photoelectrochemical (PEC) solar cells application. The photoconversion efficiency of fabricated ZnO NRs photoelectrode is highly dependent on the conditions of pre-deposited seed layer. In present work, concentration of sol was varied from 0.10 M to 0.70 M and spun coated on ITO glass substrate to achieve homogenous ZnO nanoparticles (NPs) film. As-deposited ZnO NPs was grown into nanorods by simplified hydrothermal method. X-ray diffraction (XRD), field emission scanning electron microscopy (FESEM) and energy dispersive X-ray spectroscopy (EDX) were applied to examine the structural, morphological and elemental properties of ZnO thin film, respectively. Meanwhile, films' optical properties were studied by ultraviolet-visible (UV-Vis) and photoluminescence (PL) spectroscopy. Change in thickness of prepared ZnO samples was measured with stylus profilometer. Also, electrochemical impedance spectroscopy (EIS) investigated the recombination resistance of deposited films. Photoelectrochemical analysis was carried out on both ZnO NPs and NRs by linear sweep voltammetry (LSV) under chopped illumination. The optimum concentration for ZnO NPs seed layer was found to be 0.30 M.

ICSSST2019-115

Synthesis of Silver Nanoparticles by Plasma-Assisted Hot-Filament Evaporation for Luminance Enhancement of Organic Light Emitting DiodeAbtisam Hasan Hamood Al-Masoodi^{1,a}, Boon Tong Goh^{1,b} and Wan Haliza Binti Abd Majid¹¹Low Dimensional Materials Research Center, Department of Physics, Faculty of Science, University of Malaya, 50603 Kuala Lumpur, Malaysia^aabtalmasoodi@gmail.com, ^bgohbt@um.edu.my

Abstract. Silver (Ag) nanoparticles were synthesized using plasma-assisted hot-filament evaporation. This technique showed deposition of the nanoparticles in high-density with uniformity in the size and interparticles separation. The size and interparticles separation are the main factors of the variation of the localized surface plasmon resonance characteristics of the nanoparticles. The Ag nanoparticles was an additional layer in a typical organic light emitting diode (OLED). The OLED with Ag nanoparticles layer resulted the low driving voltage with high luminance compared to the OLED without Ag nanoparticles layer. The effects of the deposition of Ag nanoparticles layer on the OLED luminance are discussed.

ICSSST2019-138

The Optical Properties of Thin Films Tin Oxide with Triple Doping (Aluminum, Indium, and Fluorine) for Electronic DeviceA. Doyan^{1,2,a*}, Susilawati^{1,2,b}, M. Taufik^{2,c}, S. Hakim^{1,d}, L. Mulyadi^{1,e}¹Master of Science Education Program, University of Mataram, Lombok, West Nusa Tenggara, Indonesia.²Physics Education, FKIP, University of Mataram, Lombok, West Nusa Tenggara, Indonesia.^aaris_doyan@unram.ac.id, ^bsusilawatihambali@unram.ac.id, ^ctaufik@unram.ac.id, ^dsyamsulhakim@unram.ac.id, ^elalumulyadi93@unram.ac.id

Abstract. Tin oxide (SnO₂) thin film is a form of modification of semiconductor material in nano size. The thin film study aims to analyze the effect of triple doping (Aluminum, Indium, and Fluorine) on the optical properties of SnO₂: (Al + In + F) thin films. Aluminum, Indium, and Fluorine as doping SnO₂ with a mass percentage of 0, 5, 10, 15, 20, and 25% of the total thin film material. The addition of Al, In, and F doping causes the thin film to undergo changes in optical properties, namely the transmittance and absorbance values undergoing changes. The transmittance value is 84.24, 86.44, 87.74, 89.34, 90.84, and 94.34 which is at a wavelength of 420 nm for the lowest to highest doping percentage, respectively. The absorbance value increased with increasing doping percentage at 350 nm wavelength of 0.52, 0.76, 0.97, 1.05, 1.23, and 1.29 for 0, 5, 10, 15, 20, and 25% doping percentages, respectively. The absorbance value is then used to find the gap energy of the SnO₂: (Al + In + F) thin film of the lowest doping percentage to the highest level. i.e. 3.60, 3.55, 3.51, 3.47, 3.42, and 3.39 eV. Thin film activation energy also decreased with values of 2.27, 2.04, 1.85, 1.78, 1.72, and 1.51 eV, respectively for increasing percentage of doping. The thin film SnO₂: (Al + In + F) which experiences a gap energy reduction and activation energy makes the thin film more conductive because electron mobility from the valence band to the conduction band requires less energy and faster electron movement as a result of the addition of doping.

ICSSST2019-156

Influence of Target to Substrate Distance on Structural, Microstructure and Optical Properties of Sputtered Gd-doped ZnO Thin Films

Nur Amaliyana Raship^{1,a}, Siti Nooraya Mohd Tawil^{1,b*}, Nafarizal Nayan^{2,c}, Khadijah Ismail^{1,d}, Muliana Tahan^{3,e} and Anis Suhaili Bakri^{3,f}

¹Department of Electrical and Electronic Engineering, Universiti Pertahanan Nasional Malaysia (UPNM), 57000 Kem Sungai Besi, Kuala Lumpur, Malaysia

²Microelectronic and Nanotechnology-Shamsuddin Research Centre (MiNT-SRC), Universiti Tun Hussein Onn Malaysia (UTHM), 86400 Parit Raja, Batu Pahat, Johor

³Faculty of Electrical and Electronic Engineering, Universiti Tun Hussein Onn Malaysia (UTHM), 86400 Parit Raja, Batu Pahat, Johor

^aliyanaraship@gmail.com, ^{b*}nooraya@upnm.edu.my, ^cnafa@uthm.edu.my, ^dkhadijah@upnm.edu.my, ^emulianathn15@gmail.com, ^fanishjbakri92@gmail.com

Abstract. The influence of target to substrate distance on Gd-doped ZnO thin films properties were investigated. Gd-doped ZnO thin films with three distance between a target to substrate range from 12.0, 13.5 and 15.0 cm were deposited on glass substrates using sputtering technique. The structural, element analysis, microstructure and optical properties of the thin films were characterized using x-ray diffraction (XRD), energy dispersive x-ray (EDX), atomic force microscope (AFM) and UV-Vis spectra, respectively. The XRD results show that all the samples have hexagonal wurtzite structure of ZnO without any other impurities peaks. The sharp and intense peak was observed at 13.5 cm of target to substrate distance which exhibits good crystallinity compared to others. EDS result confirms the presence of Gd elements which successfully substitute as a dopant in ZnO matrix for all deposited films. AFM images revealed that the surface topology has smooth and uniform surface with low roughness observed at 13.5 cm. All deposited films exhibit good transparency within visible region with transmittance above 90 %. The bandgap value decrease with increasing in target to substrate distance, being 3.18, 3.15, 3.13 eV for 12.0, 13.5 and 15.0 cm, respectively. The results suggest that Gd-doped ZnO thin films prepared at 13.5 cm of target to substrate distance is the best condition.

Advanced Material Synthesis and Crystal Growth Technology

ICSSST2019-018

From Kaolin to Kalsilite: The Effect of KOH Concentrations and Reaction TemperatureEddy F. Yusslee^{1,a*}, Nur Hazwani Dahon^{2,b}, Mohd Azrul Abdul Rajak^{3,c}, Nur Fadzilah Basri^{4,d} and Sazmal E. Arshad^{5,e}¹Faculty of Science and Natural Resources, Universiti Malaysia Sabah, Malaysia.²Preparatory Centre For Science and Technology, Universiti Malaysia Sabah, Malaysia.³Preparatory Centre For Science and Technology, Universiti Malaysia Sabah, Malaysia.⁴Preparatory Centre For Science and Technology, Universiti Malaysia Sabah, Malaysia.⁵Faculty of Science and Natural Resources, Universiti Malaysia Sabah, Malaysia.^{a*}eddy@ums.edu.my, ^bnurhazwani@ums.edu.my, ^cazrulrajak88@gmail.com, ^ddilabasri@ums.edu.my, ^esazmal@ums.edu.my

Abstract. Kalsilite has been synthesis using kaolin as silica and alumina precursors via hydrothermal method with the addition of KOH as potassium source. The effects of KOH concentrations and reaction temperature have been investigated. XRD graphs and SEM images indicated the formation of kalsilite after hydrothermal reaction of kaolin at 190°C in 0.75 M KOH solution for 21 hours. Higher KOH molarity increases the crystallinity of the product while zeolite W was formed at lower KOH concentration. On the other hand, the 190°C is sufficient to convert the kaolin to kalsilite, however at lower temperature, zeolite W has been found as the dominant product.

Ceramics and Glasses

ICSSST2019-066

Elastic Properties of Sodium Potassium Borotellurite Glass SystemR.Hisam ^{a*}, Nurul Farhana Abu Seman^b and Syima Asyurah Syuhaimi^c^{1,2,3}Faculty of Applied Sciences, Universiti Teknologi MARA, 40450 Shah Alam, Selangor, Malaysia^arosdiyana@salam.uitm.edu.my, ^bfarhanaabuseman@gmail.com, ^casyurah_me94@yahoo.com

Abstract. Glasses with the composition $70[(1-x) B_2O_3 + xTeO_2] + 15Na_2O + 15K_2O$ ($x = 0, 0.1, 0.2, 0.3, 0.4$ and 0.5 mol%) were prepared by melt quenching method to elucidate the elastic behaviour due to borate anomaly. Structural investigation of glass samples were carried out by X-ray diffraction (XRD) and Fourier transform infrared (FTIR) spectroscopy while elastic properties were studied by measuring both longitudinal and shear velocities. FTIR analysis revealed the presence of BO₄ and BO₃ vibration groups. Ultrasonic velocity measurements showed both longitudinal, v_L and shear, v_s velocities increased up to 0.3 mol% before decreasing with further addition of TeO₂. Independent longitudinal, C_L and shear, μ moduli along with Young's modulus, Y , and poisson's ratio, σ recorded maximum values at $x=0.3$ mol% of TeO₂ content due to the compactness of the glass systems and caused the increase in rigidity and stiffness of the glasses which were suggested to be related to the borate anomaly. Beyond 0.3 mol % of TeO₂ content, the decrease in the elastic moduli was due to weakening of the stiffness of the glass network.

ICSSST2019-082

 γ -Ray Shielding Parameter of Barium-Boro-Tellurite GlassAzuraida Amat, Halimah Mohamed Kamari^a, Ishak Mansor^b, Hasnimulyati Laoding^c, Noor Fadhilah Rahmat^d

UPNM

^ahmk6360@gmail.com, ^bishak_mansor@nuclearmalaysia.gov.my, ^chasniemulyati@gmail.com, ^dfadhilah@upnm.edu.my

Abstract. Boro-tellurite glasses have recently been attracting the attention of several researchers as a tremendous optical device and shielding material. In this work, we have synthesized boro-tellurite glasses with barium oxide (BaO) by melt quenching technique. The structural and shielding property changes after adding of barium oxide in boro-tellurite glass were studied using Fourier Transform Infrared (FTIR) and Lead Equivalent Thickness measurement (LET), respectively. The results show that the bismuth oxide increases glass density, changes the glass structure, and increases the radiation shielding properties. Changes in the glass structure are due to atomic rearrangements and formation of non-bridging oxygen (NBO). The density of boro-tellurite glass system increased when BaO content increased, which is due to the high molecular weight of BaO and the increasing number of non-bridging oxygen (NBO) atoms in the glass structure. In addition, the mass attenuation coefficient, μ_m of the glass system increases as BaO concentration increases and the half value layer, HVL and mean free path, MFP of 30BaBTe glass is better than some standard concretes.

v

ICSSST2019-103

Experimental and Theoretical Approach on The Elastic Properties of $50\text{B}_2\text{O}_3-(50-x)\text{Na}_2\text{O}-x\text{Fe}_2\text{O}_3$ Glasses

Syafawati Nadiah Mohamed

UiTM

Abstract. In this study, a series of borate-based glass with composition $50\text{B}_2\text{O}_3-(50-x)\text{Na}_2\text{O}-x\text{Fe}_2\text{O}_3$ was prepared using the melt-quenching method to investigate the effect of Fe_2O_3 doping on elastic properties. The variation of ultrasonic velocities, independent elastic moduli and Debye temperature with Fe_2O_3 showed a general decrease for $x \leq 0.2$ mol% before increasing to a maximum at 0.2 mol% Fe_2O_3 . This result coincided with the ionic to electronic transition region as previously reported. A large decrease in elastic moduli for $x \leq 0.2$ mol% indicated a decrease in stiffness because of an increment of NBO, thereby enabling ionic conductivity. Meanwhile, the presence of Fe_2O_3 as glass former for $x > 0.2$ mol% induced electronic hopping. In addition, analysis of bulk compression and ring deformation model showed that the addition of Fe_2O_3 caused a gradual increase for $x \leq 0.2$ mol% before decrease for $x > 0.2$ mol%, indicating that ring deformation was increased in the ionic region but decreased in the electronic region.

ICSSST2019-111

Structural and Ionic Conductivity of $Mg_{0.5}Ti_2(PO_4)_3$ NASICON-Structured Ceramic ElectrolytesN. A. Mustafa^{1, a*}, N. S. Mohamed^{2, b}¹Faculty of Applied Sciences, Universiti Teknologi MARA, 40450 Selangor, Malaysia.²Centre for Foundation Studies in Science, University of Malaya, 50603 Kuala Lumpur, Malaysia.^{a*}nuramalina@uitm.edu.my, ^bnsabirin@um.edu.my

Abstract. Magnesium is a promising electrolytes material for solid state rechargeable batteries as magnesium is environmentally benign, cheap and possessed high energy density. Therefore, in this study, magnesium based NASICON-structured ceramic electrolytes, $Mg_{0.5}Ti_2(PO_4)_3$ were synthesized using solid state reaction method. Then, the effects of sintering temperature from 600 °C to 750°C to the structural and electrical properties of $Mg_{0.5}Ti_2(PO_4)_3$ ceramic electrolytes were studied. X-ray diffraction analysis showed that the prepared electrolytes can be indexed to a rhombohedral NASICON-type symmetrical structure ($R\bar{3}c$) with some minor impurities. Meanwhile, Fourier Transform Infrared analysis showed that the entire region was dominated by the vibration of PO_4 tetrahedral. Ionic conductivities of the electrolytes were studied using electrochemical impedance spectroscopy in the frequency range of 1 Hz to 10 MHz at room temperature. Sample sintered at 750°C showed the highest conducting value for both bulk and grain boundary conductivity, $1.11 \times 10^{-6} \text{ Scm}^{-1}$ and $4.76 \times 10^{-9} \text{ Scm}^{-1}$. These results indicated the suitability of the $Mg_{0.5}Ti_2(PO_4)_3$ to be exploiting further for potential applications as solid electrolytes in electrochemical devices.

ICSSST2019-136

Effect of Li Substitution on the Structure and Electrical Properties of Potassium Sodium Niobate PiezoceramicsZalita binti Zainuddin, Muhammad Faisal Mustaqim bin Kamal^a, Lubna binti Nadzir^b

Fakulti Sains dan Teknologi, Universiti Kebangsaan Malaysia

^afaisal_mustaqim@yahoo.com, ^blubna.nadzir@gmail.com

Abstract. Study on the effect of lithium substitution on the properties of potassium sodium niobate (KNN) piezoceramic has been conducted. This element was selected due to its ability to overcome the weakness in KNN stoichiometry during its production process. $(K_{0.5}Na_{0.5})_{1-x}Li_xNbO_3$ samples with composition of $x = 0.00, 0.02, 0.04, 0.06$ and 0.08 has been synthesized using sol-gel method. This study includes the characterization of structure, microstructure and electrical properties of the samples. XRD spectrum analysis showed that Li substitution has resulted in the production of tetragonal structured samples. Raman spectroscopy showed that Li substitution does not change the basic NbO_6 octahedron structure and confirms the existence of perovskite structure in the materials. All samples have cuboid shaped grains with a slight deterioration of the grains shape for samples with $x = 0.06$ and 0.08 . The highest Curie temperature, T_c was obtained for $x = 0.08$ sample at 485°C. All samples were confirmed to have ferroelectric properties based on the formation of sigmoid shape hysteresis loop. The coercive electric field, E_c varies slightly while the remnant polarization, P_r decreases with the increment of Li content. All samples were poled with a 4.0kV/cm dc voltage for piezoelectric constant measurement and the highest piezoelectric constant, d_{33} obtained is 181 pC/N for $x = 0.08$ sample.

ICSSST2019-153

Structural and Elastic Properties of Binary Bismuth Borate Glass SystemsNuraidayani Effendy, Sidek Hj Ab Aziz^a, Halimah Mohamed Kamari^b, Mohd Hafiz Mohd Zaid^c

Department of Physics, Faculty of Science, UPM

^asidek@upm.edu.my, ^bhalimahmk@upm.edu.my, ^cmhmzaid@upm.edu.my

Abstract. A series of binary bismuth-borate glass systems were successfully fabricated. The density was determined by using Archimedes principle. By addition of bismuth oxide content, the density of glass samples increased. The amorphous nature with no discrete and sharp peak of bismuth-borate glass systems was revealed by XRD analysis. Elastic moduli were measure and calculated at room temperature and taken at 5 MHz. The result were showed that the variation of elastic moduli decreased with the increasing of bismuth oxide content. It was due to the bismuth oxide which acts as network modifier.

ICSSST2019-165

Effect of Tungsten Oxide on Elastic Properties of Zinc Borotellurite Glass SystemHalimah Mohamed Kamari, Faznny Mohd Fudzi^a, Nazirul Nəzrin Shahrol Nidzam^b, Nur Syahirah Mat Tajudin^c

UPM

^afaznnyf@gmail.com, ^bnazirulnazrin@ymail.com, ^cnursyahirahupm@gmail.com

Abstract. Zinc borotellurite glass system doped tungsten oxide was synthesized by melt quenching method. X-ray Diffraction (XRD), Fourier Transform Infrared (FTIR) spectroscopy and elastic measurement was used to characterize the prepared samples. An amorphous nature of glass samples was determined by XRD. As tungsten oxide increases, the density decreases and molar volume increases. The longitudinal and shear velocity were measured at room temperature. The elastic properties, Poisson's ratio, microhardness and softening temperature were calculated from the measured density and ultrasonic velocity at room temperature. The elastic moduli such as longitudinal modulus, shear modulus, bulk modulus and Young's modulus give a variation trend with the increase of tungsten oxide.

Crystallography

ICSSST2019-144

Influence of Ruthenium Doping on the Structural and Magnetic Properties of $\text{Pr}_{0.67}\text{Ba}_{0.33}\text{Mn}_{1-x}\text{Ru}_x\text{O}_3$

Zakiah Mohamed

Fakulti Sains Gunaan Universiti Teknologi Mara 40450 Shah Alam, Selangor, Malaysia

zakiah626@uitm.edu.my

Abstract. In this paper, we report the structural, morphological and magnetic properties of ruthenium doping at manganese site in $\text{Pr}_{0.67}\text{Ba}_{0.33}\text{MnO}_3$ manganites. The Rietveld refinement of X-ray powder diffraction (XRD) data shows that the $\text{Pr}_{0.67}\text{Ba}_{0.33}\text{MnO}_3$ and $\text{Pr}_{0.67}\text{Ba}_{0.33}\text{Mn}_{0.9}\text{Ru}_{0.1}\text{O}_3$ crystallizes in an orthorhombic perovskite structure with Pnma space group. Doping with ruthenium shows increment in the lattice parameter and the unit cell volume. Small change in both Mn-O-Mn bond angle and bond distance is observed with ruthenium doping. Field Emission Scanning Electron Microscopy (FESEM) was used to examine the surface morphology of samples. Fourier Transform Infrared Spectroscopy (FTIR) reveal the manganese-oxygen as well as metal-oxygen bonds appeared at the band of 600 cm^{-1} and 900 cm^{-1} respectively. AC susceptibility measurements studies confirm that the samples exhibit paramagnetic to ferrimagnetic transition at 130 K and 153 K for $\text{Pr}_{0.67}\text{Ba}_{0.33}\text{MnO}_3$ and $\text{Pr}_{0.67}\text{Ba}_{0.33}\text{Mn}_{0.9}\text{Ru}_{0.1}\text{O}_3$ sample respectively.

v

Devices and Materials for Biology and Medicine

ICSSST2019-059

Preliminary Study: Entrance Surface Dose Verification using Nanodot Optically Stimulated Luminescence (OSL) For Chest X-Ray Examinations in 4 Health Clinic in PerakM.T. Saidin¹ and A.A Rahman¹¹School of Physics, Universiti Sains Malaysia Main Campus, 11800 Minden, Penang.

tarmizi7879@yahoo.co.uk

Abstract. The study was conducted to determine the patient dosimetry received in carrying out an X-ray Examination Procedure at the Perak Health Clinic. As a result of the study the ESD measurement of the procedure will be recorded. There are a number of diagnostic procedures implemented at the Health Clinic where most of the cases are for Chest PA imaging procedures. Therefore, dosimetry measurements for Chest PA imaging procedures will be recorded where the exposure factor used is usually used by the radiography at the Health Clinic. The Clinic sample involved 4 clinics which have machines less than 10 years of use and installation. Sampling of Health Clinic chosen because machines with less than 10 years of using and installation not include under the second national survey conducted from 2005 to 2009 under Ministry of Health Malaysia. The measurement of the dosimetry ESD will use the OSL nanodot ($\text{Al}_2\text{O}_3:\text{C}$) placed on the Perspex phantom with a thickness of 10 cm and recorded in the unit of mGy. Dosimetry ESD units measured using OSL nanodot for the Chest PA imaging procedure for the Perak Health Clinic recorded and reported as mean, median, first and third quartile values. Basically the recorded ESD measurements are found to be lower than the guideline level set for Chest PA X-ray examination in Malaysia as a guide for the Dose Reference Level (DRL) recommended by the Ministry of Health Malaysia is 0.9 mGy and also by the International Atomic Agency (IAEA) is 0.4 mGy.

ICSSST2019-092

An Antifouling Electrode as a Sensing Platform for the Development of an Electrochemical Immunosensor for the Determination of Glycosylated Hemoglobin (HbA1c)Safura Taufik^{1,a*} and Justin Gooding^{2,3,4,b}¹Department of Chemistry and Biology, Centre for Defense Foundation Studies, National Defense University of Malaysia, Sungai Besi Camp, 57000 Kuala Lumpur²School of Chemistry, ³Australian Centre for Nanomedicine, ⁴ARC Centre of Excellence in Convergent Bio-Nano Science and Technology, University of New South Wales, Sydney NSW 2052, Australia^asafura@upnm.edu.my, ^bjustin.gooding@unsw.edu.au

Abstract. In this project, fabrication of an antifouling electrode based on electrode-organic layer-nanoparticles construct is discussed which will then be utilized as a sensing platform for the development of electrochemical immunosensor for the detection of HbA1c, a diabetes biomarker. Antifouling electrode is required to overcome the main challenge in electrochemical biosensors, when they are exposed to biological media, there is the possibility of interference from nonspecific protein adsorption, referred to as biofouling. In this work, gold nanoparticles (AuNPs) and ethylene oxides are used as materials to fabricate the antifouling electrode. An electrochemical immunosensor based on indirect sandwich format is then used for the detection of HbA1c where it is based on the antigen-antibody interaction on the electrode surface. The determination of HbA1c (antigen) is based on the catalysis of the substrate by the enzyme labels immobilised on the 'sandwich' modified electrode surface, which the reduction of the substrate will generate an electric signal on the electrode surface. The indirect sandwich immunoassay was developed using an IgG secondary antibody conjugated to horseradish peroxidase (HRP) as the enzyme label and ferrocenemethanol (FcMetOH)/H₂O₂ was used as the enzyme mediator/substrate system. The reduction current obtained from the electrocatalytic reaction of mediator is proportional to the concentration of Ab2-HRP conjugate, thus, it is indirectly proportional to the concentration of HbA1c. The specificity of the immunosensor towards detecting the HbA1c is achieved against different antigen such as HbA₀ and HSA as well as against unmatched detection antibody, anti-biotin antibody. The results demonstrate great specificity and antifouling behaviour of the developed immunosensor allowing it for further application in whole human blood.

Electrochemical and Solid State

ICSSST2019-026

Carboxymethyl Chitosan Based Biopolymer Electrolyte with Imidazolium Ionic LiquidI.J. Shamsudin^{a*}, H.Hanibah^b, A. Ahmad^c, N. H. Hassan^c^aChemistry Department, Centre for Defence Foundation Studies, National Defence University of Malaysia, 57000 Kuala Lumpur, Malaysia.^bCentre of Foundation Studies, Universiti Teknologi Mara, cawangan Selangor, Kampus Dengkil, 43800 Dengkil, Selangor, Malaysia.^c School of Chemical Sciences and Food Technology, Faculty of Science and Technology, Universiti Kebangsaan Malaysia, 43600, Bangi, Selangor, Malaysia.

*intanjuliana@upnm.edu.my

Abstract. Solid biopolymer electrolyte based on carboxymethyl chitosan (CMChi) has been successfully prepared with ionic liquid 1-butyl-3-methylimidazolium acetate, [Bmim][OAc] as the charge carrier. The strong interactions of the ionic liquid with the biopolymer host is detected by several changes in the FTIR spectra. The decreased percentage of the crystallinity index derived from the XRD diffractograms suggests the amorphous nature of the film prepared. SEM observations showed formation of the linkages due to the plasticizing effect of [Bmim][OAc]. Higher amount of [Bmim][OAc] leads to the enhancement in the ionic conductivity, σ . The highest σ achieved is $(3.05 \pm 0.35) \times 10^{-3} \text{ S cm}^{-1}$ measured at ambient temperature. The highest conducting electrolyte achieved high electrochemical stability up to $\pm 2.8 \text{ V}$ measured by linear sweep voltammetry (LSV). Transference number measurement confirms that ions are the major contributor in the conduction of electrolyte with ± 0.980 ion transference number.

ICSSST2019-132

Synthesis and Characterization of $\text{Li}_2\text{FeP}_2\text{O}_7$ Composite by Sol-gel MethodMaziidah Hamidi^{1,2}, Oskar Hasdinor Hassan^{3*}¹Faculty of Applied Sciences, Universiti Teknologi MARA, 40450 Shah Alam, Selangor, Malaysia²Institute of Sciences, Universiti Teknologi MARA, 40450 Shah Alam, Selangor, Malaysia³Faculty of Art and Design, Universiti Teknologi MARA, 40450 Shah Alam, Selangor, Malaysia

*oskar@salam.edu.my

Abstract. A $\text{Li}_2\text{FeP}_2\text{O}_7$ cathode material was prepared using a simple citric acid-assisted sol gel method in a controlled synthesis N_2 environment. Information on the crystal structure of the monoclinic $\text{P}2_{1/c}$ space group and structure was determined with x-ray diffraction (XRD) and supported with rietveld refinement, Fourier transform infrared microscopy (FTIR), field emission scanning electron microscopy (FESEM), galvanostatic cycling of a fabricated half-cell were investigated at different current density.

Material and Energy

ICSSST2019-041

The Effect of Etching Conditions on CdS/CdTe Solar Cells EfficiencyN. A. Abdul-Manaf^{1*} and I. M. Dharmadasa²

¹Physics Department, Centre for Defence Foundation Studies, National Defence University of Malaysia, Kem Sungai Besi, 57000 Kuala Lumpur, Malaysia.

²Electronic Materials and Sensors Group, Materials and Engineering Research Institute, Faculty of Arts, Computing, Engineering and Sciences, Sheffield Hallam University, Sheffield S1 1WB, United Kingdom.

*azlian@upnm.edu.my

Abstract. This paper reports the effect of etching process on CdS/CdTe solar cells performance. Two type of etchants were used in surface treatment on CdTe solar cells prior to gold (Au) contact. Diluted potassium dichromate ($K_2Cr_2O_7$) with addition of 2 ml concentrated sulphuric acid (H_2SO_4) was used as acidic etchant and a mixture of diluted sodium hydroxide (NaOH) and sodium thiosulphate ($Na_2S_2O_3$) was used as alkaline etchant. The power conversion efficiency (PCE), η of CdTe solar cells etched with only acidic etchant showed the highest PCE and short-circuit current density, J_{sc} with $\eta = 5.1\%$ and $J_{sc} = 36 \text{ mA/cm}^2$. More detailed information is used to measure the lifetime and stability of devices. The fabricated device with acidic etchant shows good stability and lifetime with 0.1% degradation rate per month.

ICSSST2019-055

Texturization of SiNW Process for P-Type Silicon WaferMohd Norizam Md Daud^a, Nurul Aqidah Mohd Sinin^b, Suhaila Sepeai^{c*} and Kamaruzzaman Sopian^d

Solar Energy Research Institute, Universiti Kebangsaan Malaysia, 43600 Bangi, Selangor, Malaysia

^amohdnorizam@ukm.edu.my, ^bnurulaqidah88@yahoo.com, ^{c*}suhailas@ukm.edu.my, ^dksopian@ukm.edu.my

Abstract. Silicon surface texturization is required for high efficiency solar cells. Texturing process can reduce reflection and improve light trapping. Textured silicon nanowires (SiNWs) show a great potential for energy applications compare to planar and textured wafer due to the light trapping and antireflection properties. This study presents the various surface of p-type Si wafer; planar, textured and textured SiNW. Silicon nanowires were fabricated on p-type Si (111) wafer with 200 μm thickness using a single step metal assisted chemical etching (MACE) process. The surface morphology, optical properties and the optical transmission near band gap of the textured wafer is measured with custom-designed rear infra-red (IR) transmission measurement system. Si wafer with the textured SiNW surface causes more pyramidal micro structure on the surface of p-type silicon wafer and have more light absorption than the planar and textured wafer.

ICSSST2019-081

Ferroelectric and Pyroelectric Effect of Annealed Copolymer P(VDF-TrFE)Nurazlin binti Ahmad^{1,2,a*}, Wan Haliza binti Abd. Majid^{1,b}, Norhana binti Abd. Halim^{2,c} and Azuraida binti Amat^{2,d}¹ Low Dimensional Materials Research Centre, Department of Physics, University of Malaya, Kuala Lumpur 50603, Malaysia.² Physics Department, Centre for Defence Foundation Studies, Universiti Pertahanan Nasional Malaysia, 57000 Sungai Besi, Kuala Lumpur, Malaysia.^anurazlin@upnm.edu.my, ^bq3haliza@um.edu.my, ^cnorhana@upnm.edu.my, ^dazuraida@upnm.edu.my

Abstract. This work reports the effect of annealed copolymer polyvinylidene fluoride-trifluoroethylene, P(VDF-TrFE) films on their ferroelectric and pyroelectric properties. P(VDF-TrFE) solutions of 5 wt% were pipetted on glass substrate via spin coating method and thermally annealed at temperatures between 80 °C and 140 °C in order to increase their crystallinity. The investigation has identified the optimal annealed films suitable for sensors and energy harvesting application. It was found that the copolymer P(VDF-TrFE) films annealed at 100 °C shows the highest percentage of crystallinity (75.3 %), remnant polarization (76.7 mC/m²) and pyroelectric coefficient (31 μC/m²K) with the most dominant ferroelectric beta-phase which correspond to the all trans (TTTT) conformation in the polymer chain alignment.

v

ICSSST2019-167

Effect of Film Thickness on Electrochemical Properties of LiCo_{0.6}Co_{0.4}O₂ Cathode Material for Solid Oxide Fuel Cell ApplicationWan Nor Anasuhah Wan Yusoff^{1,a}, Nurul Akidah Baharuddin^{1,b*}, Mahendra Rao Somalu^{1,c} and Andanastuti Muchtar^{1,2,d}¹Fuel Cell Institute, Universiti Kebangsaan Malaysia, 43600, UKM Bangi, Selangor, Malaysia²Centre for Engineering Materials and Smart Manufacturing (MERCU), Faculty of Engineering and Built Environment, Universiti Kebangsaan Malaysia, 43600, UKM Bangi, Selangor, Malaysia.^aanasuhahwanyusoff@gmail.com, ^{b,*} akidah@ukm.edu.my, ^cmahen@ukm.edu.my, ^dmuchtar@ukm.edu.my

Abstract. Newly developed lithiated cathode material for solid oxide fuel cell (SOFC) application performance can be shown by mean of impedance spectroscopy study. The extensive impedance spectroscopy study of LiCo_{0.6}Ni_{0.4}O₂ (LCNO) cathode using samarium doped ceria (SDC) electrolyte to form an LCNO/SDC/LCNO symmetrical cell with different thickness were analyzed and so did the different microstructures. Thus, these symmetrical cells were subjected to scanning electron microscopy (SEM) analysis to acquire further knowledge on the relation of film thickness and impedance. As per stated in the literature review for SOFC electrodes that porous electrode was needed for excellent performance as well as valuable insight about engineering characteristics such as the electrochemical utilization thickness. All the impedance measurement was acquired in the operating temperature of 500 °C-800 °C for the complete elucidation of the impedance. These symmetrical cells were further characterized by electrical conductivity to study the LCNO cathode material in the correlation of the impedance study. Both SEM and electrical conductivity analysis were able to exhibit valuable physical and chemical materials parameters extracted from the analysis. Physical materials parameters were extracted from the analysis, which was in excellent accordance with literature values. From the combined impedance study and literature review, it is clear that optimum film thickness theory is the most suitable framework for any porous SOFC electrode evaluation.

ICSSST2019-168

An Overview of Working Principle and Criteria for Composite Cathode in Solid Oxide Fuel Cell

Azreen Junaida Abd Aziz^{1,a}, Nurul Akidah Baharuddin^{1,b*}, Mahendra Rao Somalu^{1,c} and Andanastuti Muchtar^{1,2,d}

¹Fuel Cell Institute, Universiti Kebangsaan Malaysia, 43600, UKM Bangi, Selangor, Malaysia

²Centre for Engineering Materials and Smart Manufacturing (MERCU), Faculty of Engineering and Built Environment, Universiti Kebangsaan Malaysia, 43600, UKM Bangi, Selangor, Malaysia

^aareen82@hotmail.com, ^{b*}akidah@ukm.edu.my, ^cmahen@ukm.edu.my, ^dmuchtar@ukm.edu.my

Abstract. A composite electrode exhibits a low activation polarization by spreading the electrochemically active area within the volume of the electrode. Composite cathodes offer the possibility of developing a high-performance electrode for intermediate temperature (600-800°C) SOFC operation via its significant role in determining the kinetics of oxygen reduction reaction (ORR). Lower ORR will result in less anion O²⁻ to be transferred through the electrolyte component. The transferred anions generally react with cation H⁺ from an anode to produce electrons transferred via the outer circuit to the cathode side to participate in ORR again. This basic working principle explains the importance of mixed ionic-electronic conductor (MIEC) behavior in the cathode for the high electrochemical performance of SOFCs. To ensure the SOFCs is robust and long-lasting, the inter-component compatibility is essential, especially in operating temperature around 600-800°C where the components experience an extreme thermal and mechanical stress. To improve the cathode performance, the use of composite cathodes has been approached where the electrolyte phase is mixed with the cathode material throughout the dry or wet procedures. It also helps to improve the MIEC property as well as improving the inter-component compatibility. The historical of composite cathode development of SOFC application, including its basic principle and criteria, will be review in this article. Furthermore, the overall performance of as-synthesized composite cathode in term of microstructural, electrochemical reaction and inter-component compatibility are briefly discussed. At the end of this article, the prospect of the composite cathode will be suggested.

Metal and Alloy

ICSSST2019-101

Influence of Zr Additive on the Reduction Behaviour of MoO₃ in Carbon Monoxide Atmosphere

Alinda Samsuri^{1,a*}, Mohd Nor Latif^{2,3,b}, Norliza Dzakaria^{4,c}, Fairous Salleh^{5,d}, Maratun Najiha Abu Tahari^{5,e}, Tengku Shafazila Tengku Saharuddin^{6,f} and Mohd. Ambar Yarmo^{5,g}

¹Department of Chemistry and Biology, Centre for Defence Foundation Studies, Universiti Pertahanan Nasional Malaysia, Kem Perdana Sungai Besi, 57000 Kuala Lumpur, Malaysia.

²PERMATApintar National Gifted Centre, Universiti Kebangsaan Malaysia, 43600 Bangi, Selangor, Malaysia.

³Department of Chemical & Process Engineering, Faculty of Engineering and Built Environment, Universiti Kebangsaan Malaysia, 43600 Bangi, Selangor, Malaysia.

⁴School of Chemistry and Environment, Faculty of Applied Sciences, Universiti Teknologi MARA, Cawangan Negeri Sembilan, Kampus Kuala Pilah, Pekan Parit Tinggi, 72000 Kuala Pilah, Negeri Sembilan, Malaysia.

⁵School of Chemical Sciences and Food Technology, Faculty of Science and Technology, Universiti Kebangsaan Malaysia, 43600 UKM Bangi, Selangor Darul Ehsan, Malaysia.

⁶Faculty of Science and Technology, Universiti Sains Islam Malaysia, Bandar Baru Nilai, 71800, Nilai, Negeri Sembilan, Malaysia.

^aalinda@upnm.edu.my, ^bmohdnor@ukm.edu.my, ^cnorlizadzakaria75@gmail.com, ^dfairoussalleh@gmail.com, ^emaratunnajiha@gmail.com, ^ftengkushafazila@gmail.com, ^gambar@ukm.edu.my

Abstract. The reduction of molybdenum trioxide, MoO₃ by using carbon monoxide, CO have been studied by temperature programmed reduction (TPR), X-ray diffraction (XRD), Brunauer-Emmett-Teller (BET) and TEM analysis. The TPR results show that the reduction peak of MoO₃ with 20% CO in nitrogen begins at 560°C. Since the melting point of MoO₃ is 795°C, reduction of MoO₃ to MoO₂ need to complete at temperature lower than the melting point. If the reduction of MoO₃ is not completed below this temperature, it will end up as a fused mass. 3% zirconium addition to modified MoO₃ reliable to lower the reducing temperature of MoO₃. The TPR results show that the reduction peak of doped MoO₃ are slightly shifts to lower temperature as compared with the pure MoO₃. The interaction between zirconium and molybdenum ions leads to this slightly decrease of the reduction temperature of zirconium doped MoO₃. Based on the characterization of the reaction products using XRD, it confirmed that the reduction of MoO₃ to MoO₂ by CO consists of two reduction stages, namely, Mo⁶⁺ → Mo⁵⁺ and Mo⁵⁺ → Mo⁴⁺. Reduction of pure MoO₃ to MoO₂ was a consecutive reaction with the intermediate products Mo₉O₂₆ and Mo₄O₁₁. However, only intermediate product Mo₄O₁₁ formed with doping of zirconium to MoO₃. It can be seen that doping with zirconium has a remarkable influence in the reduction process of the MoO₃ powders.

ICSSST2019-141

The Role of Sr on Microstructure and Mechanical Properties of Al A356 Reinforced Al₂O₃ Composite

Anne Zulfia

Department of Metallurgy and Materials, Faculty of Engineering, Universitas Indonesia, Kampus Baru Universitas Indonesia, Depok 16424 Indonesia

anne@metal.ui.ac.id

Abstract. Aluminium alloy A356 reinforced with Al₂O₃ metal matrix composites (MMCs) have been produced by stir casting process. The strontium was added to molten Al A356 is to improve mechanical properties of composites. The strontium used was varied from 0.046 wt-% to 0.070 wt-% while Al₂O₃ was kept constant 10Vf-%. The aim of this research is to study the effect of Sr on microstructure and mechanical properties of Al A356/Al₂O₃ composite. The A356 was melted at 800°C and mixed with Al-5TiB, Al-5Sr and Mg as master alloy of matrix then flushed with argon to remove all the gas bubble from liquid aluminium and stirred for 2 minutes afterwards it was poured with Al₂O₃ particles and stirred again for 3 minutes to distribute the Al₂O₃ particles in molten Al matrix. The composites produced then characterised both microstructural analysis and mechanical properties. The maximum strength, elongation and hardness of composites were achieved at 0,046 wt-% Sr with the value of 185 MPa, 4.00% and 45.3 HRB, while strength, elongation and hardness of unreinforced were 101 MPa, 2,72% and 40 HRB respectively and further addition of Sr mechanical properties decreased. The increase in the strength is due to the refinement of Mg₂Si primary in the matrix.

v

ICSSST2019-180

Effect of Titanium and Aluminium Addition on Microstructure and Corrosion Behaviour of AISI 430 Ferritic Stainless Steel Welds

Nabil Bensaid ^{1,2 a*}, Mohamed Farid Benlamnour ^{1,2,b}, Riad Badji ^{1,c}, Sabah Senouci ^{3,d}, Tahar Saadi ^{1,e}, Yazid Laib dit Leksir ^{3,f}, Amar Boutagane ^{1,g}, Mohamed Hadji ^{2,h}

¹Research Center in Industrial Technologies CRTI, Cheraga 16014, Algiers, Algeria.

²Laboratoire des Aeronefs, University of Blida1, Route de Soumaa, Blida 9000, Algeria.

³Solids solutions laboratory, physics faculty USTHB, BP 32, El-Alia, Algiers, Algeria.

⁴Département de génie climatique, Université constantine1, Constantine 25000, Algérie.

^an.bensaid@crti.dz, ^bf.benlamnour@crti.dz, ^cr.badji@crti.dz, ^dSabah.senouci@yahoo.fr, ^eta_saadi@enst.dz, ^fyaziddl@yahoo.fr, ^ga.Boutagane@crti.dz ^hhadji_n@yahoo.com.

Abstract. Ferritic stainless steels are classified as such because the predominant metallurgical phase present is ferrite. These steels are characterized by good resistance to stress corrosion cracking (SCC), pitting corrosion, crevice corrosion (particularly in chloride environments), higher thermal conductivity, low coefficient of heat dilation and lower cost, when compared to austenitic stainless steels. The combination of low cost and good properties has made ferritic stainless steel more and more attractive in various application fields, such as, heat exchangers, petroleum refining equipment, storage vessels, protection tubes, solar water heaters, and exhaust manifold applications. However, ferritic stainless steel steels are associated with many problems during the welding process. These problems are the martensite formation and grain growth, causing a reduction of ductility and toughness. For these reasons, until recently, the application of this group steels is limited in welded structures. The aim of this study is to investigate the influence of Titanium and Aluminum addition on the microstructure and corrosion behaviour of AISI 430 ferritic stainless steel welds produced by gas tungsten arc welding was investigated. It's observed that the addition of aluminium (Al) or titanium (Ti) reducing the grains size, increase the equiaxed grains fraction and improve the mechanical properties with varying degrees. While the addition of mixture (Al+Ti) leads to better improving in mechanical properties and reducing of grains size up to 85%. The details of tensile tests, optical microscopic observations, microhardness, tensile test and Scanning electron microscopy (SEM) fractography, are discussed.

ICSSST2019-181

Effect of Filler Metal Types on Microstructure and Mechanical Behavior of HSLA-X70/304L SS Dissimilar Welds

Mohamed Farid Benlamnour ^{1,2,a*}, Nabil Bensaid ^{1,2,b}, Sabah Senouci ^{3,c}, Tahar Saadi ^{1,d}, Yazid Laib dit Leksir ^{3,e}, Amar Boutagane ^{1,f}, Riad Badji ^{1,g}, Mohamed Hadji ^{2,h}

¹Research Center in Industrial Technologies CRTI, Cheraga 16014, Algiers, Algeria.

²Laboratoire des Aeronefs, University of Blida1, Route de Soumaa, Blida 9000, Algeria.

³Solids solutions laboratory, physics faculty USTHB, BP 32, El-Alia, Algiers, Algeria.

⁴Département de génie climatique, Université constantine1, Constantine 25000, Algérie.

^af.benlamnour@crti.dz, ^bn.bensaid@crti.dz, ^cSabah.senouci@yahoo.fr, ^dta_saadi@enst.dz, ^eyaziddl@yahoo.fr, ^fa.Boutagane@crti.dz, ^gr.badji@crti.dz, ^hhadji_n@yahoo.com

Abstract. The aim of this study is to investigate the effect filler metal types on microstructure and mechanical properties of dissimilar welds between HSLA-X70 high strength steel alloy and 304L austenitic stainless steel produced by automatic tungsten arc welding (TIG). The weld joints were prepared using E304L, E316L, E2209L, and E7010 filler metal. The mechanical characteristics obtained from hardness, tensile and impact testing, were correlated to the optical and SEM microscopy, to establish a relationship between filler metal composition and the microstructures in different weld regions. It is concluded that E2209 filler metal lead to improve in the resilience characteristics and tenacity with a slight reduction in the ultimate tensile strength and hardness.

ICSSST2019-184

Mechanical Properties of Highly Deformed Sn-3.0Ag-0.5Cu Solder Wire

Norliza Ismail¹, Azman Jalar^{1,2*}, Maria Abu Bakar²

¹Pusat Pengajian Fizik Gunaan, Fakulti Sains & Teknologi, Universiti Kebangsaan Malaysia (UKM), 43600 Bangi, Selangor, Malaysia

²Institut Kejuruteraan Mikro & Nanoelektronik (IMEN), Universiti Kebangsaan Malaysia (UKM), 43600 Bangi, Selangor, Malaysia

*azmn@ukm.edu.my

Abstract. In this study mechanical properties of highly deformed Sn-3.0Ag-0.5Cu (SAC305) lead-free solder wire was investigated. SAC305 solder wire underwent tensile test with 0.1 mms⁻¹ strain rate at room temperature, 25°C and at 120°C chamber condition. Mechanical properties of deformed solder wires were evaluated from stress strain curve of tensile test followed by nanoindentation test. Micromechanical behavior of deformed solder wires was determined using nanoindentation multicycle method. Results shows that deformed SAC305 solder wire at room temperature have a high yield stress compared to SAC305 solder wire at 120°C temperature. Hardness values of deformed SAC305 solder wire are higher than SAC305 solder wire at 120°C temperature. Decreasing of hardness values in SAC305 solder wire at 120°C is due to existence of thermal. In addition, thermal induced the softening behavior of deformed SAC305 solder wire.

ICSSST2019-185

Synthesis and Characterization of Copper Selenide and Tin Selenide Powders by Mechanical Alloying MethodLoh Yen Nee¹, Zainal Abidin Talib^{1*}, Zulkarnain Bin Zainal², Josephine Liew Ying Chyi¹¹Department of Physics, Faculty of Science, Universiti Putra Malaysia, 43400 UPM Serdang, Selangor, Malaysia²Department of Chemistry, Faculty of Science, Universiti Putra Malaysia, 43400 UPM Serdang, Selangor, Malaysia

*zainalat@upm.edu.my

Abstract. This paper reports on the synthesis of Copper Selenide (CuSe) and Tin Selenide (SnSe) powders by high energy planetary ball milling, starting from elemental powders. Synthesis time and velocity have been optimised to produce CuSe and SnSe materials. The structural, compositional, morphological and optical properties of the synthesised samples have been analyzed by X-ray diffraction (XRD), transmission electron microscopy (TEM), Field Emission Scanning Electron Microscopy (FESEM) and UV-Vis. The low-temperature phase selection of the binary compound in this system is seen as a direct consequence of the thermodynamic facilitation, coupled with the capability of mechano-chemical synthesis to aid in overcoming kinetic constraints.

v

Nanoscience and Nanotechnology

ICSSST2019-087

Synthesis Optimization and Characterization of Chitosan-coated Magnetite Nanoparticles Extracted from Mill Scales Waste

Nur Asyikin Ahmad Nazri^{1,3,a*}, Raba'ah Syahidah Azis^{1,2,b}, Abdul Halim Shaari^{2,c}, Hasfalina Che Man^{4,d}, Ismayadi Ismail^{1,e}

¹Material Synthesis and Characterization Laboratory (MSCL), Institute of Advanced Technology (ITMA), Universiti Putra Malaysia, 43400 Serdang Selangor.

²Department of Physics, Faculty of Science, Universiti Putra Malaysia, 43400 Serdang Selangor.

³Center of Foundation Studies, Cawangan Selangor, Universiti Teknologi MARA, 43800 Dengkil, Selangor, Malaysia.

⁴Department of Biological and Agricultural Engineering, Faculty of Engineering, Universiti Putra Malaysia, 43400 Serdang, Selangor, Malaysia.

^aasyikin2750@uitm.edu.my, ^brabaah@upm.edu.my, ^cahalim@upm.edu.my, ^dhasfalina@upm.edu.my, ^eismayadi@upm.edu.my

Abstract. The optimization of the self-assembly coating method of chitosan onto magnetite nanoparticles which is extracted from mill scales waste has been successful with the assist of ultrasonication. First, via self-assembly of positively charged Chitosan and negatively charged magnetite nanoparticles. Samples from stirring method also has been prepared to compare with the sonicated samples. High Resolution Transmission Electron Microscopic (HR TEM) images showed that well dispersed of the magnetite nanoparticles and chitosan was occurred. Surface charges of the nanocomposites were carried out by using Zetasizer to measure the changes in zeta potential caused by the different coating method. It was found that the different mixing method has the greatest influence on the dispersity when measured over a range of zeta potential as well as surface charges. Sonication process helps to optimize the dispersity of the chitosan and magnetite. Hence, the coating process produce better results. Stirring method is only allowed agglomerated magnetite covered with chitosan non-uniformly while with sonication, every single particles is coated uniformly by the chitosan. Chitosan is one of the cation polymer widely used as a good potential modifier. Since magnetite is an amphoteric solid, which is pH dependent. Therefore, to allow self assembly to occur between the chitosan onto the magnetite the pH must controlled to an optimum pH. These polymer magnetic nanocomposites has high magnetite loading content, and showed unique pH-dependent behaviours on the zeta potential. The modified magnetite with chitosan was believed to have higher potential for magnetic separation in waste water treatment with higher value of adsorption.

ICSSST2019-096

Effect of TEOS on the Synthesis of Silica-coated Iron Oxide NanoparticlesNurul Izza Taib^{1, a *}, Nur Diyana Syazwani Zambri^{2, b}, Famiza Abd Latif^{2, c} and Zakiah Mohamed^{2, d}¹Faculty of Applied Sciences, Universiti Teknologi MARA, Perak Branch, Tapah Campus, 35400 Tapah Road, Perak, Malaysia.²Faculty of Applied Sciences, Universiti Teknologi MARA, 40450 Shah Alam, Selangor, Malaysia.^aizza257@uitm.edu.my, ^bndiyana1811@gmail.com, ^cfamiza@uitm.edu.my, ^dzakiah626@uitm.edu.my

Abstract. In targeted drug delivery system, the drug is embedded in SiO₂ that will be transported to the targeted area by coating it on Fe₃O₄ nanoparticle. In this study, this SiO₂ has been coated on the surface of Fe₃O₄ (Fe₃O₄@SiO₂) by hydrolysis and condensation of tetraethyl orthosilicate (TEOS) under alkaline medium at 80°C. It was found that only 500 μL TEOS is required to obtain the best coated Fe₃O₄ core structures which has been confirmed from its TEM micrograph. FTIR analyses revealed the formation of Si-O-Si bonds at 1084.2–1101.4 cm⁻¹ hence confirmed that SiO₂ has been successfully coated the Fe₃O₄ core. From the FESEM analyses, the average size of silica was ~ 50 -70 nm. EDX of the Fe₃O₄@SiO₂ showed that silica had been effectively bonded onto the surface of Fe₃O₄. The VSM measurements confirmed the superparamagnetic properties of Fe₃O₄@SiO₂ that is desirable for biomedical applications.

v

ICSSST2019-106

Determination of Hygroscopic Growth and Water Activities of Continentals and Desert AerosolsM. D. Audu¹, I. G. Geidam², I. B. Kinga³¹Department of Physics Federal College of Education (Tech), Potiskum, Nigeria.²Department of Physics Yobe State University Damaturu, Nigeria.³Department of Integrated Science Education Federal College of Education (Tech), Potiskum, Nigeria.¹mdabdulpot29@gmail.com

Abstract. The hygroscopic growth of atmospheric aerosols influences human health, Earth climate and atmospheric chemistry. In this paper the microphysical properties such as radii, number concentration, volume mix ratio etc. were extracted from optical properties of aerosols and cloud (OPAC), the ZSR (Zdanavskii, Stokes and Robinson) is used to compute the hygroscopic growth of the aerosols mixture and modified Köhler equation was also used to predict water activities and kelvin effect at eight different values of relative humidity 0%, 50%, 70, 80, 90, 95, 98, and 99%. We observed that hygroscopic growth of atmospheric aerosols of Continental Clean, Continental pollutant, Continental average and Desert increased with the increasing relative humidity and for the water activity the highest value was found in desert aerosols ($a_w = 1.36$) at 50% RH and the lowest was observed in continental aerosols ($a_w = 0.38$) at 0% RH also for p -value ($p < 0.05$) the data fitted the equations very well.

ICSSST2019-149

Facile Synthesis and Characterizations of Silver Nanoparticle-Reduced Graphene Oxide HybridNurul Izrini Binti Ikhsan^{1,2,a*}, Nurul Ain Mohamed Zamri^{1,b}¹Faculty of Applied Sciences, Universiti Teknologi Mara (UiTM), 40450 Shah Alam, Malaysia.²Ionic Materials and Devices, Universiti Teknologi Mara (UiTM), 40450 Shah Alam, Malaysia.^{a*}nurulizrini@gmail.com, ^bainnnz96@gmail.com

Abstract. Here, we report the synthesis of silver nanoparticle-reduced graphene oxide (AgNPs-rGO) hybrid for facile and eco-friendly method. Silver nanoparticles (AgNPs) were successfully deposited on reduced graphene oxide (rGO) sheets to (AgNPs-rGO) hybrid using lemon extract as a reducing and stabilizing agent. The products form a stable aqueous solution without any surfactant stabilizers and this makes it possible to produce (AgNPs-rGO) hybrid on a large scale using low-cost solution processing technique. The synthesis of nanohybrid was monitored at different ratio of reducing agent (1:1, 1:2, 1:4) and characterized using UV-Visible (UV-Vis) absorption spectrum, X-ray diffraction (XRD) and Raman spectroscopy analyses. From UV-Vis absorption spectrum, the (AgNPs-rGO) (1:1) hybrid result shows the sharp peak at 433 nm indicating the accomplishment formation of AgNP on the surface of rGO sheets. Completely spherical Ag nanoparticles (NPs) were found at (AgNPs-rGO) (1:1) hybrid with an average particle size of 21 nm. Furthermore, (AgNPs-rGO) (1:1) hybrid exhibit fast electron-transfer kinetics for electrochemical reaction of Fe (CN)₆^{3-/4-} redox couple, suggesting the potential applications for electrocatalysis and electrochemical sensor.

ICSSST2019-154

DFT and Spectroscopic Study of a Zin-porphyrin Beta-substitution with Indene-dioxo Group for Potential Dye-sensitized Solar Cell (DSSCs) use

Alvie Lo Sin Voi, Keith C. Gordon, Pawel Wagner; David L. Officer

alvielo@gmail.com, keith.gordon@otago.ac.au

Abstract. Dye-sensitized Solar Cells (DSSCs) attract great attention due to potential low cost and relatively high solar conversion. Porphyrin have optical properties and electronic structure that can be suitable for DSSCs. In this study, the substitution effect of indene-dioxo group at the beta-position is investigated using spectroscopy and quantum chemistry to look at how the electron withdrawing group at beta-position can alter the electronic structure of the molecule. Density functional theory (DFT) and the time dependent DFT (TDDFT) couple with spectroscopy technique were employed. The study reveals that the substitution has resulted in redshift and broadening of its solar absorption spectra due to the appearance of new absorbant band. The additional band can be attributed to the indene-dioxo group. In addition, the substitution also improves the unidirection of the charge transfer character which is important for the DSSCs process. This finding can be benefited for the design of new efficient sensitizer.

ICSSST2019-186

Comparative Study on Micronized and Nanosized *Carica Papaya* Seed Modified Pullulan as Biocoagulant in Wastewater TreatmentDeong Jing Lie^{1, a}, Mazatuszihah Ahmad^{2, b} * and Nur Sabrina Azhar^{3, c}¹Faculty of Engineering Technology, Universiti Tun Hussein Onn Malaysia, Malaysia²Biotechnology-Sustainable Material (B-SMAT) Focus Group, Advanced Technology Centre (ATC), Faculty of Engineering Technology, Universiti Tun Hussein Onn Malaysia, Malaysia³Faculty of Engineering Technology, Universiti Tun Hussein Onn Malaysia, Malaysia^adn160283@siswa.uthm.edu.my, ^b*maza@uthm.edu.my, ^cdn160167@siswa.uthm.edu.my

Abstract. Plant-based coagulants have been used as an alternative to replace chemical coagulant in wastewater treatment. So far, limited information was found on the incorporation of biocoagulant to natural polymers and the effect of particle size upon wastewater treatment application. Thus, this study was conducted to explore the effectiveness of micronized and nanosized *Carica Papaya* (CP) seed modified pullulan as biocoagulant. The biocoagulant were prepared at different composition of CP to pullulan, with the CP content range from 1% to 9%. The biocoagulant were characterized via particle size distribution and Fourier transform infrared spectroscopy (FTIR). Biocoagulant produced was used to treat municipal wastewater. The treated wastewater quality was analyzed by jar test method with dosage of biocoagulant used was 0.6 g/L. The result showed that the micronized CP at D10, D50 and D90 was 0.3675 μm , 0.8433 μm and 1.9537 μm respectively. The nanosized CP was 0.4473 nm (D10), 2.3758 nm (D50) and 2.9938 nm (D90). It was found that at 3% micronized CP and 7% nanosized CP were able to reduce turbidity up to 59.65% and 65.27% respectively. Both size of biocoagulant slightly changed the pH of treated wastewater, increased in dissolved oxygen (DO) and reduced in total suspended solid (TSS) of treated wastewater. Overall, nanosized CP was found more effective than micronized CP.

Optical and Dielectric Materials

ICSSST2019-025

Pt Coated Carbon Nanotubes for Optical Limiting Applications

Noor Aisyah Ahmad Shah^{1,a}, Siti Zulaikha Ngah Demon^{2,b}, Farah Nabila Diauddin^{3,c}, Norli Abdullah^{1,d}, Norherdawati Kasim^{1,e}, Ganesan Krishnan^{4,f}

¹Jabatan Kimia & Biologi, Pusat Asasi Pertahanan, Universiti Pertahanan Nasional Malaysia, Kem Sungai Besi, 57000 Kuala Lumpur, Malaysia.

²Jabatan Fizik, Pusat Asasi Pertahanan, Universiti Pertahanan Nasional Malaysia, Kem Sungai Besi, 57000 Kuala Lumpur, Malaysia.

³Fakulti Sains dan Teknologi Pertahanan, Universiti Pertahanan Nasional Malaysia, Kem Sungai Besi, 57000 Kuala Lumpur, Malaysia.

⁴Laser Centre, Ibnu Sina Institute for Scientific & Industrial Research (ISI-SIR), Universiti Teknologi Malaysia, 81310 Johor Bahru, Johor, Malaysia

^aaisyah@upnm.edu.my, ^bzulaikha@upnm.edu.my, ^cfarnad242@gmail.com, ^dnorli.abdullah@upnm.edu.my, ^eherdawati@upnm.edu.my, ^fk.ganesan@utm.my

Abstract. Platinum/multi-wall carbon nanotubes (Pt/MWCNTs) was prepared through chemical reduction and characterized by UV-vis spectrophotometer, transmission electron microscopy (TEM), scanning electron microscopy (SEM) and Raman spectroscopy. Through this chemical reduction, Pt ions were reduced by the addition of sodium dodecyl sulfate (SDS), and Pt was in-situ deposited on the exterior walls of MWCNTs. Finally, the Pt/MWCNTs in ethanol suspension was investigated with continuous wave laser and z-scan measurement at 532 nm to study its optical limiting properties. The results show the optical limiting of Pt/MWCNTs is remarkable in comparison to the MWCNTs as suspensions.

Organic Materials and Application

ICSSST2019-008

Vibrational Spectroscopy Analysis of Oligomer Blend Film

Siti Zulaikha Ngah Demon^{1, a*} and Nursaadah Ahmad Poad^{1,b}

¹Pusat Asasi Pertahanan, Universiti Pertahanan Nasional Malaysia, Kem Sungai Besi, Kuala Lumpur 57000, Malaysia.

^{a*}zulaikha@upnm.edu.my, ^bnursaadah_ahmadpoad@yahoo.com

Abstract. Organic semiconductor materials can be utilized in production of flexible electronic displays. Spin-coating fabrication of biodegradable polylactic acid (PLA) and small molecule 3''-didodecyl-2,2':5',2'':5'',2''-quarterthiophene (4T) blend was introduced to demonstrate the feasibility of processing oligomers at ambient atmosphere. High molecular weight polylactic acid served as binding matrix to the small molecule and to promote film homogeneity across the ITO substrate. PLA and 4T were successfully blended as amorphous film determined by atomic force microscope. The complementary vibrational studies using ATR-FTIR and Raman spectroscopies are able to identify the characteristics of thiophene rings and alkyl functional group of 4T with and without the presence of polymer. Our result implied the change of molecular orientation of 4T that is known for standing formation to lying formation after introduction of polymer. The microscopic information of oligomers is crucial in future flexible electronics applications.

ICSSST2019-126

Corrosion Inhibition of Mild Steel by Electrodeposited Poly(M-Aminophenol) CoatingSabrina M Yahaya^{1*}, M K Harun¹, R. Rosmamuhamadani²¹ Department of Applied Chemistry, Faculty of Applied Sciences, Universiti Teknologi MARA, 40450 Shah Alam, Selangor, Malaysia.² Department of Material Technology, Faculty of Applied Sciences, Universiti Teknologi MARA, 40450 Shah Alam, Selangor, Malaysia.

*sabrina@salam.uitm.edu.my

Abstract. Electrochemical impedance spectroscopy (EIS) was used to study the corrosion protection properties of poly (m-aminophenol) (PMAP) coatings in 0.5 M NaCl aqueous solution towards mild steel electrode. The coatings properties interpreted through Nyquist and Bode EIS plots. Data from the Nyquist and Bode plots were used to model the equivalent electrical circuit (EEC) that described the overall coating performance. Data obtained showed that PMAP coatings experienced a significant drop in total impedance followed by the development of an electrochemical reactions on coating/metal interface indicating gradual degradation of the PMAP coatings. The coatings were characterized by Fourier transform infrared (FTIR) spectroscopy and scanning electron microscopy (SEM). The appearance of broad absorption band at 1082 cm⁻¹ attributed to stretching vibration of the C–O–C ether group supports the electropolymerization of PMAP coatings. The micrograph of SEM indicates the formation of a dense and continuous PMAP coatings.

Polymer and Composite

ICSSST2019-002

Fatigue Lifetime Prediction of Bamboo Laminated Composites

Aidy Ali*, Faiz Othman, and M. K. Faidzi

Department of Mechanical Engineering, Faculty of Engineering

Universiti Pertahanan Nasional Malaysia (UPNM) National Defense University of Malaysia (NDUM) Kem Sg. Besi, 57000, Kuala Lumpur, Malaysia.

Tel: +6 017-2496293; Fax: +6 038-946-7122

*saidynaidy@gmail.com

Abstract. It is evident that laminated reinforced composite are successfully prolonging the life of composites compared to particle and fiber type of reinforced composites method. The question on how this laminated composites take up the fatigue loading is crucial in order to give sound confident to industry replacing their design from metal to composites based. The lack of confident and uncertainties' life of composites components become an issue to designer to shift from metal based to composites based especially when the design required to be done in short time. The works gives prediction of fatigue lifetime of laminated bamboo composites. The model work well and the accuracy of prediction is acceptable with below than 10 % errors.

ICSSST2019-088

Conversion of Bacterial Cellulose to Cellulose Nitrate with High Nitrogen Content as Propellant Ingredient

Siti Hasnawati Jamal^{1,a}, Nursyafiqah Jori Roslan^{2,b}, Noor Aisyah Ahmad Shah^{1,c}, Siti Aminah Mohd Noor^{1,d}, Ong Keat Khim^{1,e}, Wan Md Zin Wan Yunus^{2,f}

¹Department of Chemistry and Biology, Center for Defence Foundation Studies, National Defence University of Malaysia, 57000 Kuala Lumpur, Malaysia.

²Department of Defence Science, Faculty of Defence Science and Technology, National Defence University of Malaysia, 57000 Kuala Lumpur, Malaysia.

^ahasnawati@upnm.edu.my, ^bsyafiqahjr@gmail.com, ^caisyah@upnm.edu.my, ^ds.aminah@upnm.edu.my, ^eongkhim@upnm.edu.my, ^fwanmdzin@upnm.edu.my

Abstract. Nitrocellulose has attracted great interest amongst researchers due to its uses in wide range of products including paint and gun propellant. Therefore, this work focuses on the synthesis of nitrocellulose using two different sources of cellulose; plant and bacterial. It is important to obtain cellulose nitrate with high percentage of nitrogen content so that it can be used as an ingredient in propellant. The synthesis of cellulose nitrate was carried out via nitration method using different sources of cellulose; *nata de coco* and kapok (*Ceiba pentadra* L). The samples were then characterized by elemental analysis, Fourier transform infrared (FTIR) spectroscopy and surface electron morphology (SEM). Elemental analysis was performed to determine percentage of nitrogen content attached to the cellulose. FTIR shows the presence of NO₂ groups in nitrocellulose, proving that it was successfully synthesized by nitration method.

ICSSST2019-119

Effects of Ammonium Bromide on Methylcellulose Biopolymer Electrolytes in Optical and Electrical Studies

Siti Nurhaziqah Abd Majid^{1,a}, Afiqah Qayyum Ishak^{1,b}, Nik Aziz Nik Ali^{1,c*}, Muhamad Zalani Daud^{2,d}, Hasiah Salleh^{3,e}

¹School of Fisheries and Aquaculture Sciences, University Malaysia Terengganu, 21030 Kuala Nerus, Terengganu, Malaysia

²School of Ocean Engineering, University Malaysia Terengganu, 21030 Kuala Nerus, Terengganu, Malaysia

³Center for Foundation and Liberal Education, University Malaysia Terengganu, 21030 Kuala Nerus, Terengganu, Malaysia

^anurhaziqahmajid@gmail.com, ^baqizqayyum@gmail.com, ^{c*}nikaziz@umt.edu.my, ^dzalani@umt.edu.my, ^ehasiah@umt.edu.my

Abstract. The development of biopolymer electrolytes based on methylcellulose (MC) has been accomplished by incorporating ammonium bromide (NB) to the polymer-salt system. The biopolymer electrolytes were prepared via solution-casting method. The conductivity and permittivity characteristics of the material were studied. The biopolymer-salt complex formation have been analysed through Fourier Transform Infrared (FTIR) spectroscopy and X-ray diffraction (XRD). The conductivity of the sample was measured by EIS HIOKI. Upon addition of 20wt.% of NB, highest conductivity of $3.25 \times 10^{-4} \text{ Scm}^{-1}$ was achieved at ambient temperature. The temperature dependence of the biopolymer electrolytes exhibit Arrhenius behaviour. This result had been further proven in FTIR study.

ICSSST2019-157

Study of π - π Interaction and Covalent Bond of Hybridized Polypyrrole with Reduced Graphene Oxide CompositesNur Atikah Md Jani^{1,a,*}, Muhammad Aidil Ibrahim^{1,b}, Tunku Ishak Tunku Kudin^{1,c}, Oskar Hasdinor Hassan^{2,d},
Ab Malik Marwan Ali^{5,e}¹Ionics Materials & Devices Research Laboratory (iMADE), Institute of Science, Universiti Teknologi MARA, 40450 Shah Alam, Selangor, Malaysia²Faculty of Art and Design, Universiti Teknologi MARA, 40450 Shah Alam, Selangor, Malaysia³ Faculty of Applied Sciences, Universiti Teknologi MARA, 40450 Shah Alam, Selangor, Malaysia^anuratikahmdjani@yahoo.com, ^baidilibrahim1991@yahoo.com, ^ctunkuishak@gmail.com,
^doskar@salam.uitm.edu.my, ^eammali@salam.uitm.edu.my

Abstract. The composition of polypyrrole (PPy) and reduced graphene oxide (rGO) are the materials that can enhance the sensitivity and selectivity of sensor devices such as a biosensor. Polypyrrole is a conducting polymer that has a unique characteristic which it can act as a transducer that converts the biological signal to an electrical signal. While graphene is a good electric conductor, have a large surface area and a great mechanical strength as it can increase the electroconductivity of a device. The combination of these great materials might produce the greatest composite to improve the transducer of a device. Hybridized composites of polypyrrole (PPy) with reduced graphene oxide (rGO) was composited by ultrasonication process as to harvest PPy/rGo with a various weight ratio of PPy:rGO 1;1, 1;2, 1;3, and 1;4 respectively. All the samples produced were observed through the Scanning Electron Microscopy (SEM), also been characterized with Fourier transform infrared spectroscopy (FTIR) and ultraviolet-visible spectroscopy (UV-Vis) to analyze the π - π interaction and hydrogen bond between the PPy and rGO as to confirm the presence of both molecules in all sample. The ratio of PPy;rGO 1;1 has the greatest interaction and most prominent compared to other ratios.

Semiconductors and Devices

ICSSST2019-152

Semiconductor Devices Lifetime Prediction Methodology for Hot Carrier Injection Tests

Mr. Yew Huang Lau

Silterra Malaysia, Kulim Hi-Tech Park, 09090 Kulim, Kedah Darul Aman, Malaysia

yewhuang_lau@silterra.com

Abstract. Hot Carrier Injection (HCI) tests in Semiconductor Reliability is one of the gating stress tests to ensure semiconductor devices last the lifetime that is promised to the customer. Typically a set of devices is subjected to three or more different stress conditions. Before hand, those devices needs to be characterized in order to determine its' electrical performance. These can be the threshold voltage, linear channel current or saturation current. Those set of devices then undergo the stress condition which has been determined beforehand. After the stress routines are completed, they have to be characterized again. The next step would be to determine what are the drift values observed. The loop of stress and characterization needs to be repeated until a predetermined drift criterion is achieved. The total time taken also has to be recorded. In modern reliability equipment, these measurements are handled automatically. In order to determine the lifetime of the device in field or actual operating condition, an extrapolation to that use condition is necessary. When performing the extrapolation, special care is needed in order to get an accurate lifetime model. In this paper, two methodologies are proposed, the global or universal data fitting methodology and the individual data fitting methodology. A set of 5V NMOS devices were subjected to HCI stress tests as described earlier. A degradation plot is obtained from these set of tests. These set of experimental data were then used to illustrate the means of the fitting methodologies. The physics behind each data fitting methodology are described. It is observed that different wearout lifetime for the 5V NMOS devices are deduced. A lognormal lifetime plot is used to illustrate this. This paper then explains why the global or universal method is preferable. Although this paper uses the HCI tests to describe the fitting methodologies, in principle it can be used in other types of semiconductor process reliability tests such as Time Dependent Dielectric Breakdown (TDDB), Negative Bias Temperature Instability (NBTI) and others.

Superconductors

ICSSST2019-047

Synthesis and Characterization of Low Density Bi-2223 Cuprates Superconductor Doped Eu₂O₃ NanoparticlesE. S. Nurbaisyatul^{1,a*}, H. Azhan^{2,b}, K. Azman^{2,c}, N. Ibrahim^{1,d}, S. F. Saipuddin^{2,e}¹Faculty of Applied Sciences, Universiti Teknologi MARA Shah Alam, 40450 Shah Alam, Selangor, Malaysia²Faculty of Applied Sciences, Universiti Teknologi MARA Pahang, 26400 Bandar Tun Abdul Razak Jengka, Pahang, Malaysia^{a*}ersyamiza@gmail.com, ^bdazhan@pahang.uitm.edu.my, ^cazman615@pahang.uitm.edu.my, ^dnoraz954@salam.uitm.edu.my, ^esitifatih7020@uitm.edu.my

Abstract. Bi_{1.6}Pb_{0.4}Sr₂Ca_{2-x}Eu_xCu₃O₈ cuprates superconductor doped with Eu nanoparticles (x = 0.00, 0.02, 0.05 and 0.07) were synthesized through conventional solid state reaction method. Crystalline sucrose was added during pelletization and burn at 400°C for two hours to create low density sample. The effect of doping Eu₂O₃ nanoparticles on the structural and superconducting properties by means of critical temperature, critical current density, X-ray diffraction (XRD) together with Field Emission Scanning Electron Microscopy (FESEM) were studied. Based on XRD analyses, the crystallographic structure has shown slightly changed from tetragonal to orthorhombic. The amount of 2223 phase gradually decreased with the increment of Eu concentration which indicates that Eu nanoparticles substitution favours the growth of 2212 phases. FESEM results showed that the plate-like grains become smaller and distributed randomly without specific alignment due to the increment of Eu concentration.

ICSSST2019-166

Enhanced Transport Critical Current Density of TI-1212 Bulk Superconductor Added with Nickel-Zinc Ferrite NanoparticlesWei Kong^{1, a*}, Nurul Auni Khalid^{2, b}, Wani Nadhirah Titingan Nizam^{3, c}, Kim Yeow Tshai^{3, d}, Ing Kong^{4, e}, Eng Hwa Yap^{5, f} and Roslan Abd-Shukor^{6, g}¹Centre for Foundation and General Studies, Infrastructure University Kuala Lumpur, Jalan Ikram - Uniten, 43000 Kajang, Selangor, Malaysia.²Faculty of Science, Universiti Putra Malaysia, 43400 Serdang, Selangor, Malaysia.³Faculty of Engineering, University of Nottingham Malaysia, Jalan Broga, 43500 Semenyih, Selangor, Malaysia.⁴School of Engineering and Mathematical Sciences, La Trobe University, Bendigo VIC 3552, Australia.⁵Faculty of Transdisciplinary Innovation, University of Technology Sydney, Broadway NSW 2007, Australia.⁶School of Applied Physics, Faculty of Science and Technology, Universiti Kebangsaan Malaysia, 43600 Bangi, Selangor, Malaysia.^akwei@iukl.edu.my, ^bnurulauni2412@gmail.com, ^ckedy5wnt@nottingham.edu.my, ^dKim-Yeow.Tshai@nottingham.edu.my, ^eI.Kong@latrobe.edu.au, ^fEngHwa.Yap@uts.edu.au, ^gras@ukm.edu.my

Abstract. High temperature superconductor TI-1212 with nominal starting composition $(\text{Ti}_{0.85}\text{Cr}_{0.15})\text{Sr}_2\text{CaCu}_2\text{O}_{7-\delta}$ was prepared using high purity oxide powders through a solid state reaction method. Small amounts of nickel-zinc ferrite nanoparticles ($\text{NiZnFe}_2\text{O}_4$) at compositions 0.01, 0.02, 0.05, and 0.10 wt. % were added to the TI-1212 superconductor. The effect of $\text{NiZnFe}_2\text{O}_4$ nanoparticles' addition on the sample's critical temperature (T_c), transport critical current density (J_c), phase formation, and morphology was studied. The samples were characterized using electrical resistance measurement, transport critical current density measurement, powder X-ray diffraction method (XRD), scanning electron microscopy (SEM), and energy dispersive X-ray analysis (EDX). Zero-resistance critical temperature ($T_{c\text{-zero}}$) was found to increase from 97 K to 99 K by increasing $\text{NiZnFe}_2\text{O}_4$ concentration. The highest transport critical current density (J_c) recorded was 3,120 mA/cm² at 77 K, which was exhibited by sample with 0.02 wt. % of $\text{NiZnFe}_2\text{O}_4$. All of the samples showed a dominant TI-1212 phase and exhibited tetragonal lattice structure in the P4/mmm space group. SEM micrographs showed close-packed microstructure with low porosity. EDX mapping showed that $\text{NiZnFe}_2\text{O}_4$ nanoparticles were well distributed in the TI-1212 samples. This study has established $\text{NiZnFe}_2\text{O}_4$ nanoparticles as effective flux pinning centers to TI-1212 superconductors and thus significantly enhanced its J_c .

ICSSST2019-188

Assessment of Magnetic Property between Fe and Ni doped ZnO Nanoparticles Synthesized by Microwave Assisted Synthetic MethodS. S. Abdullahia^{a,b,d}, G.S.M Galadanci^b, N.M. Saidu^{c,d}, J. Y.C. Liew^{b,d}^aPhysics Department, Federal University Dutse, P.M.B. 7156, Dutse, Jigawa State Nigeria^bPhysics Department Bayero University, Kano Nigeria. P.M.B.3011, Kano Nigeria^cPhysics Department, Faculty of Science, Universiti Putra Malaysia, 43400 UPM Serdang, Selangor Malaysia.^dInstitute of Advanced Technology, Universiti Putra Malaysia, 43400 UPM Serdang, Selangor, Malaysia.

sabiused1@yahoo.com, nlaily@upm.edu.my

Abstract. The emergence of Dilute Magnetic Semiconductors (DMS) with a potentials for spintronic application have attracted much researches attention, special consideration has been given to ZnO semiconductor material due to its wide band gap of 3.37eV, large exciting binding energy of 60meV and small exciton Bohr radius of 2.34nm, moreover, its ferromagnetic behavior at room temperature when doped with transition metals. $M_xZn_{1-x}O$ (M = Fe or Ni) nanoparticle was synthesized by microwave assisted synthesis method calcined at 600°C. The structural, optical and magnetic properties of these nanoparticles were studied using X-ray diffraction (XRD). UV-Visible, Photoluminescence Spectroscopy (PL) and Vibrating Sample Magnetometer (VSM) respectively. Single and secondary phase Wurtzite hexagonal crystal structure was observed for the Fe and Ni doped ZnO nanoparticles respectively. The optical property of both Fe and Ni doped ZnO samples indicate a shift in the band gap of the nanoparticles compared to undoped ZnO sample, The Photoluminescence spectra demonstrate the formation of three emission peaks. The magnetic measurement reveals a clear ferromagnetic behavior for Fe doped ZnO while a diamagnetic behavior for Ni doped ZnO. The research confirm that Fe doped ZnO material will be good material for spintronic applications.

A

absorbent, 15, 70
AC susceptibility, 82, 92
activation energy, 59, 78, 86
active layer, 49
adsorption capacity, 30, 44, 56
agglomeration, 39, 63
alpha-willemite, 29
alumina, 19, 88
Aluminum, 86, 99
amide, 38, 57, 66
amorphous, 14, 15, 16, 20, 23, 24, 28, 32, 45, 55, 74, 84, 91, 94, 106

B

battery, 37, 45, 49
biocoagulant, 105
biodegradable, 15, 75, 106
biopolymer electrolyte, 39, 94, 108
biosensor, 13, 109
borotellurite glass, 20, 21, 32, 91

C

captopril, 53, 57
carbon nanotubes, 13, 30, 57, 63, 106
catalyst, 16, 53, 65
catalytic, 13, 16
cathode, 37, 49, 94, 96, 97
ceramic, 19, 22, 24, 26, 28, 29, 32, 33, 80, 90
chitosan, 13, 39, 94, 102
chromium, 36
clay, 24, 41
Combustion Synthesis, 61
communication, 40
copper, 36, 49
co-precipitation, 13, 43, 70, 79, 82
corn, 19, 39, 64
corrosion, 36, 40, 62, 66, 99, 107
critical transition temperature, 80, 81, 82
crystal, 21, 28, 30, 33, 44, 51, 70, 80, 81, 94
crystallinity, 13, 29, 55, 74, 77, 87, 88, 94, 96
crystallization, 29, 72, 75, 77
current density, 27, 36, 40, 62, 81, 82, 94, 95, 111, 112

D

Density Functional Theory, 80
dielectric, 59, 61
dielectric loss, 59, 61
dopant, 18, 26, 27, 29, 39, 47, 79, 80, 87
drug, 53, 56, 57, 103

E

efficiency, 24, 25, 30, 40, 44, 48, 49, 53, 57, 66, 75, 85, 95
elastic properties, 25, 88, 89, 91
electrical conductivity, 17, 47, 70, 74, 96
electrical properties, 16, 20, 21, 22, 27, 63, 79, 90
electrochemical stability, 42, 45, 94
electrodeposition, 36, 84
electronic properties, 71, 72, 80
electroresistance, 68, 69
emeraldine base, 84
emission, 13, 16, 18, 23, 28, 29, 30, 32, 36, 41, 58, 61, 68, 83, 84, 85, 94
Europium, 61

F

fabrication, 18, 23, 27, 44, 47, 60, 71, 79, 93, 106
Fatigue crack growth, 73
ferroelectric, 31, 90, 96
ferromagnetic, 21, 31, 68, 70, 83, 113
ferromagnetism, 31, 83
filter, 17
First Principle Study, 80
fitting methodology, 110
Fluorine, 86

G

gamma radiation, 41
gold, 28, 38, 93, 95
graphene, 15, 16, 17, 30, 38, 48, 55, 60, 104, 109
graphite, 16, 17, 74
groundwater., 54

H

hardness, 26, 36, 41, 52, 73, 99, 100
high-performance, 56, 58, 72, 97
Hot Carrier Injection, 110
Hummer's method, 15
hydrophobic, 14, 16
hydrothermal method, 18, 25, 51, 83, 85, 88
hysteresis, 44, 73, 90

I

immunosensor, 93
impedance spectroscopy, 37, 40, 59, 66, 85, 90, 96, 107
Indium, 86
intercalation, 53, 56, 57
ion selective electrode, 35
ionic conductivity, 37, 42, 45, 89, 94
ionic liquid, 37, 49, 94
ionophore, 35
irradiated, 41, 64

K

kalsilite, 88
kaolin, 88
kapok, 108
kinetic, 44, 78, 101

L

laser, 26, 40, 67, 106
layered double hydroxide, 53, 56, 57
lifetime, 26, 95, 107, 110
lignin, 76
lithium, 45, 90
luminance, 85

M

magnesium, 42, 90
magnetic properties, 46, 70, 83, 92, 113
magnetite, 24, 44, 102
mechanical properties, 14, 36, 72, 74, 76, 99, 100
microcrystalline cellulose, 17
microhardness, 36, 91, 99
microstructure, 30, 46, 52, 61, 68, 83, 87, 90, 99, 100, 112
microwave absorption, 68, 70

microwave assisted, 43, 51, 113
mild steel, 40, 107
mill scale, 46
modulus, 24, 25, 26, 41, 52, 59, 72, 74, 75, 88, 91
molybdenum, 98

N

nanocellulose, 55, 56
nanocomposite, 13, 36, 53, 56, 57
nanofiller, 72, 77
nanohybrid, 104
nanoindentation, 41, 52, 100
nanoparticle, 20, 21, 34, 43, 103, 104
nanowire, 43, 83
nitrocellulose, 108
nonlinear coefficient, 27

O

oil palm, 47
oil sorbents, 14
optical properties, 20, 32, 61, 71, 75, 85, 86, 87, 95, 101, 103, 104

P

packaging, 41, 64, 72, 77
Payne effect, 76
penetration, 17, 64, 82
perovskite manganite, 22
photoelectrochemical, 84, 85
photoluminescence, 18, 26, 28, 29, 32, 61, 85
plasticizer, 35, 42, 74, 75, 77
polarization, 31, 36, 40, 62, 66, 90, 96, 97
Polyaniline, 18, 84
polymer electrolyte, 45, 74
polypyrrole, 109
polystyrene, 75
porous, 18, 38, 51, 96
pullulan, 105
pyroelectric, 96

R

Raman spectroscopy, 16, 75, 90, 104, 106
rare-earth, 28, 81
reflection loss, 46, 68
reinforcement, 72, 76, 77

Rietveld, 33, 49, 92
ring deformation, 25, 89
rubber, 45, 73, 76

S

samarium, 18, 20, 28, 32, 96
Scanning Electron Microscope, 26, 38, 46,
47, 62, 70
seawater, 62, 66
Seebeck coefficient, 47, 50
silica, 14, 19, 20, 26, 27, 32, 88, 103
silver, 35, 49, 63, 75, 104
solar cell, 85, 95
sol-gel method, 33, 43, 49, 83, 90
solid oxide fuel cell, 44, 96
solid-state reaction, 21, 59
spin coating, 18, 96
sputtering, 16, 87
stagnation point, 34
stainless steel, 99

V

structural properties, 13, 20, 21, 25, 28,
69, 80, 81
surface plasmon resonance, 28, 60, 63, 85
surfactant, 43, 104

T

tellurite glass, 21, 55, 89
tensile properties, 74, 76
thermal conductivity, 47
thermodynamic, 101
thermomechanical, 75, 77
thiazole, 35
tin oxide, 49
titanium, 60, 72, 99
torrefaction, 48
transport critical current density, 82, 112

U

ultrasonication, 72, 77, 102, 109
UV-Vis, 20, 21, 23, 26, 28, 32, 62, 63, 66,
83, 84, 85, 87, 101, 104, 109

W

wastewater, 30, 48, 102, 105

X

X-ray Diffraction, 13, 18, 20, 21, 22, 23,
24, 26, 28, 29, 36, 42, 46, 49, 55, 59,
61, 62, 65, 68, 69, 70, 81, 85, 87, 88,
90, 91, 94, 98, 101, 104, 108, 111, 113

Z

zirconium, 98
ZnO thin film, 85

SPECIAL THANKS TO OUR SPONSORS



PerkinElmer[®]
For the Better

Perkin Elmer Sdn. Bhd.
#2.01 Level 2, Wisma Academy
Lot 4A, Jalan 19/1
46300 Petaling Jaya, Selangor
Malaysia

ROC No : 481872-T
Phone 03-79491118
Fax : 03-79491119
www.perkinelmer.com



INTERSCIENCE SDN BHD
2, Jalan Sungai Kayu Ara 32/38, Berjaya
Industrial Park, 40460 Shah Alam, Selangor,
Malaysia.
Tel: +60 3 5740 9888
Fax: +60 3 5740 9866
Email: info@its-interscience.com
www.its-interscience.com

AMETEK Potentiostat	Retsch Solutions in Milling & Sieving Grinder	THALESNano Reactor
C-THERM TECHNOLOGIES Thermal Analyzer	büchi Reactor	JASCO FTIR
SETARAM Instrumentation KCP Technologies Thermal Analyzer	MILESTONE Microwave Digester, Extraction & Synthesis	SYMPA Particle Sizer
elementar CHALLENGE IN ANALYSIS Elemental Analyzer	HITACHI Inspire the Next XRF / LIBS	BROUKER FT-NIR
xplore Micro-compounder	ramé-hart Goniometer / Tensiometer	CARBOLITE GERO Furnace

Your Preferred Local Star



Biotek Abadi Sdn. Bhd.
16-1, Jalan Setia Indah U13/Y, Setia Alam,
40170 Shah Alam, Selangor.
T: 03-3358 0920 E: info@biotekabadi.com.my

Each of Our Brands is a STAR



MACHEREY-NAGEL

Filtration - Rapid Tests - Water Analysis - Chromatography - Bioanalysis
Filtration - Schnellteste - Wasseranalyse - Chromatographie - Bioanalyse

Haier Biomedical
Intelligent Protection of Life Science



NOVATEINBIO
Accelerator - Research and Development

SIGMA-ALDRICH



**Technical Service
Consultants Ltd**



MERCK



Perfect Binding

Stapler Tape

Comb Binding

Wire O Binding

Spiral Binding

KALAM PRINTING

No. 29C Jalan
Hentian 4,
Pusat
Hentian Kajang
Jalan Reko,
43000 Selangor

Tel: 03-8741 5407



<https://icsst19.upnm.edu.my>